NRL Report 6663

Theoretical VLF Multimode Propagation Predictions

C. B. Brookes, Jr., J. H. McCabe, and F. J. Rhoads

Communication Branch
Radio Division

December 1, 1967

NAVAL RESEARCH LABORATORY
Washington, D.C.

90

NRL Report 6663

Theoretical VLF Multimode Propagation Predictions

December 1, 1967

NAVAL RESEARCH LABORATORY
Washington, D.C.

BLANK PAGE

CONTENTS

ABSTRACT

A computer program in Fortran has been written for the Control Data Corporation (CDC) 3800 computer to predict the field strength of multimode very-low-frequency (vlf) propagation for distances from 0.5 megameters to 15 megameters.

Although the propagation parameters used in the computations appear in various forms elsewhere in the literature, the curves presented here can be directly compared with experimental data without further computations.

Curves based on the theoretical results for seawater paths are presented for frequencies between 8.0 kc/s and 30.0 kc/s for ionospheric heights of 70 km and 90 km.

PROBLEM STATUS

A final report on one phase of the problem; work on other phases continues.

AUTHORIZATION

NRL Problem R01-39
NavElecSysCom Project X-1508, Task 82205

Manuscript submitted October 25, 1967.

THEORETICAL VLF MULTIMODE PROPAGATION PREDICTIONS

INTRODUCTION

The experimental, very-low-frequency (vlf) radio wave propagation data reported by Bickel et al. (1) and Rhoads and Garner (2) show that the higher order modes are significant at distances exceeding 3 Mm (3). The theoretical work by Wait and Spies (4) indicates that the second-order and third-order modes of the transverse magnetic waves are significant, and can even be dominant, at distances greatly exceeding 3 Mm, depending upon the frequency and the height of the ionosphere. The experimental results of Rhoads and Garner (2) show close agreement with the theoretical results of Wait and Spies (4).

A computer program has been written to calculate and plot the field strength as a function of distance for each individual mode and for the resultant of multiple modes, using the values for the various parameters as given by Wait and Spies (4). This program was written in Fortran for the Control Data Corporation (CDC) 3800 computer with the output automatically plotted by a 10-in. Calcomp plotter. This program was used to calculate the theoretical field strengths given by Rhoads and Garner (2). This report is intended to present more detailed information on this computer program and to present the calculated field strengths as a function of distance for many frequencies in the vlf range.

THEORETICAL MODEL

The theoretical model used throughout this report is that of Wait (3), where the vertical electric field is given by

$$E = E_0 \frac{(d/a)^{1/2}(d/\lambda)^{1/2}}{[\sin (d/a)]^{1/2}(h/\lambda)} e^{-i\pi/4} \Sigma e^{-ixt_n} G_n(\hat{Y})\, G_n(Y)\, \Lambda_n \qquad (1)$$

with $x = \phi(ka/2)^{1/3}$ and $E_0 = 3 \times 10^5 P^{1/2}/d$. The expressions $G_n(\hat{Y})$ and $G_n(Y)$ are the height-gain functions of the nth mode, and Λ_n is the complex excitation coefficient. All the latter quantities are functions of t_n, the complex roots of the modal resonance equation $1 - A(t)\,B(t) = 0$. The functions $A(t)$ and $B(t)$ are related to the reflection coefficients of the waveguide boundaries and are given by Wait (3). The exponential within the summation is related to the more familiar propagation parameters by

$$\alpha_n = (20 \log e)(1000\, x/d)(\mathrm{Im}\ t_n) \qquad (2a)$$

and

$$(\omega/v_n) - (\omega/c) = (x/d)(\mathrm{Re}\ t_n)\ , \qquad (2b)$$

where $\mathrm{Im}\ t_n$ and $\mathrm{Re}\ t_n$ are the imaginary and real parts of t_n, respectively. The dimensions and definitions of all symbols not specifically cited are given in the Appendix.

For amplitude calculations, when both the transmitter and the receiver are on or very near the surface of the earth, both height functions become unity and the imaginary exponent external to the summation can be ignored. With these simplifications, and using the above equalities, Eq. (1) reduces to

$$E = \frac{5.2 \times 10^6 P^{1/2}}{[a \sin (d/a)]^{1/2} f^{1/2} h} \Sigma \Lambda_n e^{-i x t_n} . \quad (3)$$

The summation on the right-hand side of Eq. (3) was computed for three modes ($n = 1,2,3$), unless otherwise stated, using the numerical results of Wait and Spies (4). For convenience, the values used are given in Tables 1a and 1b. These values are for an isotropic model with an infinitely conducting ground and an exponential ionosphere with a conductivity gradient of $\beta = 0.5$ km^{-1}.

DISCUSSION

The simplified electric field strength equation,

$$E = \frac{5.2 \times 10^6 P^{1/2}}{[a \sin (d/a)]^{1/2} f^{1/2} h} \Sigma \Lambda_n e^{-i x t_n} \quad (4)$$

was used in this multimode program. The calculations were made at increments of 50 km from the transmitter for both daytime and nighttime conditions. The height of the ionosphere was taken to be 70 km and 90 km for day and night conditions, respectively. The summation portion ($\Sigma \Lambda_n e^{-i x t_n}$) of Eq. (4) was separated into the real and imaginary parts such that

$$A_n = \text{Re}\, \Lambda_n e^{-i x t_n} = 10^{(1/20)[(-d\alpha_n/1000)+\Lambda_n]} ,$$

where t_n is imaginary, and

$$\phi_n = \arg \Lambda_n + \arg e^{-i x t_n} = \Lambda_n^0 - (360 f d)/V_n .$$

Then

$$A_r e^{-i\phi_r} = \Sigma A_n e^{-i\phi_n}$$

$$= \Sigma \left[10^{(1/20)[(-d\alpha_n/1000)+\Lambda_n]} \cos (\Lambda_n^0 - (360 f d)/\Lambda_n) \right]$$

$$+ i \Sigma \left[10^{(1/20)[(-d\alpha_n/1000)+\Lambda_n]} \sin (\Lambda_n^0 - (360 f d)/\Lambda_n) \right] ,$$

where

$$A_r = \left\{ \left[\Sigma 10^{(1/20)[(-d\alpha_n/1000)+\Lambda_n]} \cos (\Lambda_n^0 - (360 f d)/\Lambda_n) \right]^2 \right.$$

$$\left. + \left[\Sigma 10^{(1/20)[(-d\alpha_n/1000)+\Lambda_n]} \sin (\Lambda_n^0 - (360 f d)/\Lambda_n) \right]^2 \right\}^{1/2}$$

and

$$\phi_r = \tan^{-1} \frac{\Sigma 10^{(1/20)[(-d\alpha_n/1000)+\Lambda_n]} \sin (\Lambda_n^0 - (360 f d)/\Lambda_n)}{\Sigma 10^{(1/20)[(-d\alpha_n/1000)+\Lambda_n]} \cos (\Lambda_n^0 - (360 f d)/\Lambda_n)} .$$

The magnitudes of the individual modes and the summation are evaluated from

$$E_i = \frac{5.2 \times 10^6 P^{1/2}}{[a \sin (d/a)]^{1/2} f^{1/2} h} A_i .$$

The multimode field-strength-prediction program discussed in this report was used to produce the graphs presented in Figs. 1 through 72. These graphs show the calculated field strength as a function of distance for individual modes and for the summation of multiple modes. The values for the individual parameters used in these calculations are given in Tables 1a and 1b, which are for $\beta = 0.5$ km^{-1}, $\sigma_g = \infty$, and for the isotropic case with a radiated power of 1 kw. The numbers on each curve refer to the mode order number(s) involved in each respective calculation.

Table 1a
Theoretical Propagation Parameters for the Daytime Ionospheric Height h = 70 km

Frequency (kc/s)	Mode	$\lvert A \rvert$ (dB)	Phase A (Degrees)	α (dB/Mm)	v/c
8.0	1	0.59	6.76	3.96	1.008013
10.0	1	0.80	6.00	2.64	1.003692
10.2	1	0.00	5.95	2.55	1.003400
10.45	1	-0.03	5.95	2.47	1.003500
12.0	1	-0.41	5.77	2.03	1.001452
	2	1.24	2.20	13.34	1.039163
13.6	1	-0.85	5.80	1.77	1.000330
	2	1.30	2.05	10.75	1.028500
14.0	1	-0.95	5.90	1.73	1.000121
	2	1.32	1.98	10.31	1.026439
14.3	1	-1.06	5.95	1.70	0.999700
	2	1.34	1.96	9.94	1.025000
14.7	1	-1.15	6.00	1.66	0.999770
	2	1.37	1.90	9.53	1.023400
15.0	1	-1.25	6.10	1.64	0.999640
	2	1.38	1.89	9.23	1.022200
15.5	1	-1.40	6.20	1.61	0.999430
	2	1.42	1.80	8.80	1.020300
15.6	1	-1.40	6.13	1.62	0.999400
	2	1.42	1.80	8.73	1.020100
16.0	1	-1.58	6.31	1.59	0.999249
	2	1.46	1.74	8.42	1.018646
16.2	1	-1.65	6.37	1.58	0.999180
	2	1.48	1.72	8.28	1.018100
16.6	1	-1.80	6.50	1.57	0.999040
	2	1.51	1.70	8.00	1.016900
17.1	1	-1.97	6.68	1.55	0.999880
	2	1.56	1.62	7.75	1.015500
17.8	1	-2.20	6.90	1.55	0.998700
	2	1.62	1.55	7.25	1.013900
18.0	1	-2.32	7.01	1.54	0.999631
	2	1.64	1.52	7.16	1.013511
	3	1.04	0.84	16.72	1.048684
18.6	1	-2.55	7.30	1.55	0.998500
	2	1.70	1.45	6.87	1.012300
	3	1.05	0.82	16.02	1.045000
19.0	1	-2.73	7.44	1.55	0.998480
	2	1.75	1.43	6.77	1.011600
	3	1.07	0.80	15.58	1.042500
19.8	1	-3.10	7.90	1.56	0.998200
	2	1.83	1.36	6.35	1.010300
	3	1.12	0.76	14.80	1.038500
20.0	1	-3.18	7.98	1.57	0.998170
	2	1.85	1.33	6.27	1.009973
	3	1.13	0.77	14.54	1.037680
21.4	1	-3.90	8.90	1.61	0.997890
	2	1.99	1.26	5.80	1.008100
	3	1.21	0.75	13.44	1.034000

Table continues.

Table 1a (Continued)

Frequency (kc/s)	Mode	$\lvert A \rvert$ (dB)	Phase A (Degrees)	a (dB/Mm)	v/c
22.0	1	-4.23	9.29	1.64	0.997790
	2	2.06	1.25	5.26	1.007377
	3	1.24	0.74	13.02	1.029731
22.3	1	-4.40	9.50	1.66	0.997730
	2	2.08	1.22	5.53	1.007100
	3	1.26	0.73	12.84	1.028500
23.4	1	-5.03	10.40	1.72	0.997570
	2	2.20	1.23	5.27	1.006000
	3	1.32	0.64	12.16	1.025500
24.0	1	-5.43	10.91	1.76	0.997481
	2	2.26	1.26	5.11	1.005486
	3	1.36	0.61	11.79	1.023943
24.5	1	-5.80	11.39	1.80	0.997400
	2	2.32	1.29	5.00	1.005100
	3	1.40	0.59	11.55	1.022700
24.9	1	-6.08	11.78	1.83	0.997350
	2	2.38	1.32	4.92	1.004820
	3	1.42	0.57	11.36	1.021800
25.0	1	-6.15	11.90	1.84	0.997320
	2	2.35	1.31	4.90	1.004700
	3	1.43	0.57	11.30	1.021700
26.0	1	-6.88	12.91	1.92	0.997198
	2	2.43	1.43	4.70	1.004019
	3	1.49	0.51	10.89	1.019458
26.1	1	-7.00	13.00	1.93	0.997180
	2	2.44	1.42	4.67	1.004000
	3	1.50	0.50	10.85	1.019500
26.8	1	-7.48	13.80	2.00	0.997100
	2	2.50	1.53	4.54	1.003580
	3	1.55	0.44	10.54	1.017800
28.0	1	-8.49	15.20	2.12	0.996952
	2	2.56	1.75	4.36	1.002911
	3	1.64	0.35	10.12	1.016026
28.5	1	-9.00	15.80	2.17	0.996880
	2	2.58	1.87	4.27	1.002700
	3	1.68	0.32	9.95	1.015200
30.0	1	-10.40	17.90	2.34	0.996700
	2	2.61	2.29	4.07	1.002018
	3	1.80	0.22	9.53	1.013200

Table 1b
Theoretical Propagation Parameters for the Nighttime Ionospheric Height h = 90 km

Frequency (kc/s)	Mode	$\lvert\Delta\rvert$ (dB)	Phase Δ (Degrees)	α (dB/Mm)	v/c
8.0	1	-0.24	6.30	2.06	1.002338
10.0	1	-1.12	6.30	1.53	1.002338
	2	1.36	2.00	8.92	1.030935
10.2	1	-1.20	6.22	1.50	0.999600
	2	1.38	1.96	8.55	1.029200
10.45	1	-1.33	6.28	1.47	0.999380
	2	1.40	1.86	8.17	1.027200
12.0	1	-2.19	6.73	1.34	0.998378
	2	1.57	1.62	6.46	1.018705
	3	1.02	0.99	15.59	1.068030
13.6	1	-3.30	7.55	1.30	0.997610
	2	1.78	1.40	5.30	1.012900
	3	1.09	1.04	12.75	1.049400
14.0	1	-3.56	7.83	1.30	0.997470
	2	1.85	1.35	5.04	1.011800
	3	1.12	1.04	12.20	1.045927
14.3	1	-3.84	8.08	1.30	0.997350
	2	1.89	1.33	4.88	1.011000
	3	1.15	1.28	11.74	1.043000
14.7	1	-4.15	8.35	1.31	0.997210
	2	1.95	1.31	4.70	1.010000
	3	1.17	1.01	11.33	1.040700
15.0	1	-4.40	8.59	1.32	0.997110
	2	2.00	1.29	4.55	1.009400
	3	1.18	1.00	10.98	1.038900
15.5	1	-4.80	9.01	1.33	0.996950
	2	2.07	1.28	4.32	1.008400
	3	1.22	0.97	10.47	1.036000
15.6	1	-4.91	9.10	1.34	0.996910
	2	2.08	1.28	4.30	1.008200
	3	1.24	0.97	10.40	1.034500
16.0	1	-5.30	9.51	1.36	0.996801
	2	2.14	1.27	4.14	1.007529
	3	1.26	0.94	10.02	1.032592
16.2	1	-5.50	9.65	1.38	0.996770
	2	2.16	1.28	4.07	1.007200
	3	1.28	0.93	9.88	1.031300
16.6	1	-5.95	10.10	1.40	0.996640
	2	2.21	1.30	3.95	1.006600
	3	1.31	0.90	9.63	1.030200
17.1	1	-6.46	10.68	1.43	0.996500
	2	2.27	1.35	3.77	1.005900
	3	1.37	0.86	9.15	1.027300
17.8	1	-7.05	11.50	1.48	0.996310
	2	2.35	1.44	3.58	1.005000
	3	1.44	0.82	8.70	1.024700
18.0	1	-7.51	11.77	1.49	0.996255
	2	2.37	1.47	3.52	1.004726
	3	1.45	0.79	8.56	1.023879

Table continues.

Table 1b (Continued)

Frequency (kc/s)	Mode	$\lvert A \rvert$ (dB)	Phase A (Degrees)	α (dB/Mm)	v/c
18.6	1	-8.25	12.55	1.55	0.996110
	2	2.42	1.60	3.38	1.004000
	3	1.52	0.74	8.20	1.021900
19.0	1	-8.75	13.08	1.58	0.996010
	2	2.45	1.70	3.28	1.003820
	3	1.56	0.70	8.00	1.020800
19.8	1	-9.90	13.20	1.66	0.995820
	2	2.49	1.94	3.11	1.003000
	3	1.66	0.60	7.60	1.018500
20.0	1	-10.20	14.51	1.68	0.995781
	2	2.49	1.99	3.07	1.002822
	3	1.68	0.60	7.52	1.017888
21.4	1	-12.40	16.60	1.83	0.995480
	2	2.44	2.59	2.82	1.001800
	3	1.87	0.46	6.95	1.014800
22.0	1	-13.48	17.59	1.90	0.995336
	2	2.40	2.88	2.73	1.001458
	3	1.93	0.42	6.78	1.013516
22.3	1	-14.00	18.00	1.94	0.995290
	2	2.37	3.00	2.68	1.001300
	3	1.98	0.37	6.65	1.013000
23.4	1	-16.00	19.76	2.07	0.995060
	2	2.22	3.65	2.67	1.000770
	3	2.14	0.27	6.34	1.011200
24.0	1	-17.15	20.75	2.14	0.994935
	2	2.11	4.01	2.50	1.000483
	3	2.22	0.21	6.19	1.010309
24.5	1	-18.20	21.52	2.20	0.996850
	2	1.99	4.36	2.44	1.000280
	3	2.29	0.17	6.06	1.009600
24.9	1	-19.00	22.10	2.25	0.996780
	2	1.88	4.64	2.41	1.000130
	3	2.35	0.13	5.97	1.009200
25.0	1	-19.20	22.30	2.26	0.994750
	2	1.86	4.70	2.40	1.000100
	3	2.38	0.16	5.95	1.009100
26.0	1	-21.30	23.86	2.38	0.994550
	2	1.54	5.44	2.35	0.999735
	3	2.52	0.05	5.74	1.007824
26.1	1	-21.60	24.00	2.40	0.994550
	2	1.50	5.50	2.32	0.999700
	3	2.55	0.03	5.70	1.007700
26.8	1	-23.00	25.00	2.48	0.994430
	2	1.25	6.10	2.30	0.999500
	3	2.64	0.00	5.56	1.007000
28.0	1	-25.63	26.85	2.62	0.994207
	2	0.73	7.08	2.29	0.999165
	3	2.84	-0.08	5.36	1.005924
28.5	1	-26.80	27.60	2.68	0.994120
	2	0.50	7.55	2.30	0.999000
	3	2.92	-0.09	5.25	1.005400
30.0	1	-30.30	29.72	2.85	0.993879
	2	-0.38	9.08	2.31	0.998689
	3	3.16	-0.08	5.03	1.004396

REFERENCES

1. Bickel, J.E., Heritage, J.L., and Weisbrod, S., "An Experimental Measurement of VLF Field Strength as a Function of Distance Using an Aircraft," U.S. Navy Electronic Laboratory Report 767, June 28, 1957

2. Rhoads, F.J. and Garner, W.E., "An Investigation of the Modal Interference of Very-Low-Frequency Radio Waves," NRL Report 6359, Oct. 27, 1965

3. Wait, J.R., "Electromagnetic Waves in Stratified Media," Oxford: Pergamon, 1962

4. Wait, J.R. and Spies, K.P., "Characteristics of the Earth-Ionosphere Waveguide for VLF Radio Waves," NBS Technical Note 300, Dec. 30, 1964

Appendix A

LIST OF SYMBOLS

E = vertical electric field (μV/m)

P = radiated power

f = transmission frequency (kc/s)

h = effective ionospheric height (km)

d = distance from the transmitter (propagation path length) (km)

t_n = complex roots of the modal equation $1 - A(t)\ B(t) = 0$

$x = (ka/2)^{1/3}\ \theta = [(\pi a/\lambda)^{1/3}\ d/a]$

Λ_n = complex mode excitation coefficient ($|\Lambda|$ dB, Λ^0)

$|\Lambda|$ dB = real part in dB

Λ^0 = imaginary part in degrees

n = mode number

α_n = mode attenuation rate (dB/Mm)

V_n = mode phase velocity

a = radius of the earth (6371 km)

λ = free-space wavelength (km)

$k = 2\pi/\lambda$

$\theta = d/a$

ω = angular transmission frequency

c = velocity of light

$A(t)$ = function related to the ionospheric reflection coefficient (Ref. 3)

$B(t)$ = function related to the ground reflection coefficient (Ref. 3)

Y = height of transmitter above ground

$\hat{Y}$ = height of receiver above ground

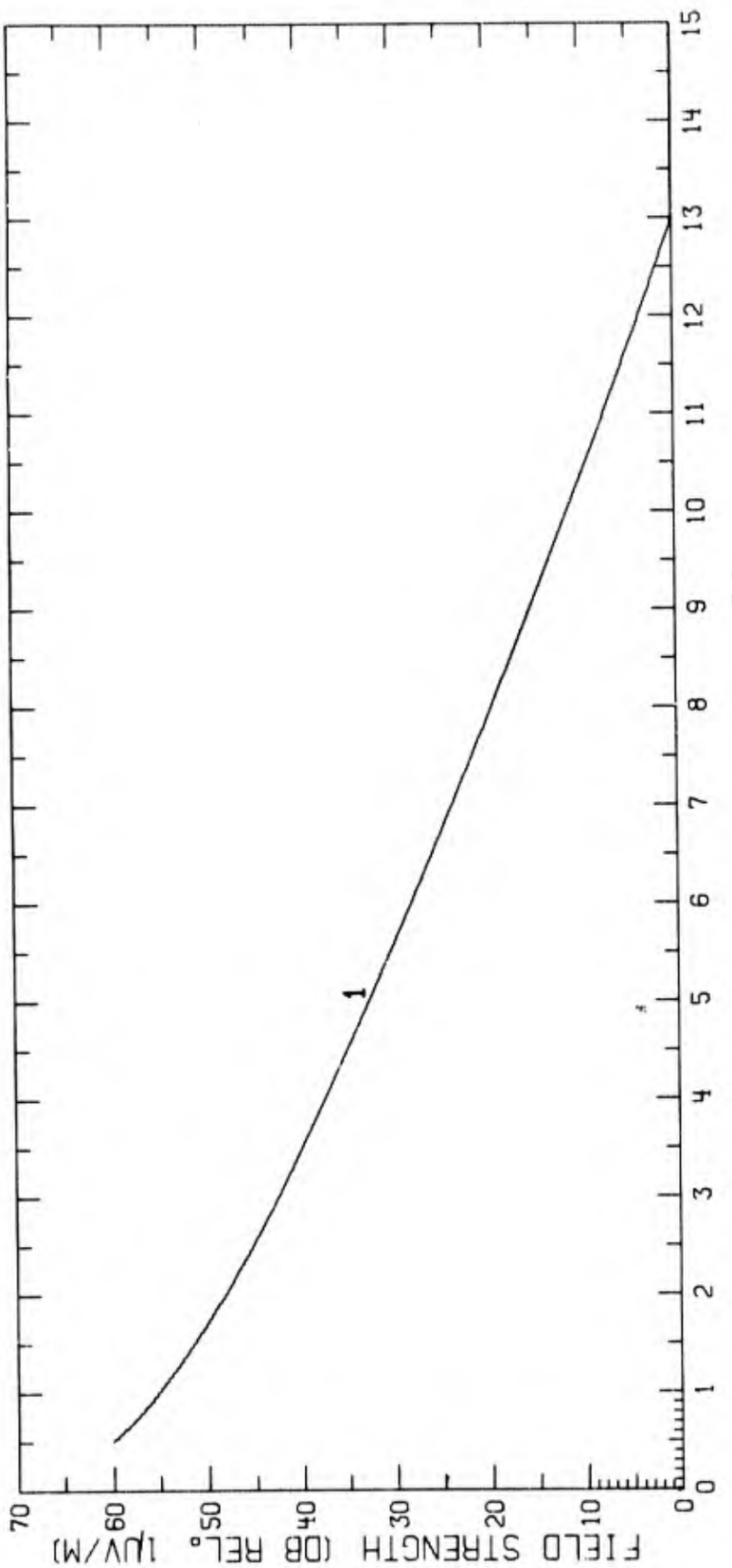

Fig. 1 - Predicted field strengths for $f = 8.0$ kc/s and $h = 70$ km

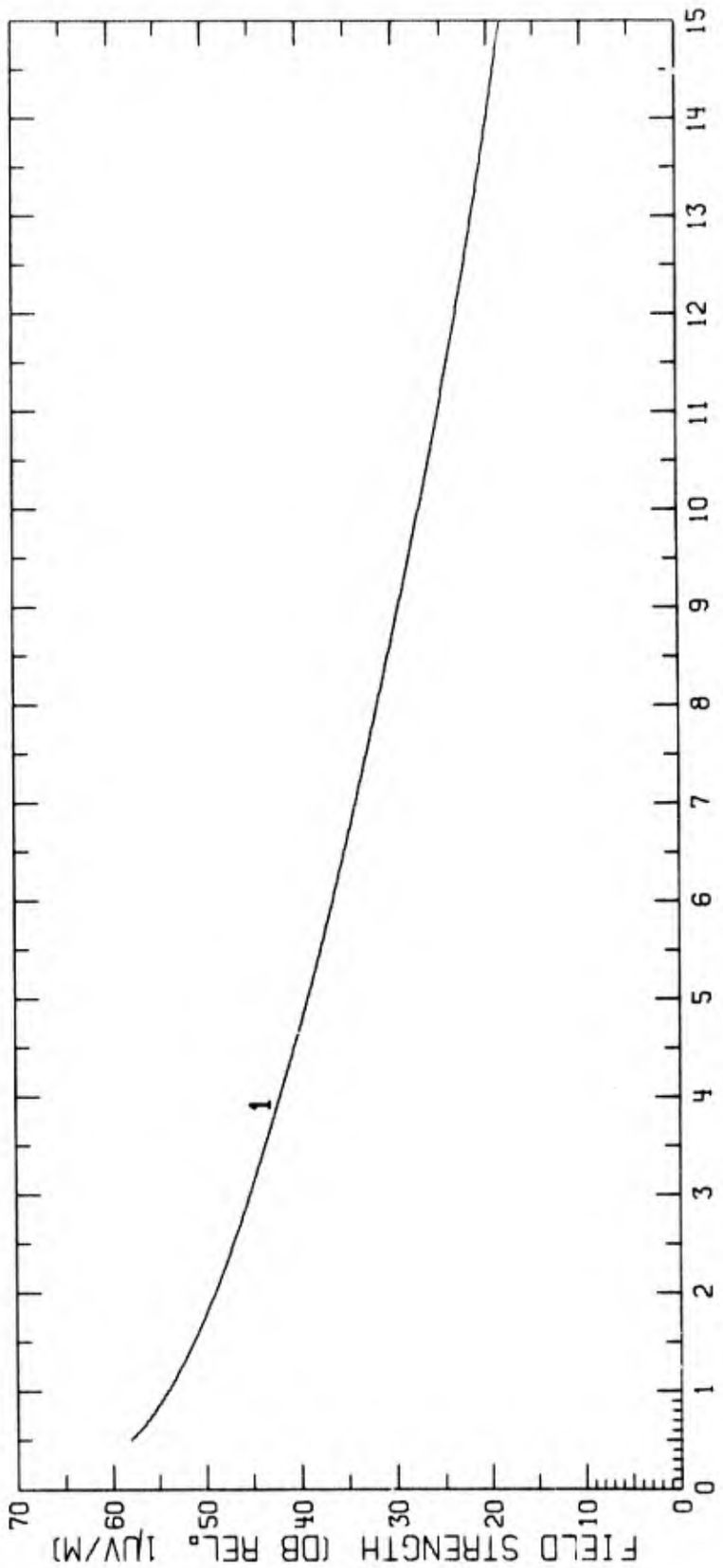

Fig. 2 - Predicted field strengths for f = 8.0 kc/s and h = 90 km

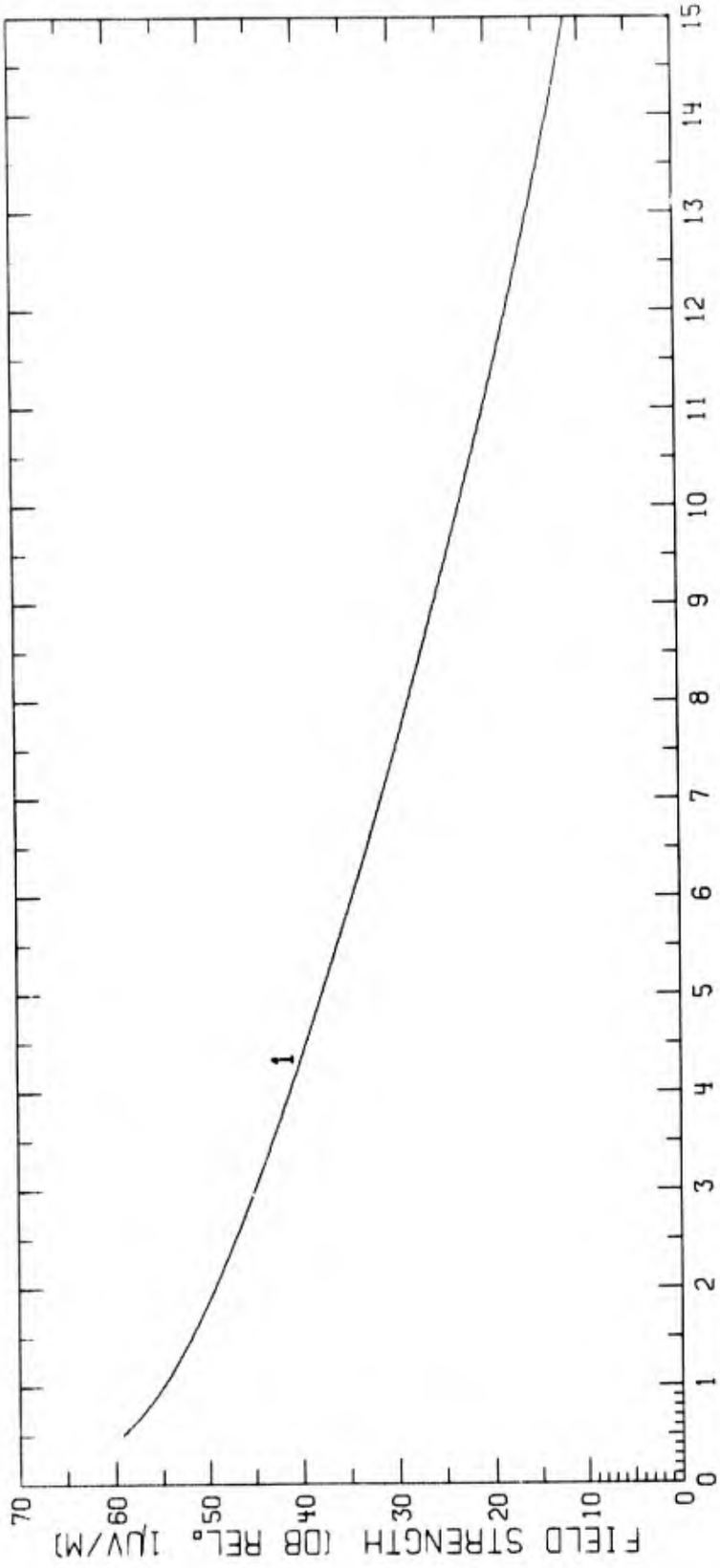

Fig. 3 - Predicted field strengths for f = 10.0 kc/s and h = 70 km

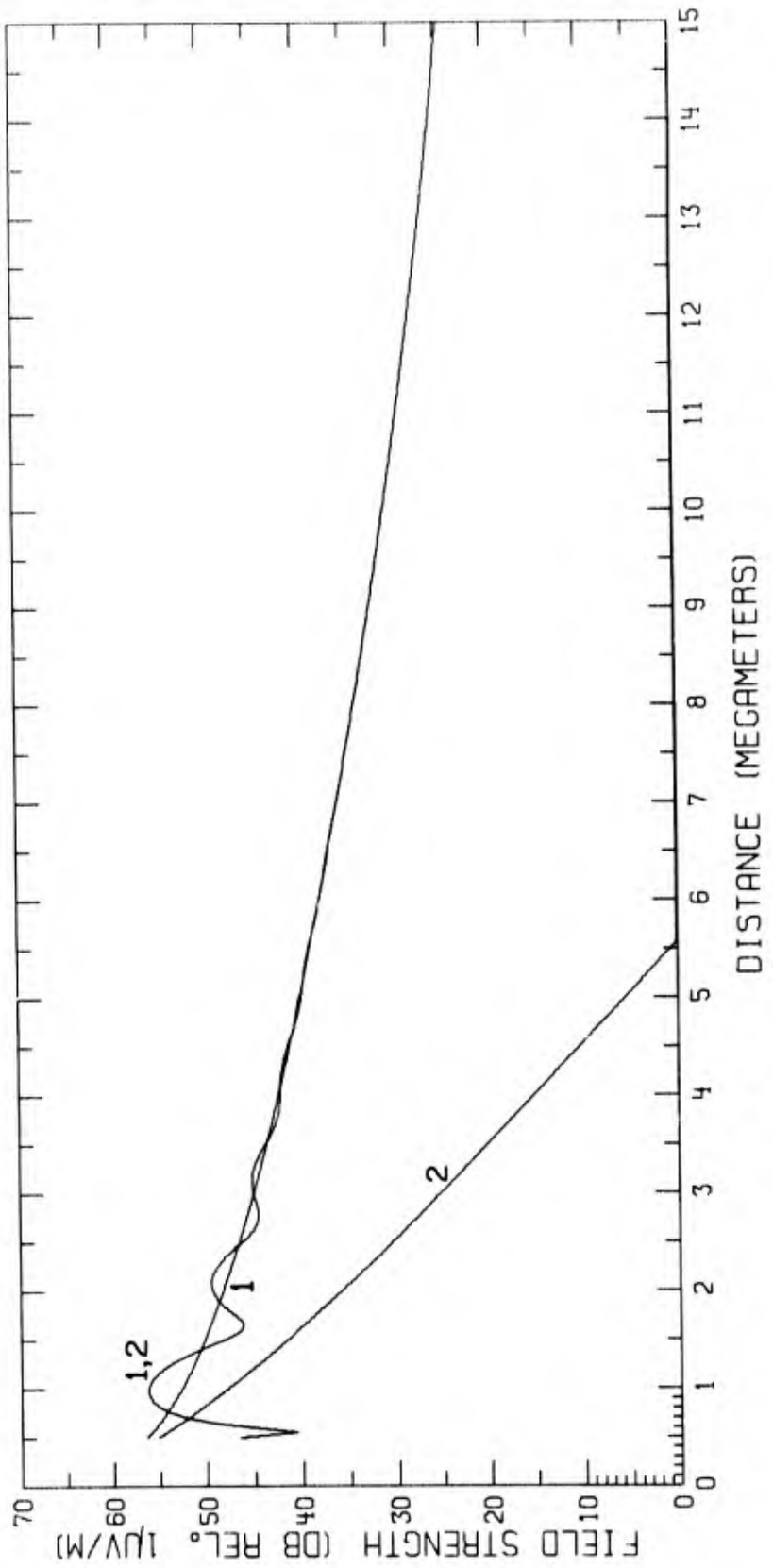

Fig. 4 - Predicted field strengths for f = 10.0 kc/s and h = 90 km

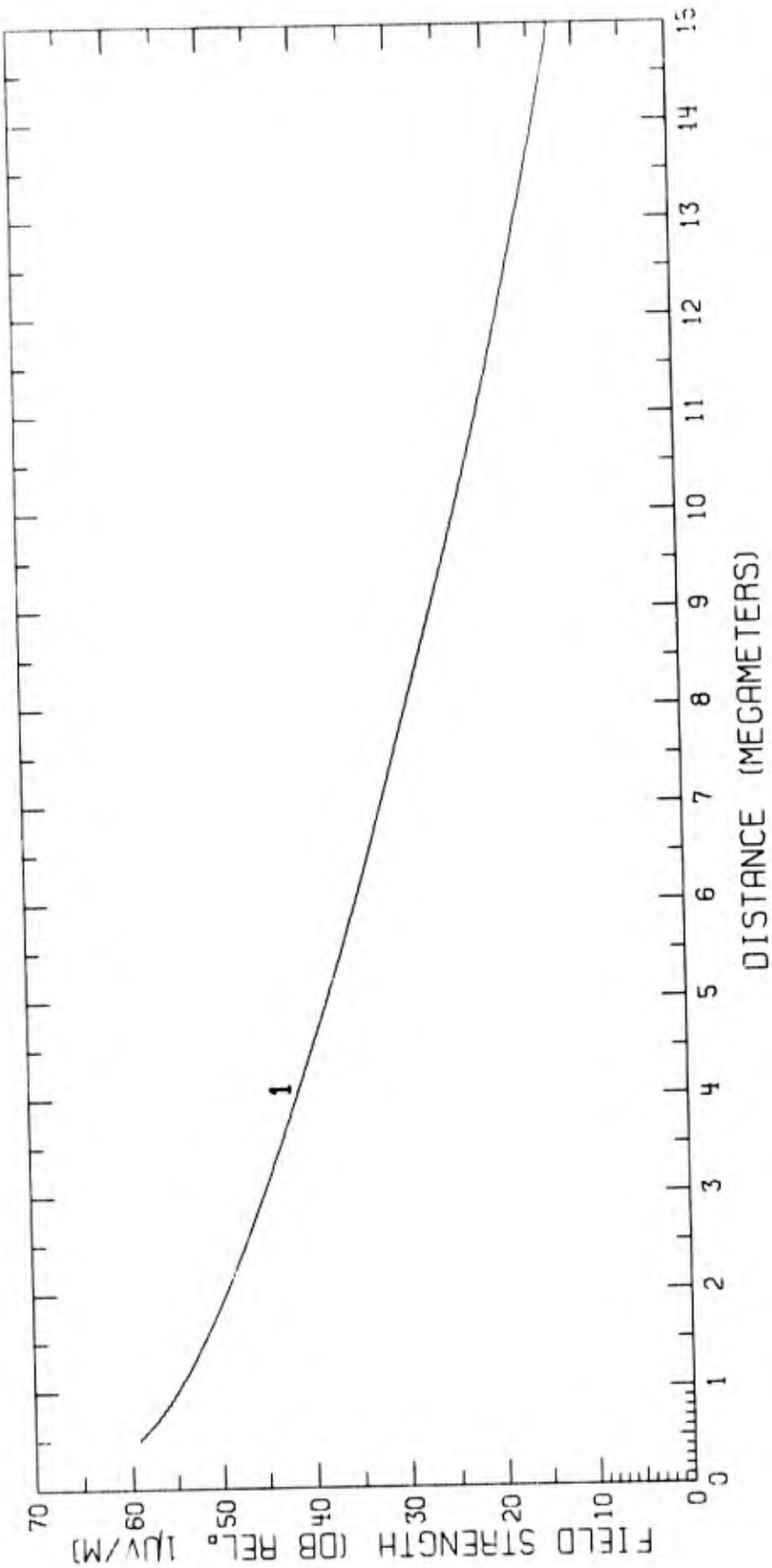

Fig. 5 - Predicted field strengths for f = 10.2 kc/s and h' = 70 km

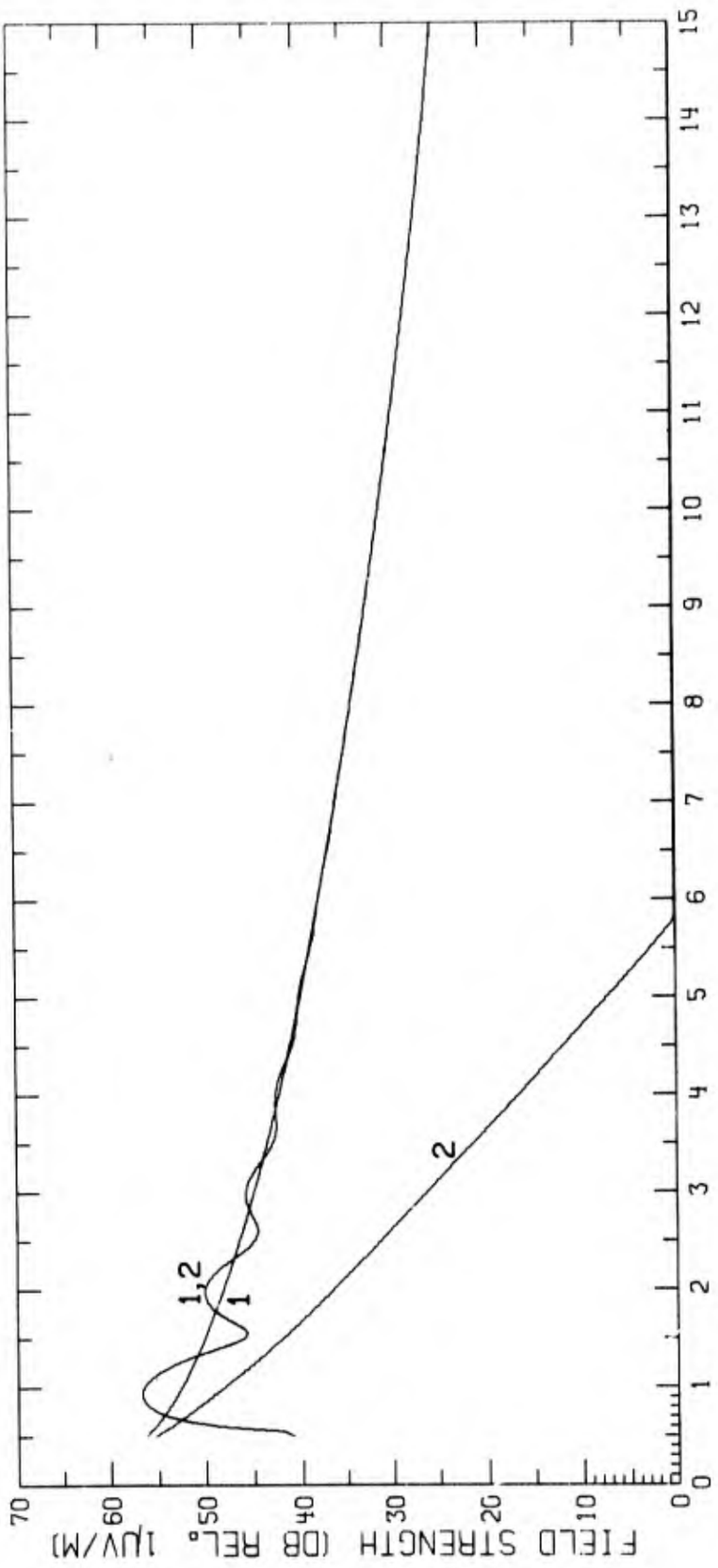

Fig. 6 - Predicted field strengths for f = 10.2 kc/s and h = 90 km

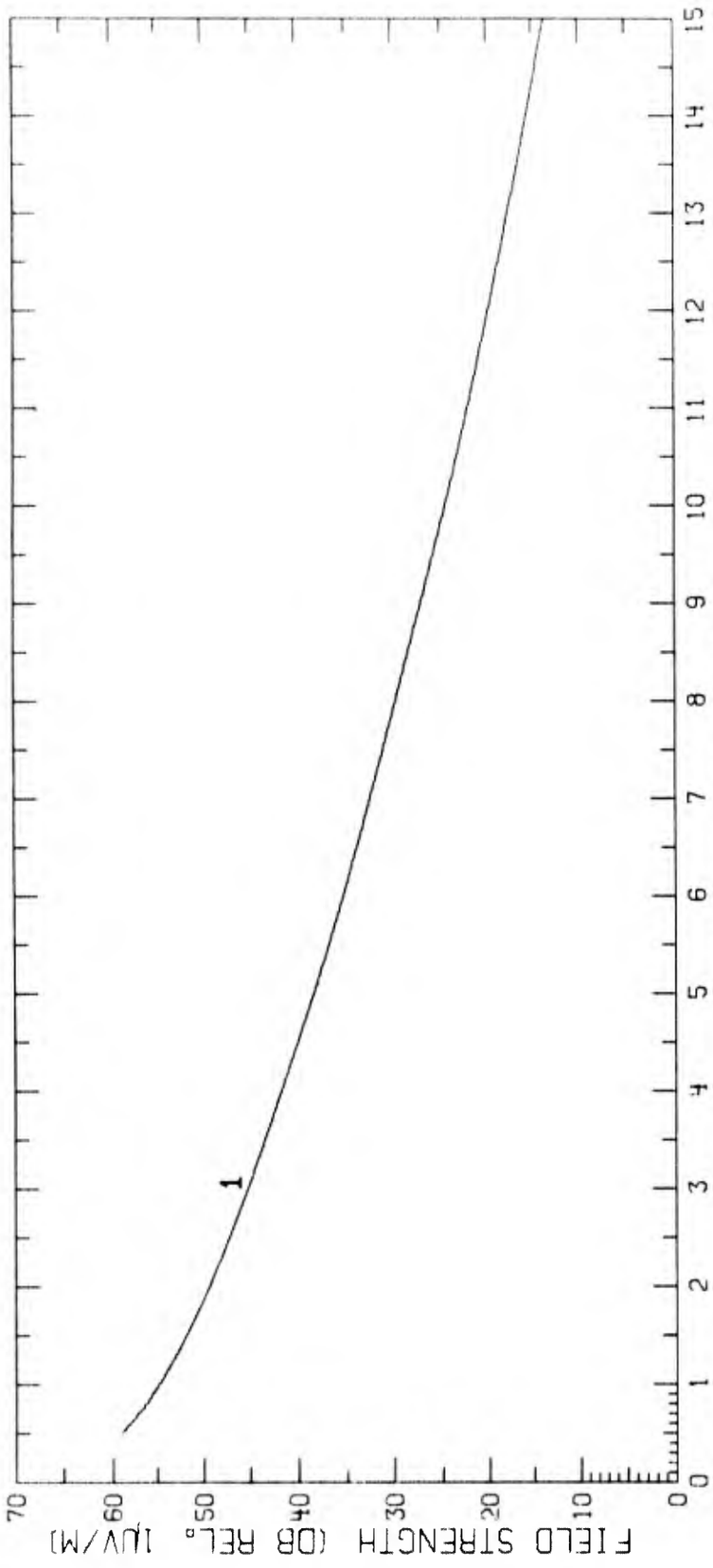

Fig. 7 - Predicted field strengths for f = 10.45 kc/s and h = 70 km

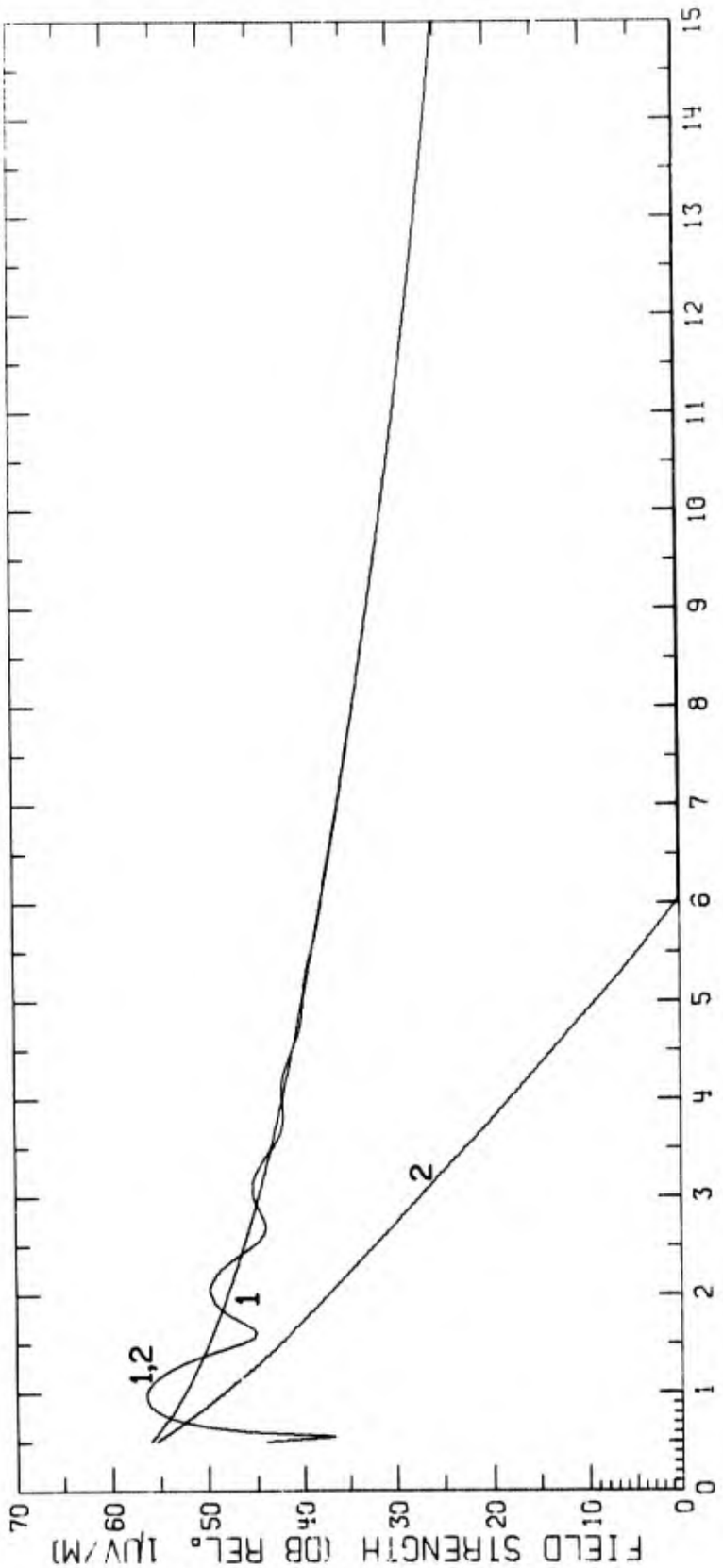

Fig. 8 - Predicted field strengths for f = 10.45 kc/s and h = 90 km

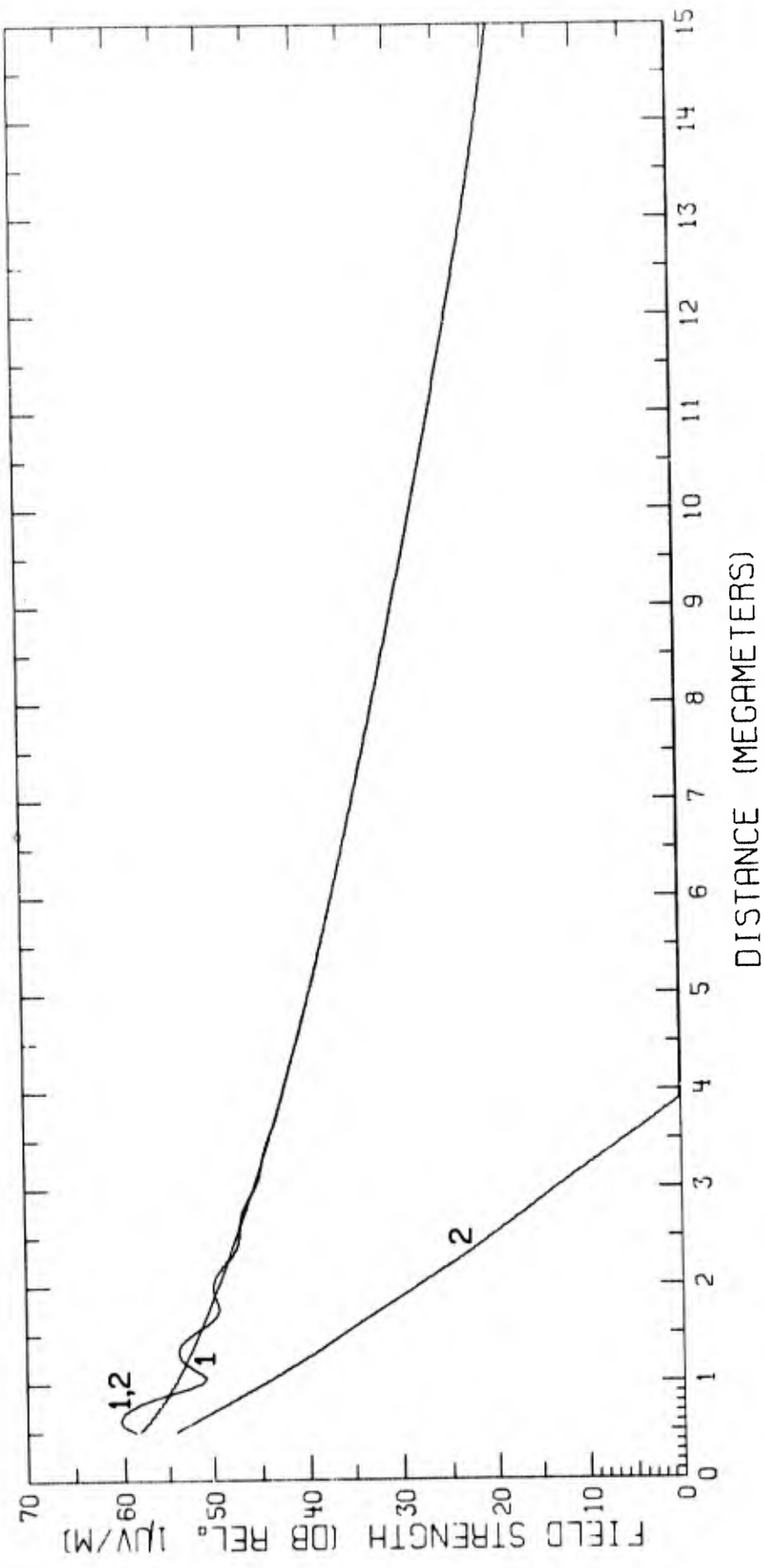

Fig. 9 - Predicted field strengths for f = 12.0 kc/s and h = 70 km

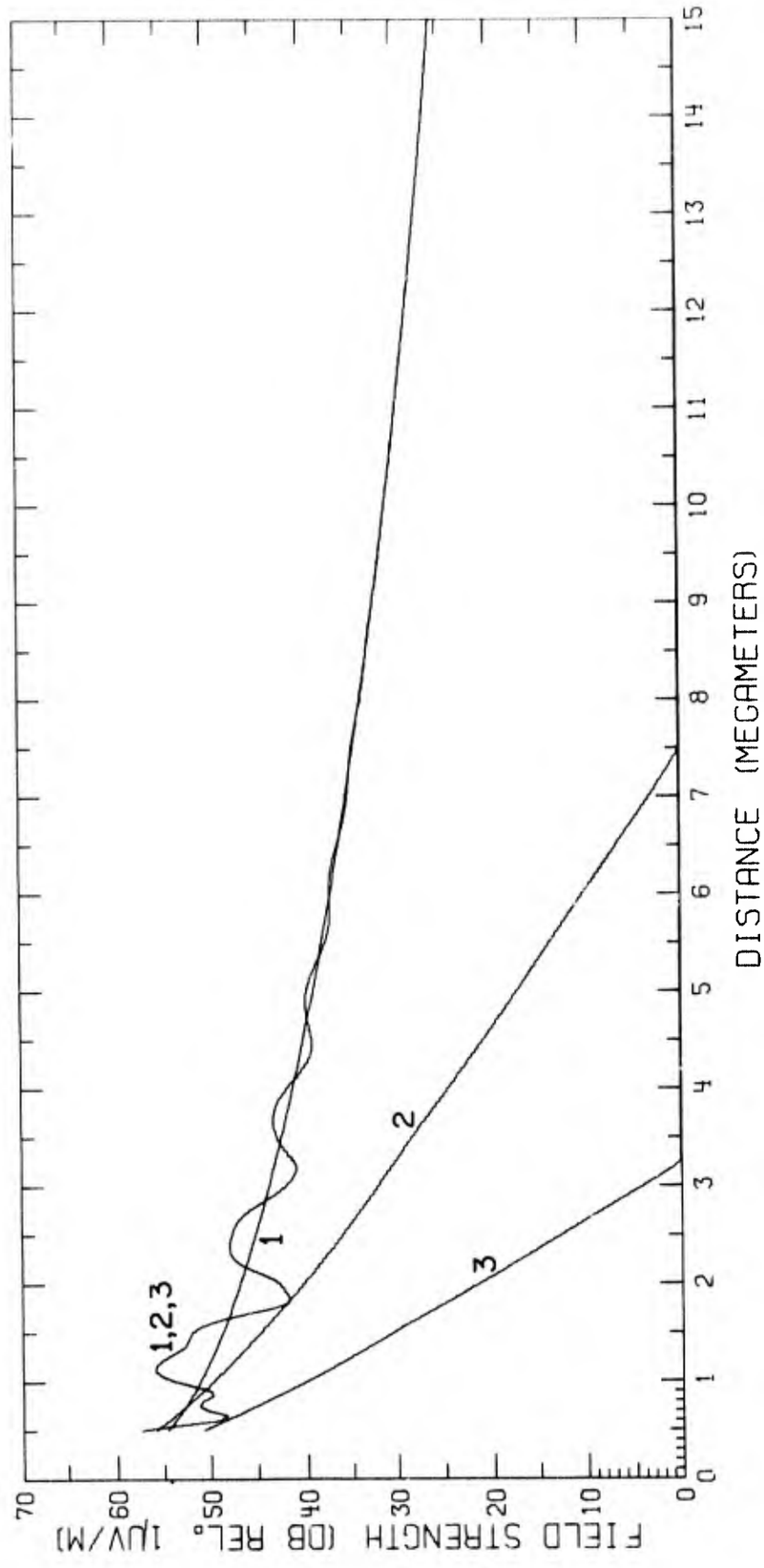

Fig. 10 - Predicted field strengths for f = 12.0 kc/s and h = 90 km

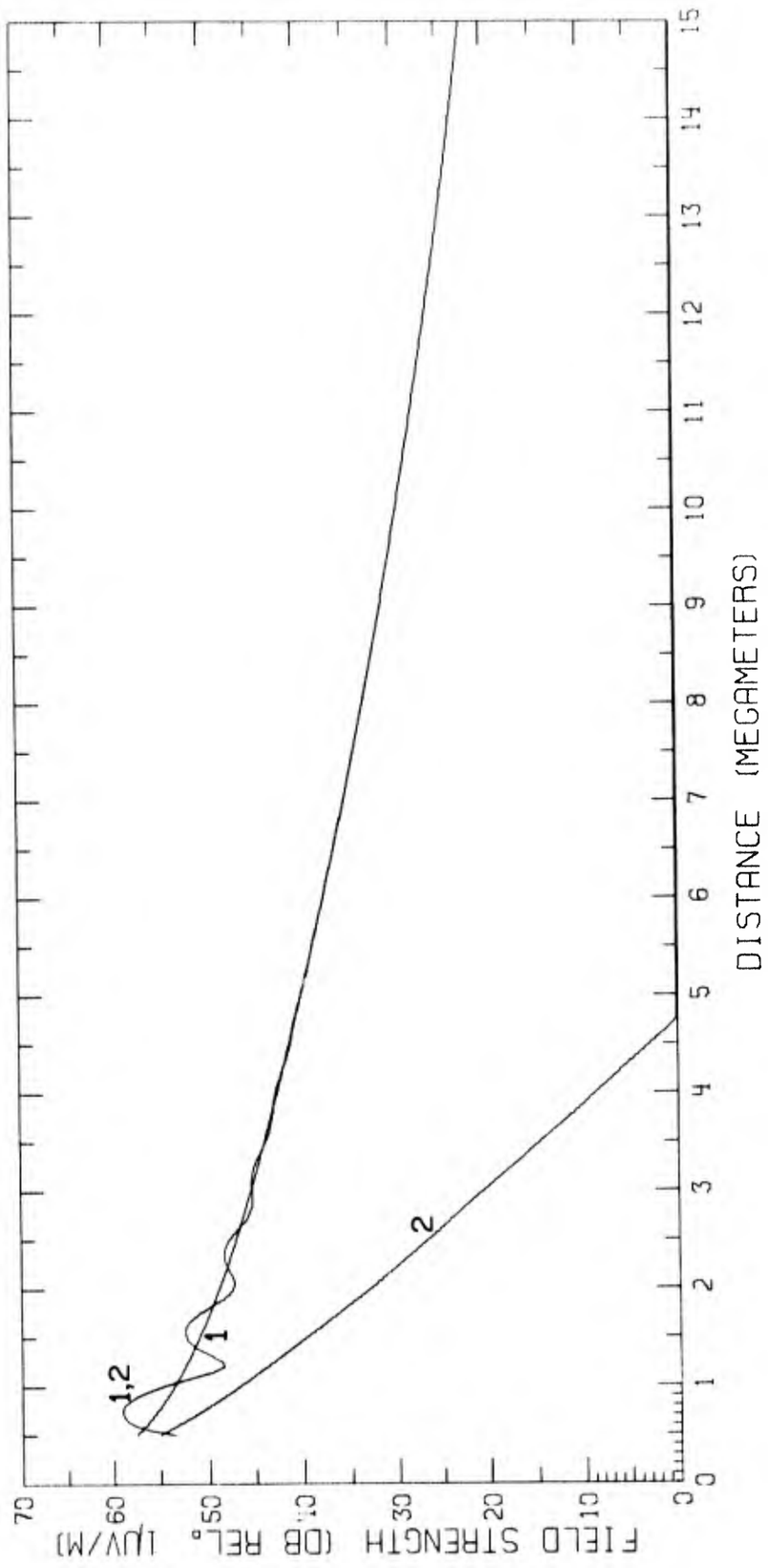

Fig. 11 - Predicted field strengths for f = 13.6 kc/s and h = 70 km

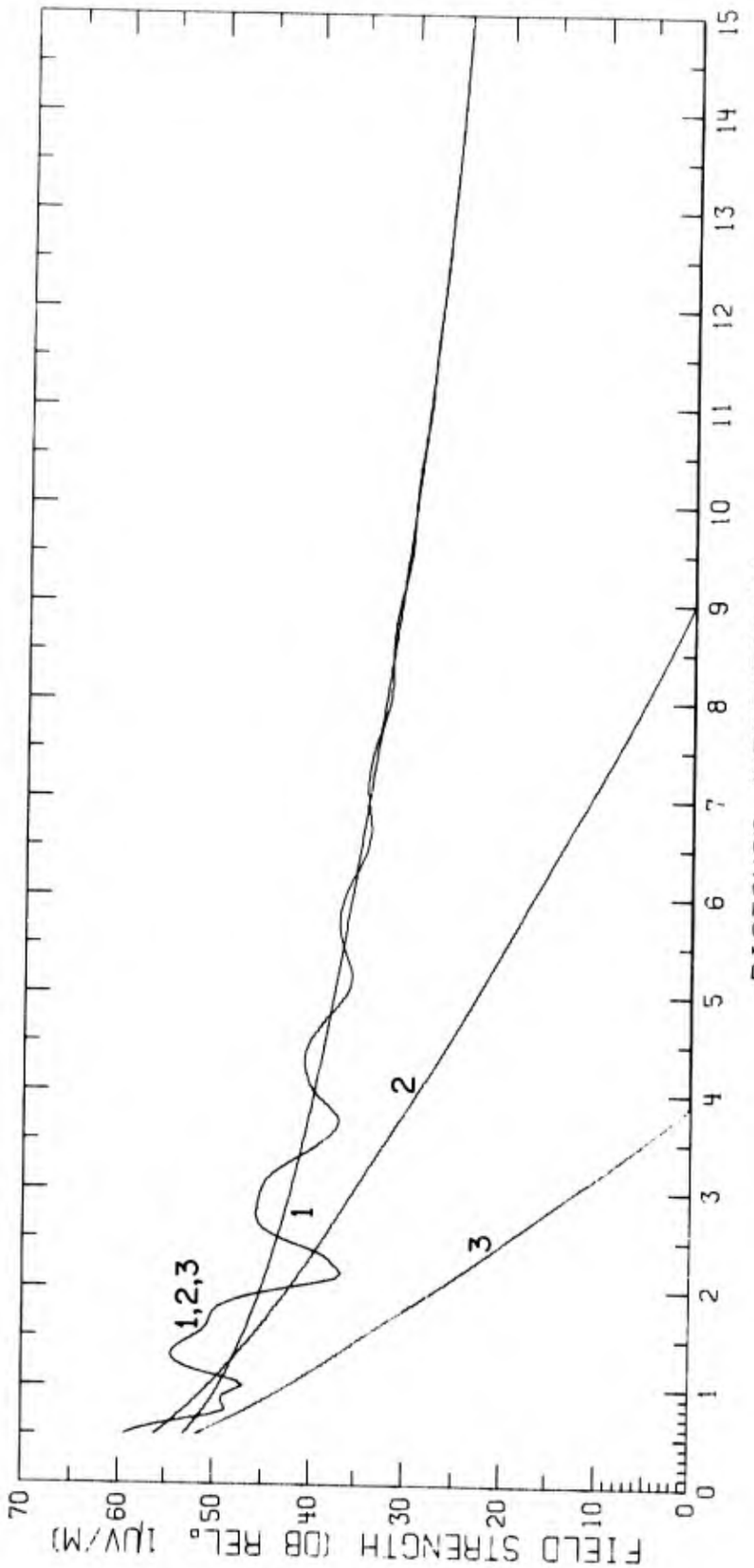

Fig. 12 - Predicted field strengths for f = 13.6 kc/s and h = 90 km

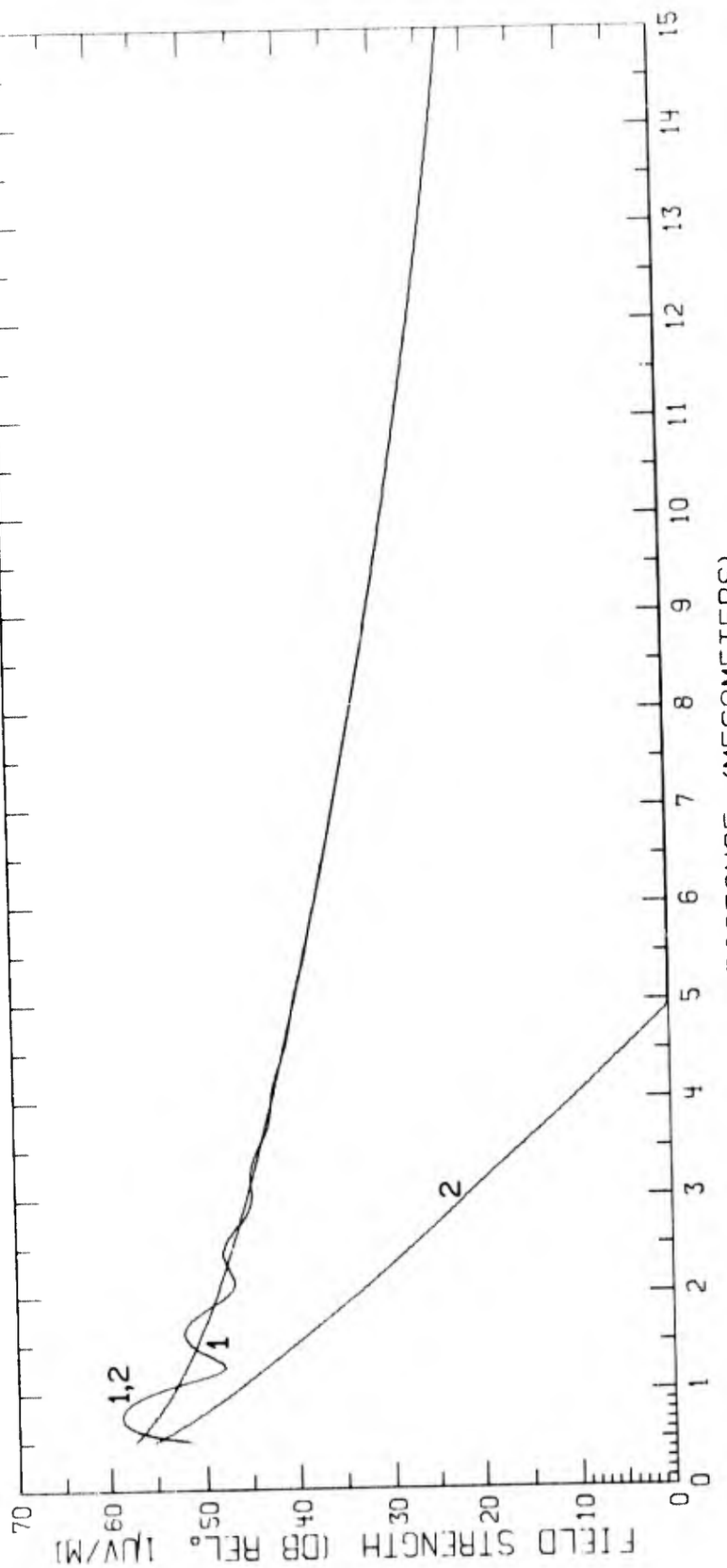

Fig. 13 - Predicted field strengths for f = 14.0 kc/s and h = 70 km

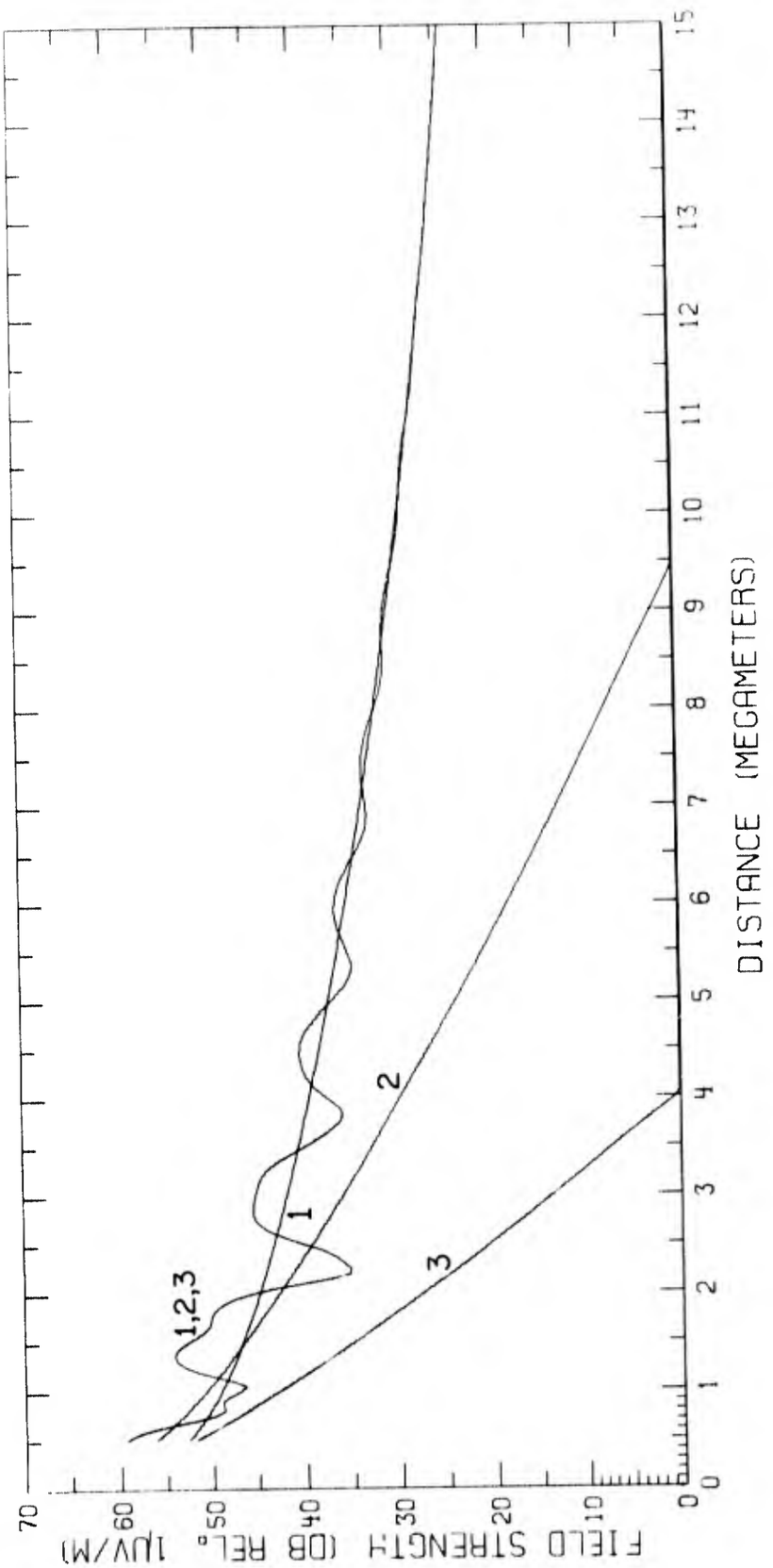

Fig. 14 - Predicted field strengths for f = 14.0 kc/s and h = 90 km

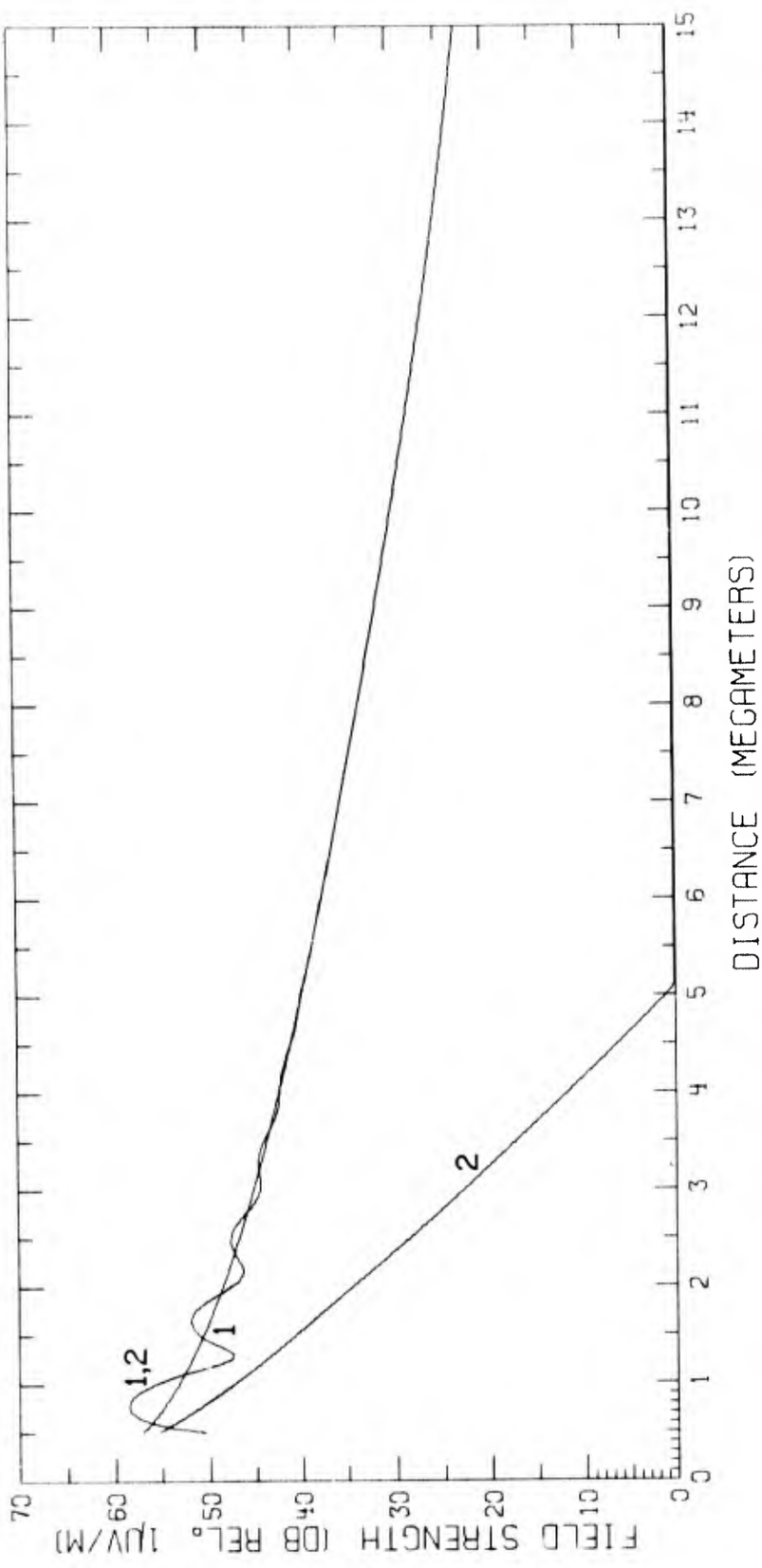

Fig. 15 - Predicted field strengths for f = 14.3 kc/s and h = 70 km

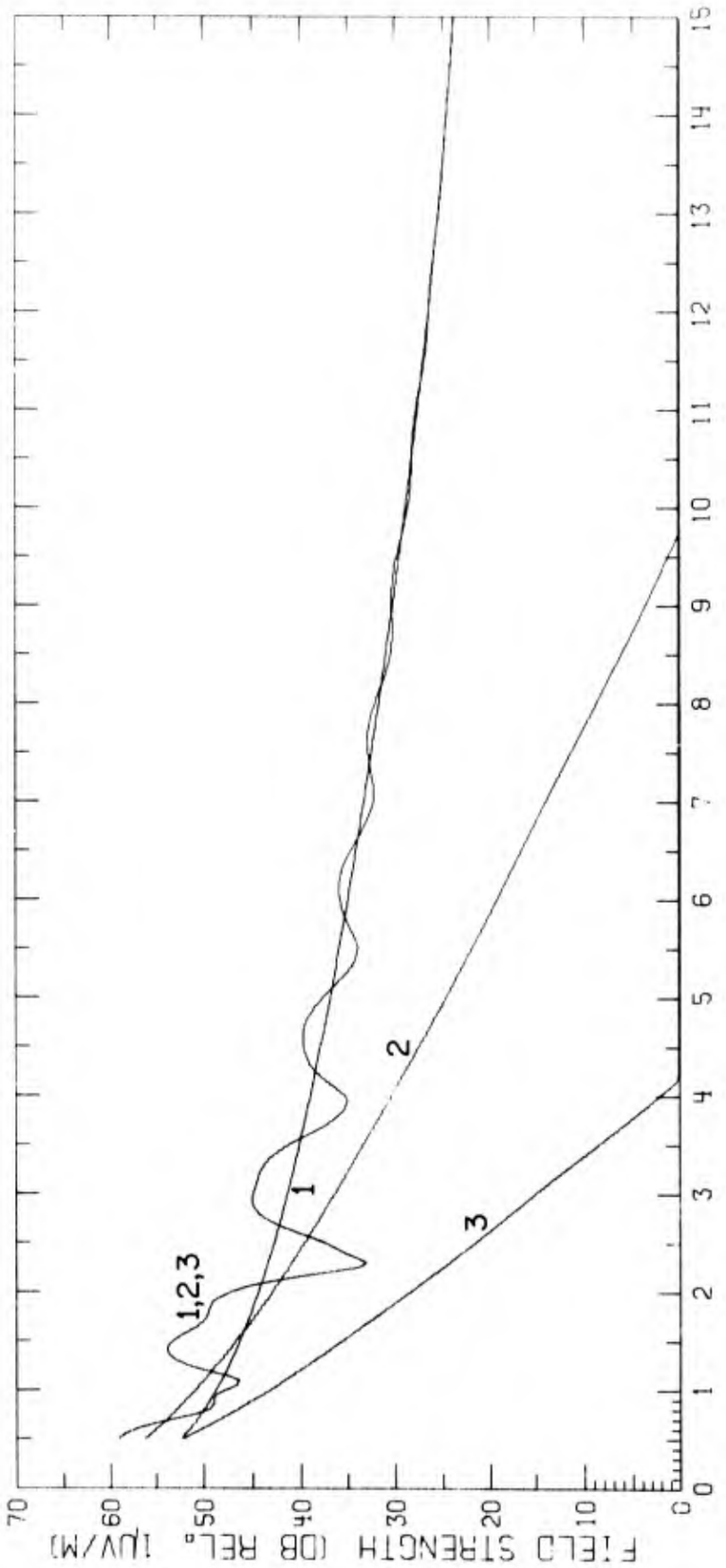

Fig. 16 - Predicted field strengths for f = 14.3 kc/s and h = 90 km

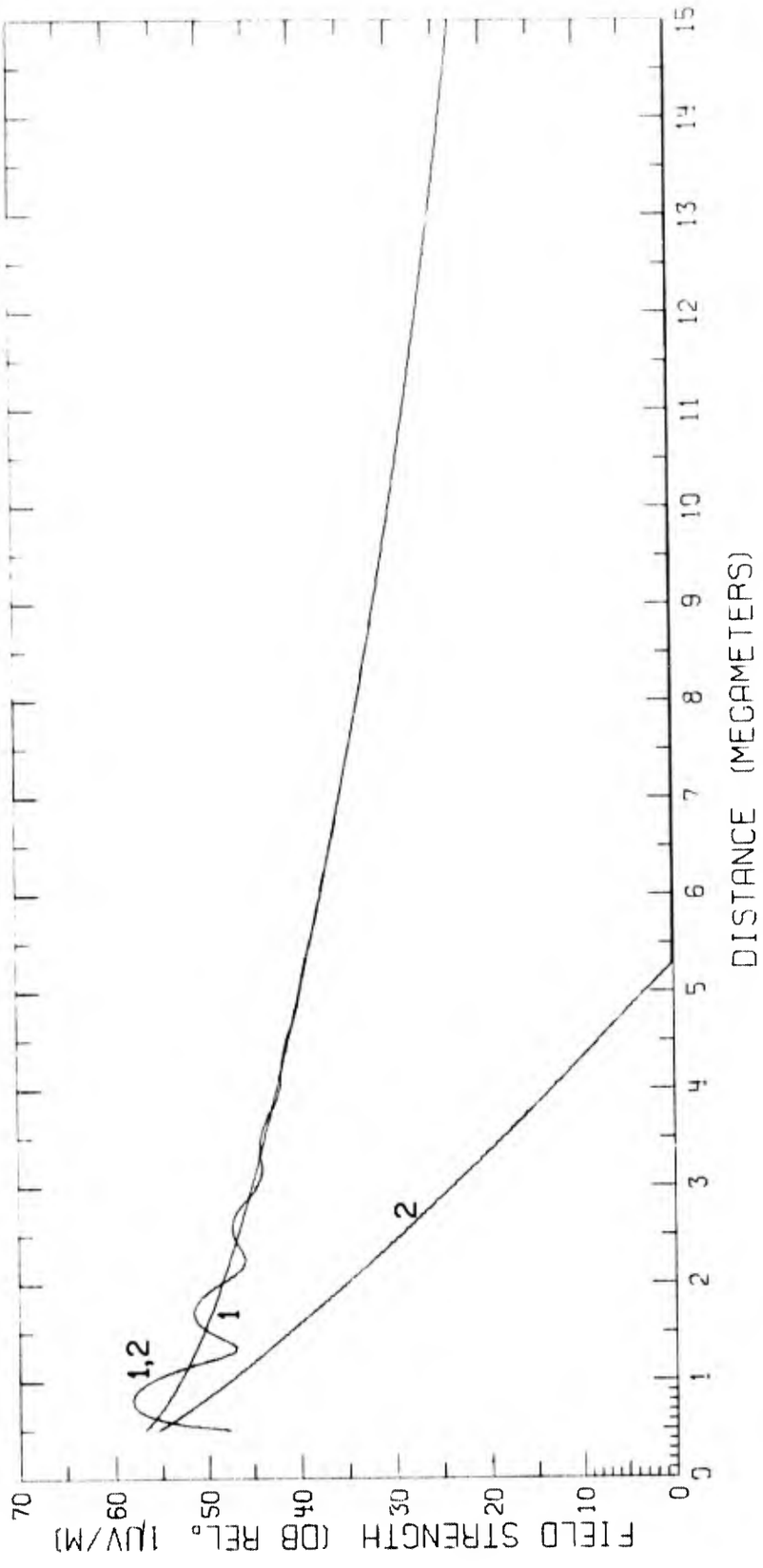

Fig. 17 - Predicted field strengths for f = 14.7 kc/s and h = 70 km

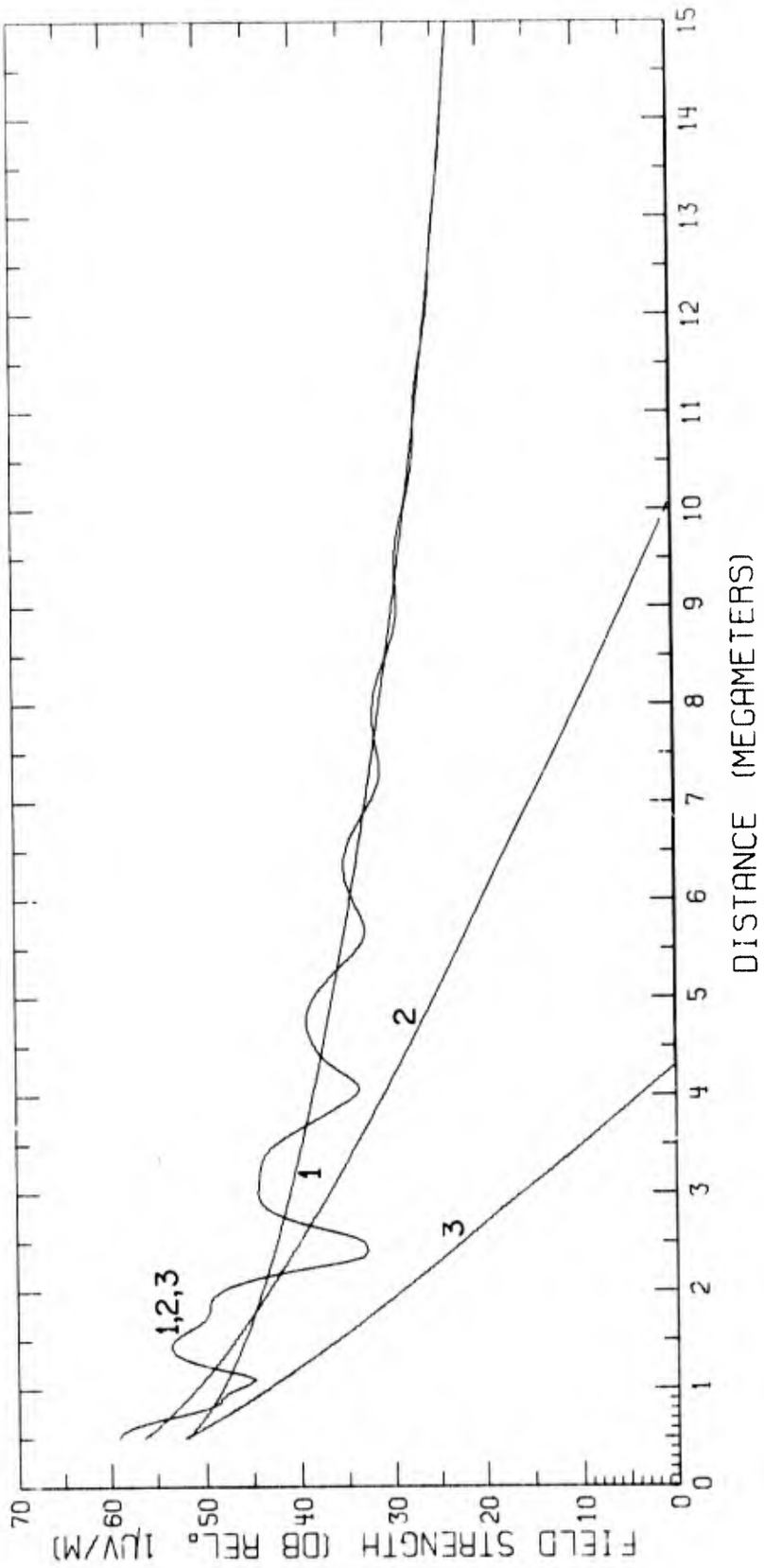

Fig. 18 - Predicted field strengths for $f \approx 14.7$ kc/s and $h = 90$ km

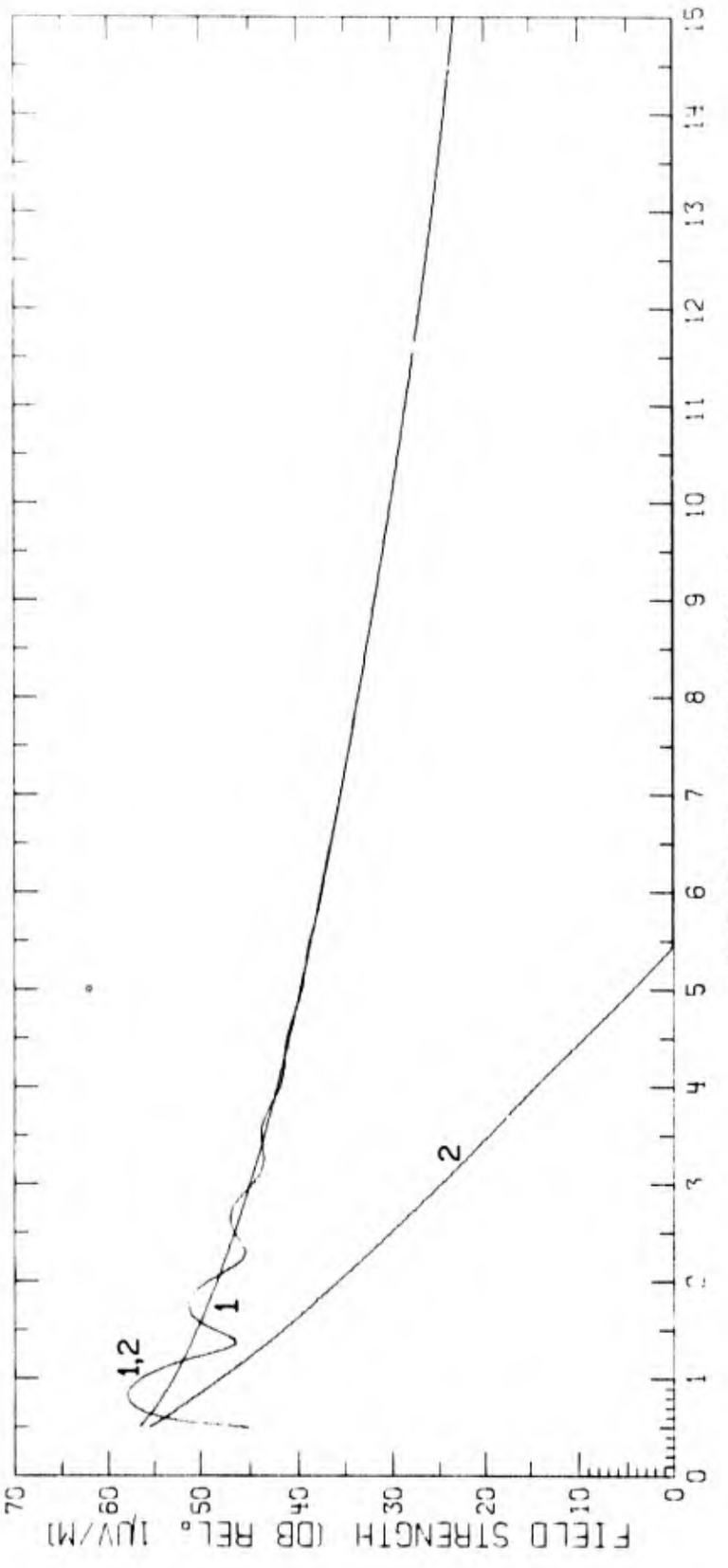

Fig. 19 - Predicted field strengths for f = 15.0 kc/s and h = 70 km

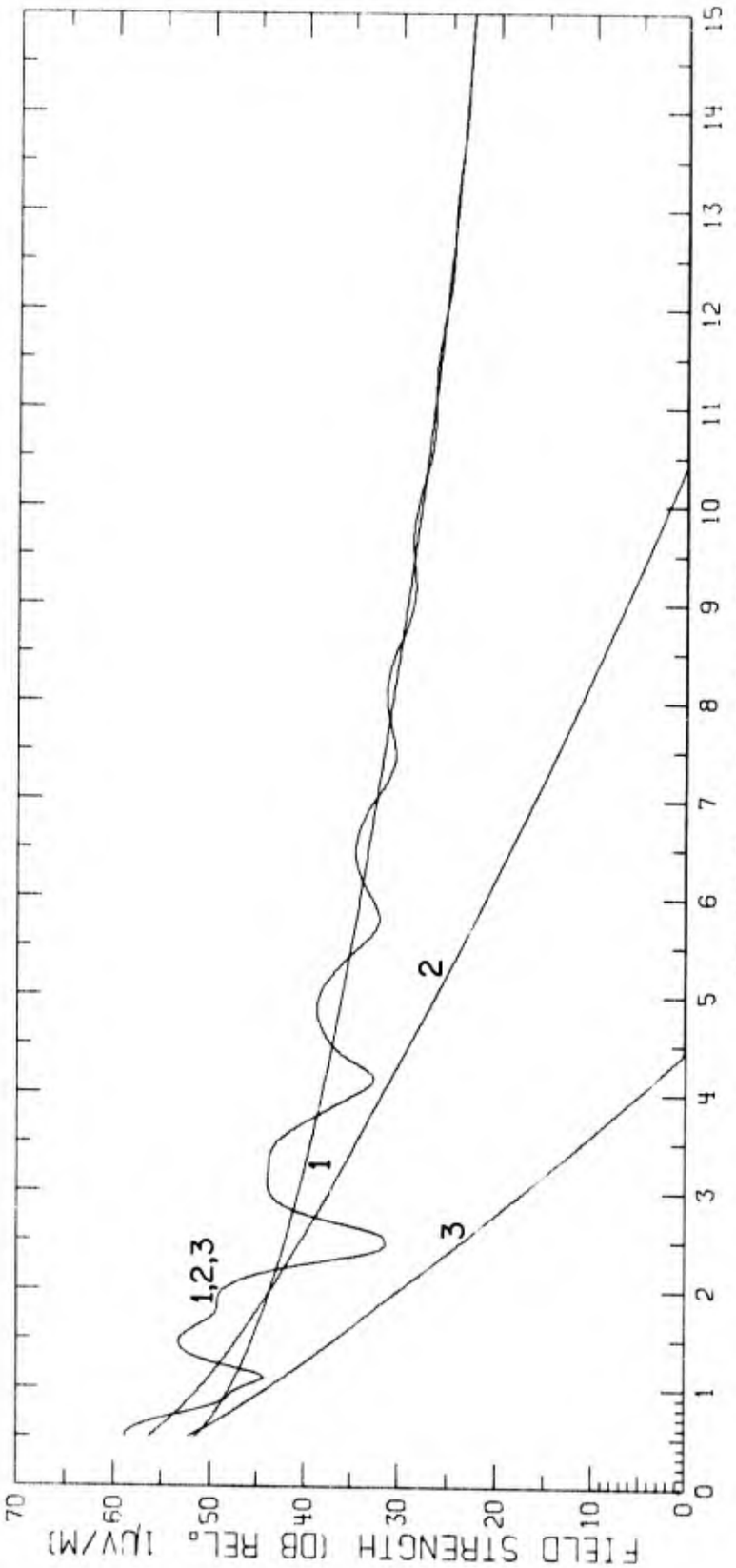

Fig. 20 - Predicted field strengths for f = 15.0 kc/s and h = 90 km

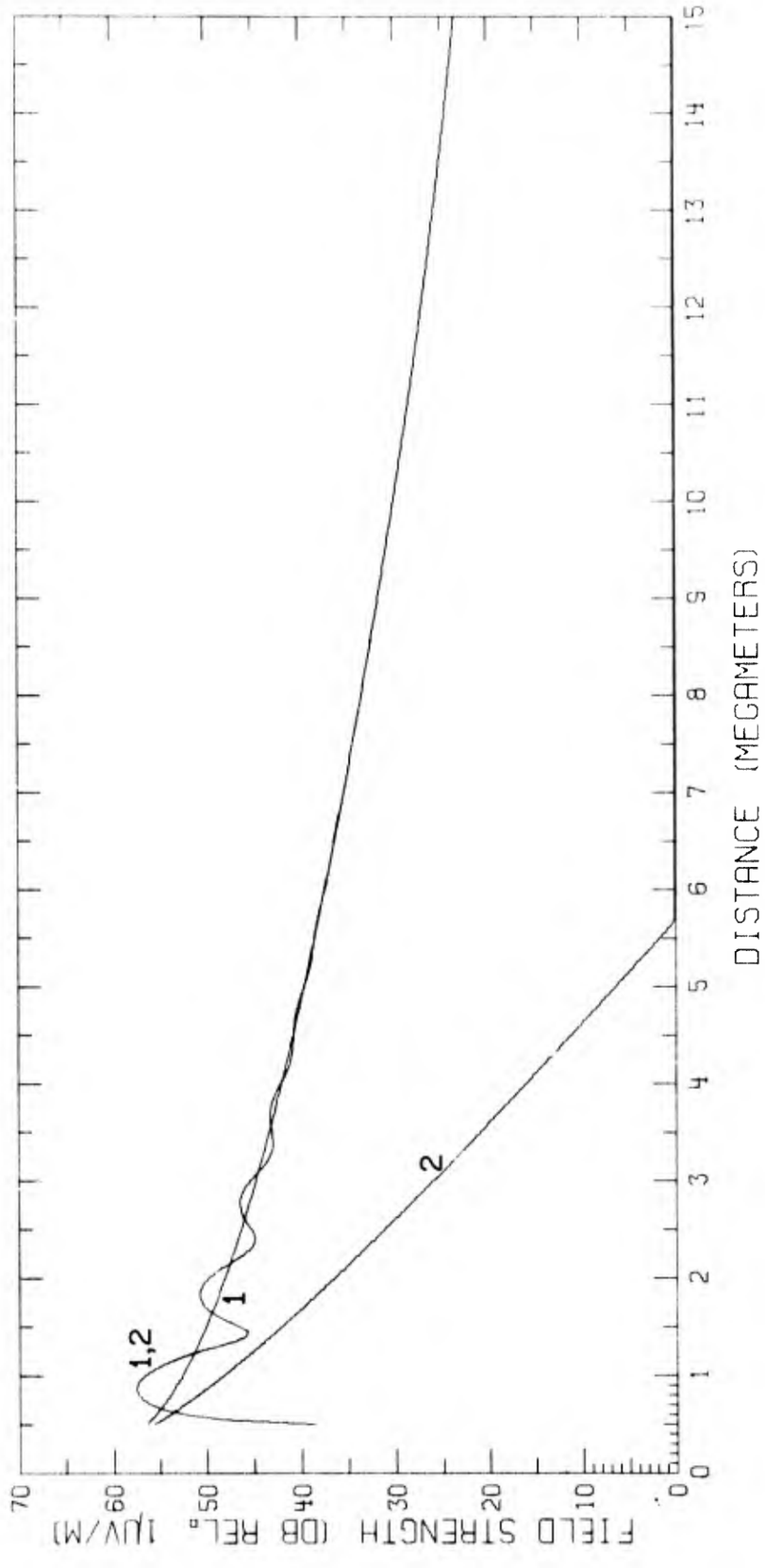

Fig. 21 - Predicted field strengths for f = 15.5 kc/s and h = 70 km

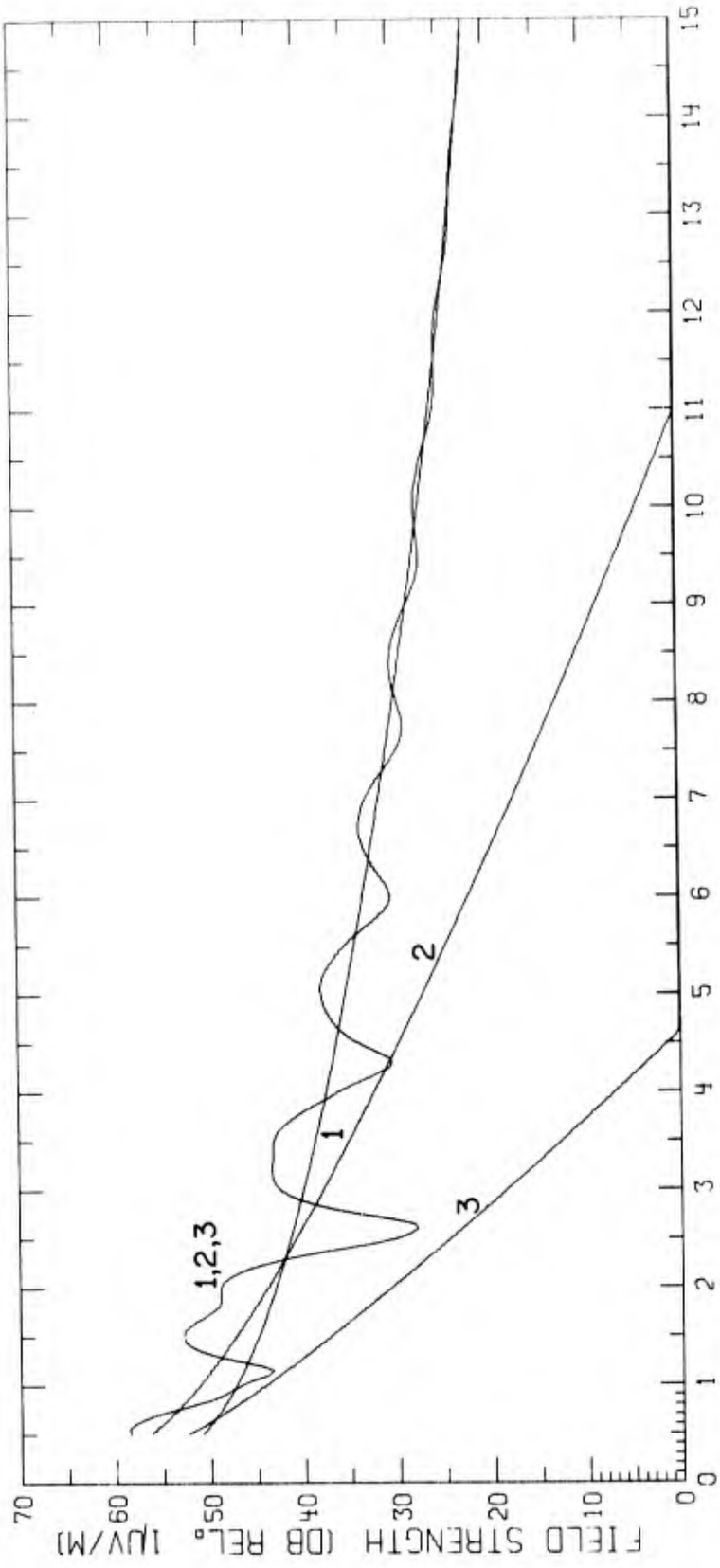

Fig. 22 - Predicted field strengths for f = 15.5 kc/s and h = 90 km

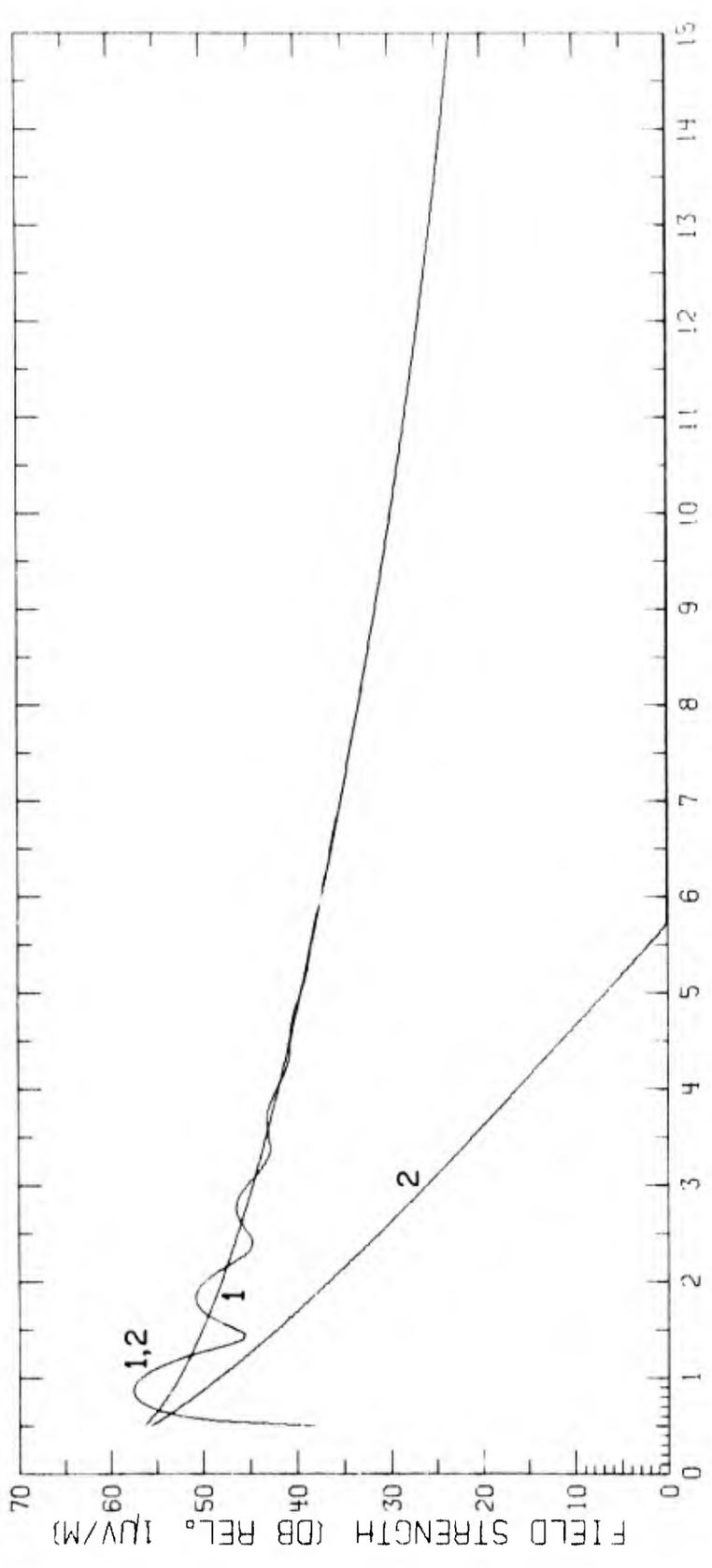

Fig. 23 - Predicted field strengths for f = 15.6 kc/s and h = 70 km

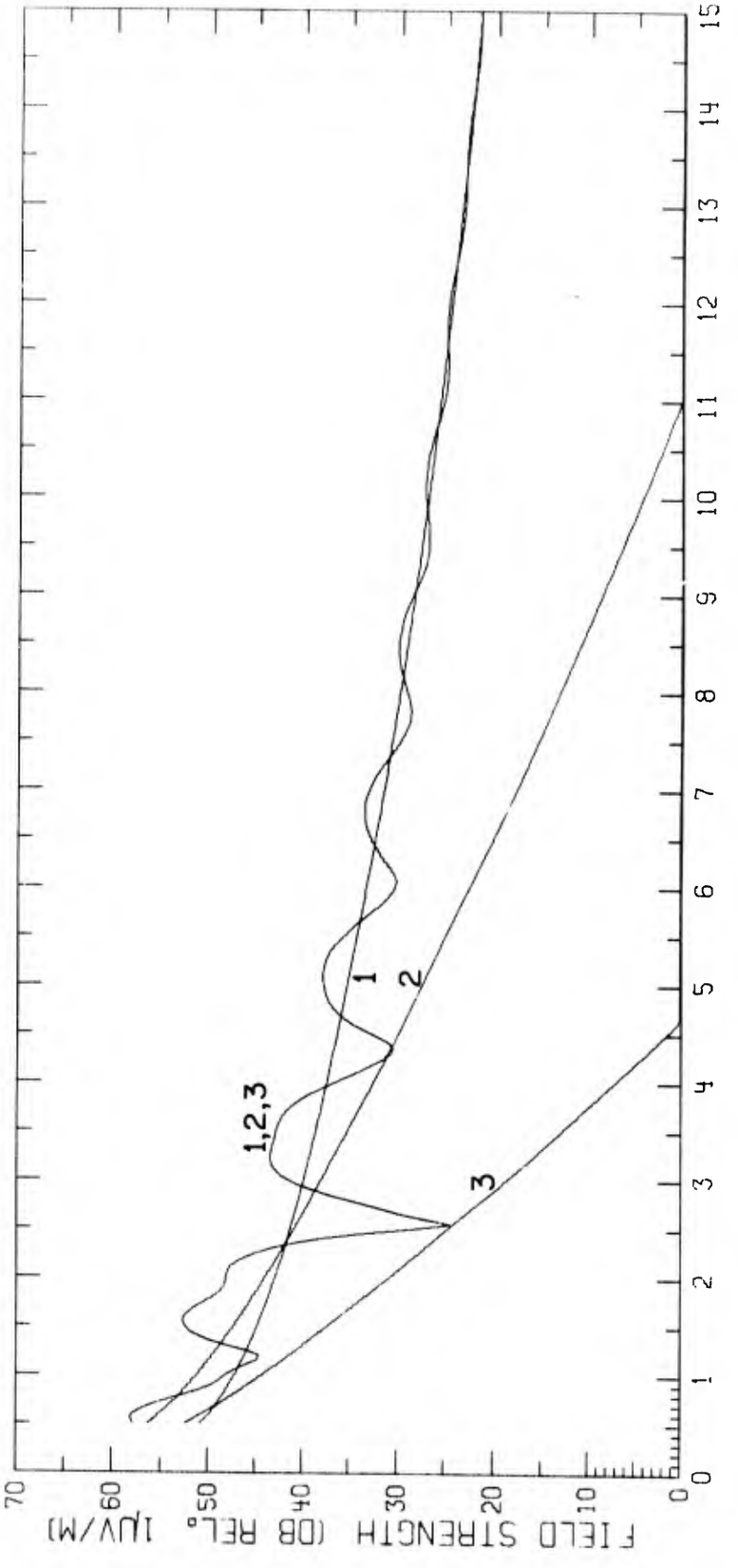

Fig. 24 - Predicted field strengths for f = 15.6 kc/s and h = 90 km

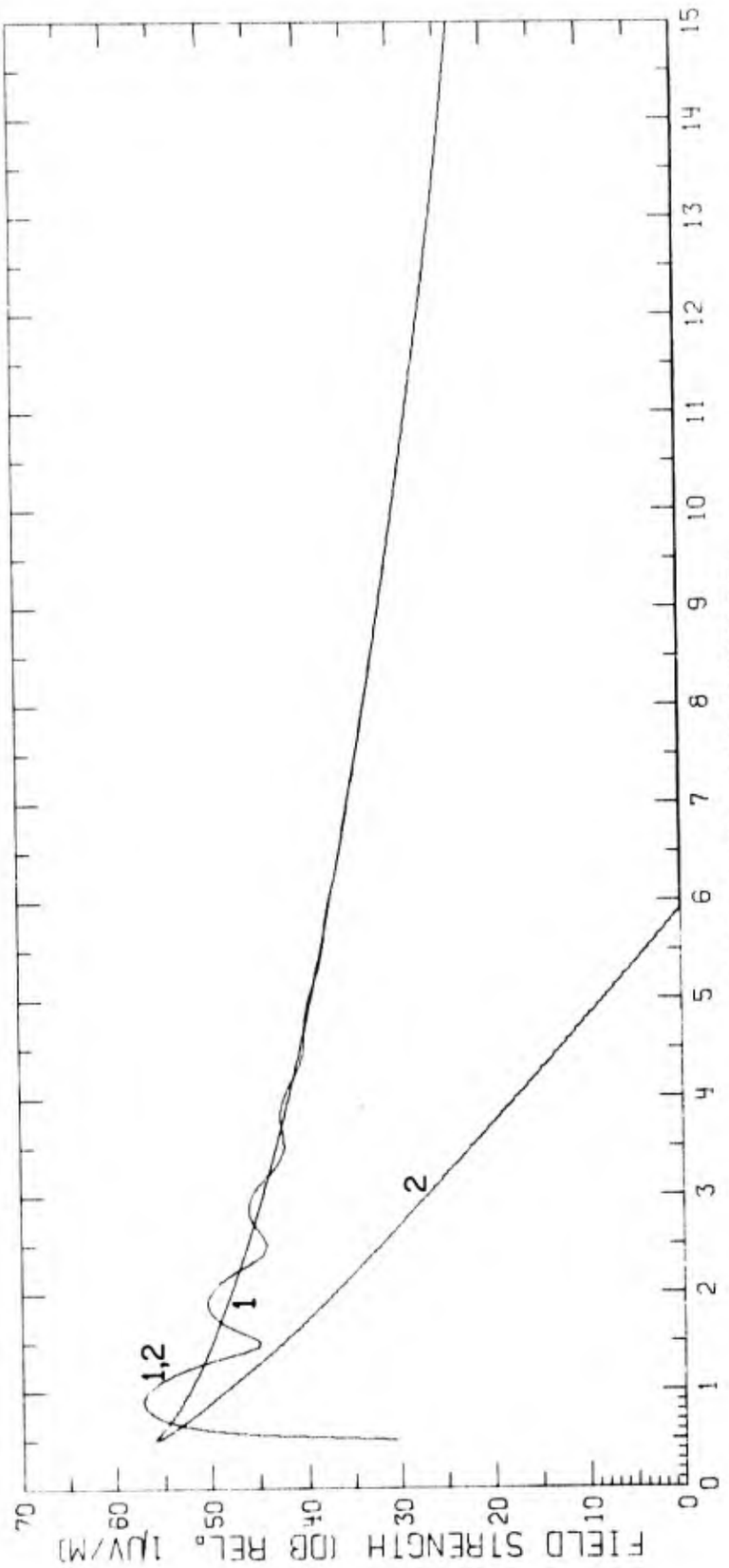

Fig. 25 - Predicted field strengths for f = 16.0 kc/s and h = 70 km

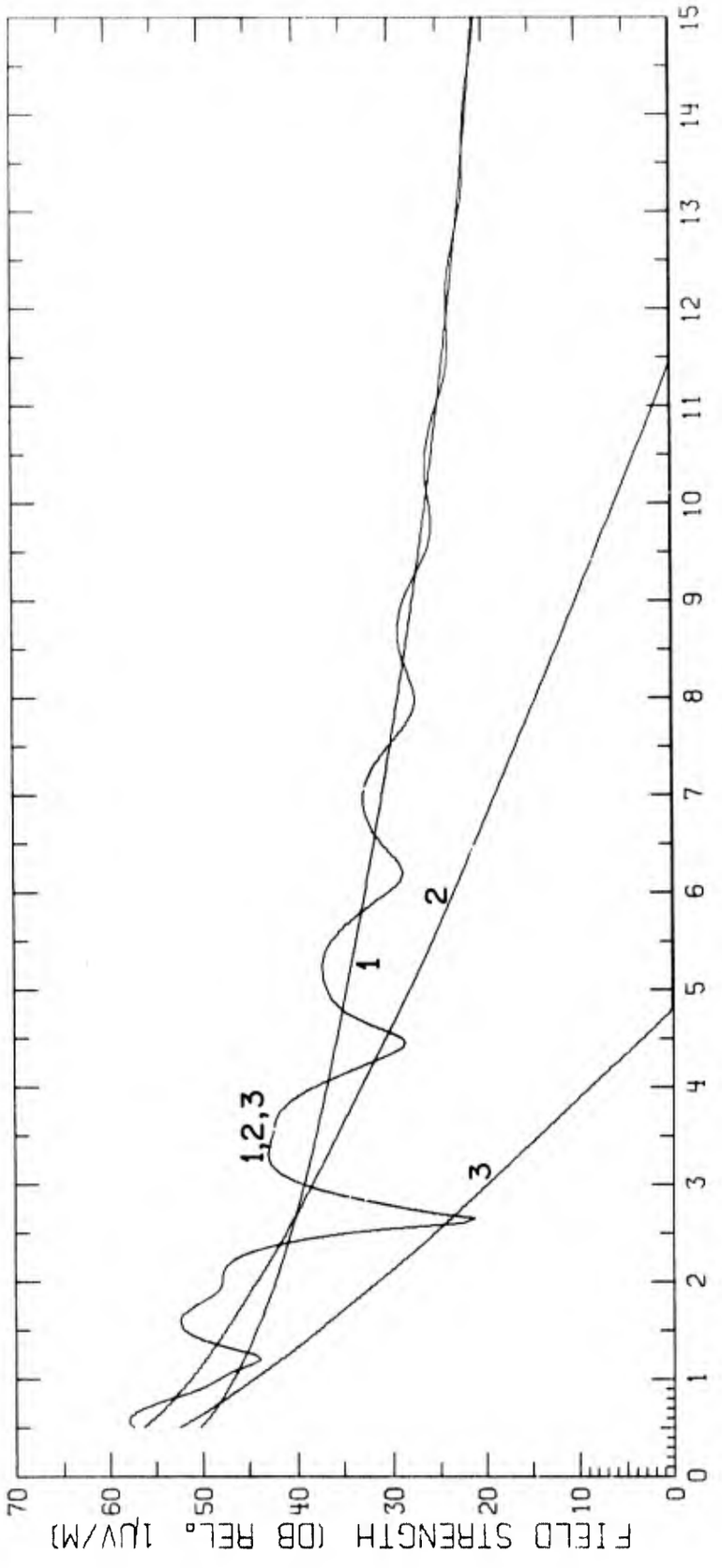

Fig. 26 - Predicted field strengths for f = 16.0 kc/s and h = 90 km

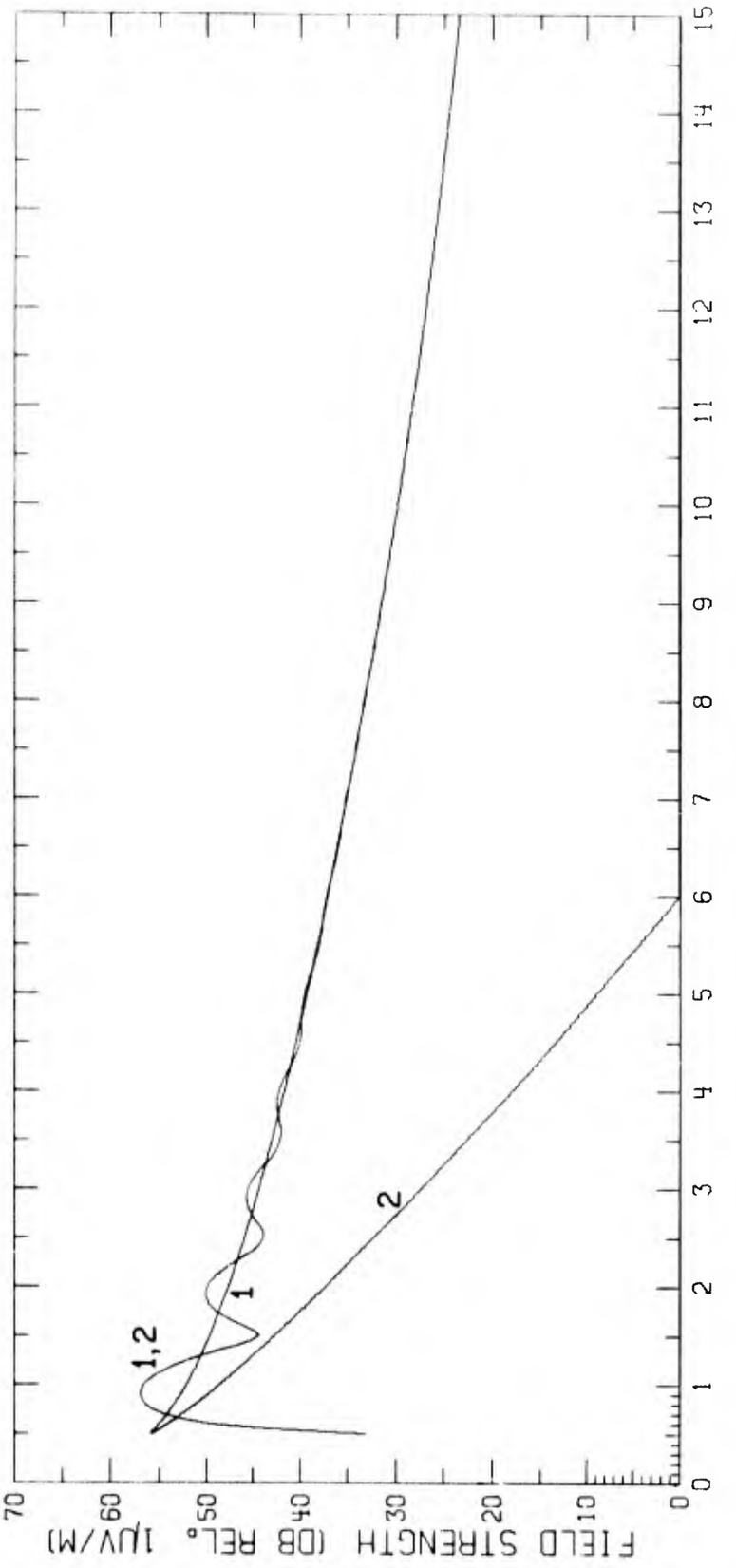

Fig. 27 - Predicted field strengths for f = 16.2 kc/s and h = 70 km

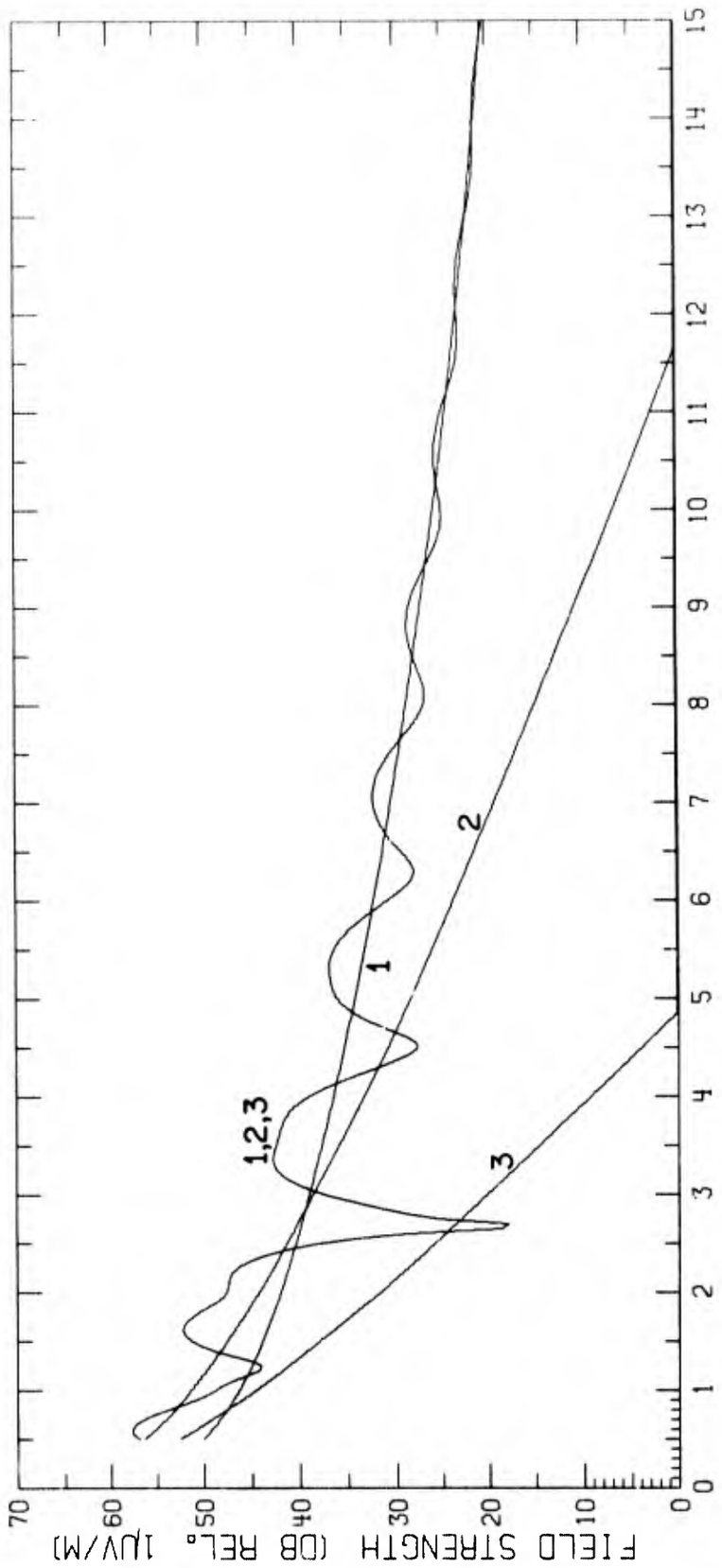

Fig. 28 - Predicted field strengths for f = 16.2 kc/s and h = 90 km

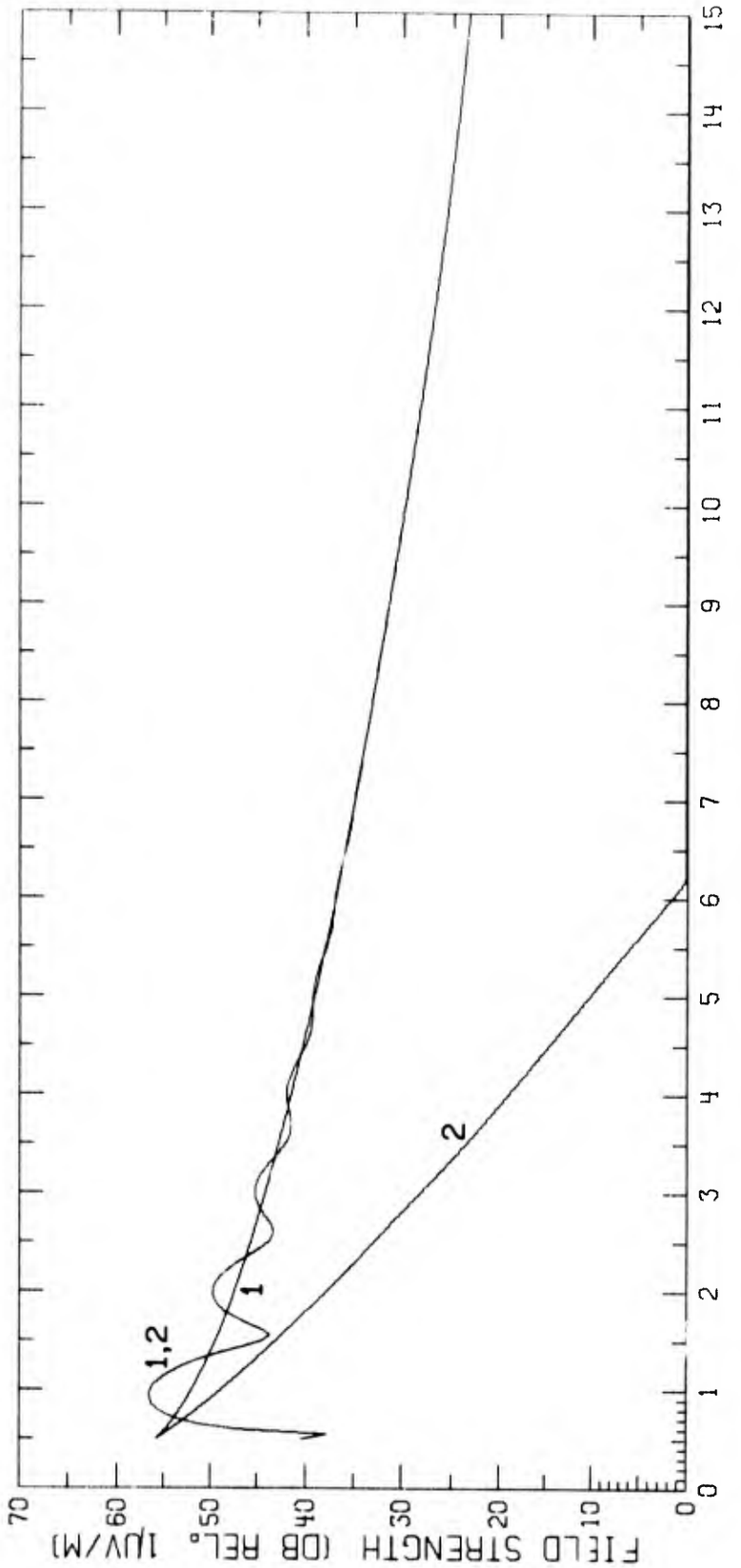

Fig. 29 - Predicted field strengths for f = 16.6 kc/s and h = 70 km

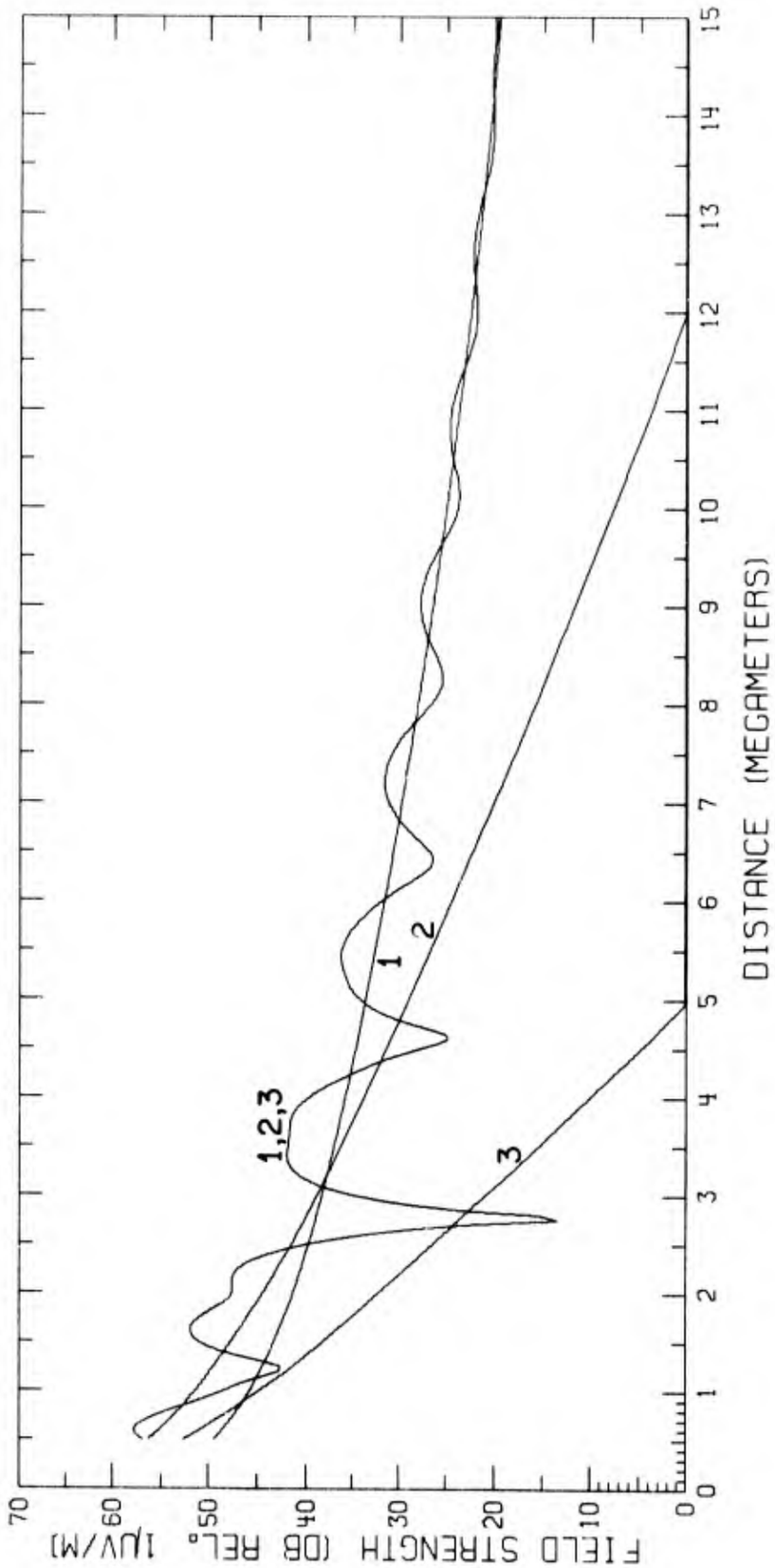

Fig. 30 - Predicted field strengths for f = 16.6 kc/s and h = 90 km

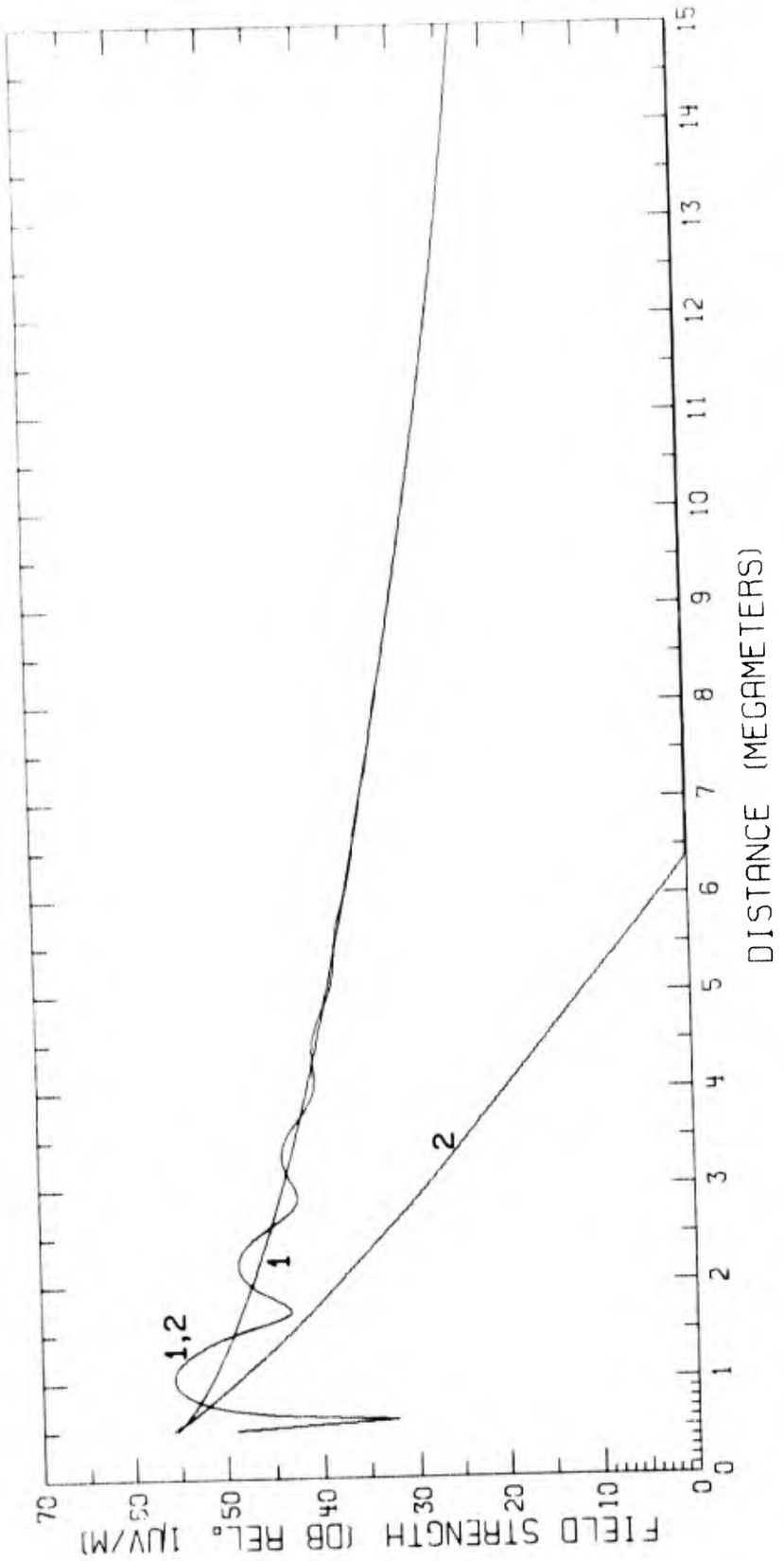

Fig. 31 - Predicted field strengths for f = 17.1 kc/s and h = 70 km

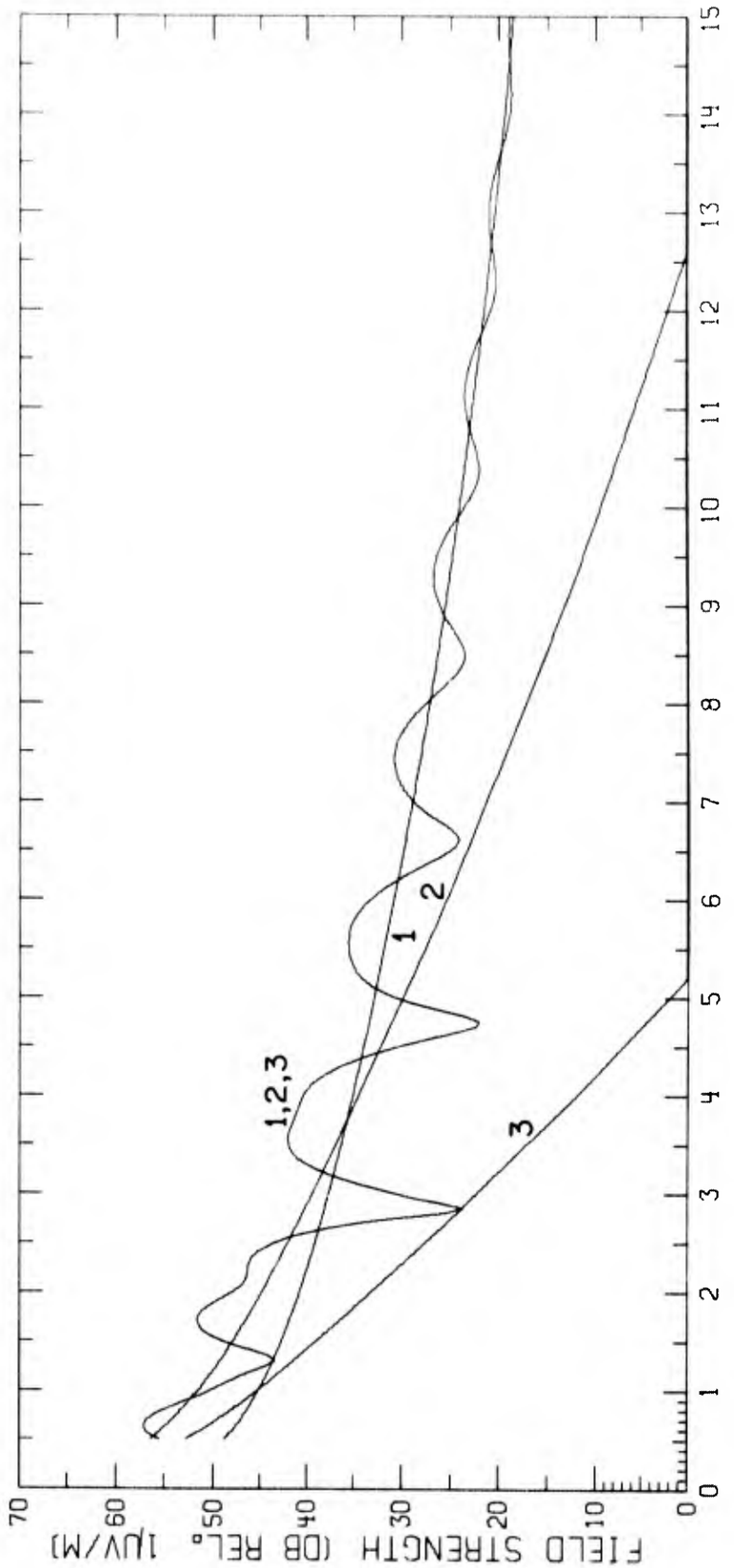

Fig. 32 - Predicted field strengths for f = 17.1 kc/s and h' = 90 km

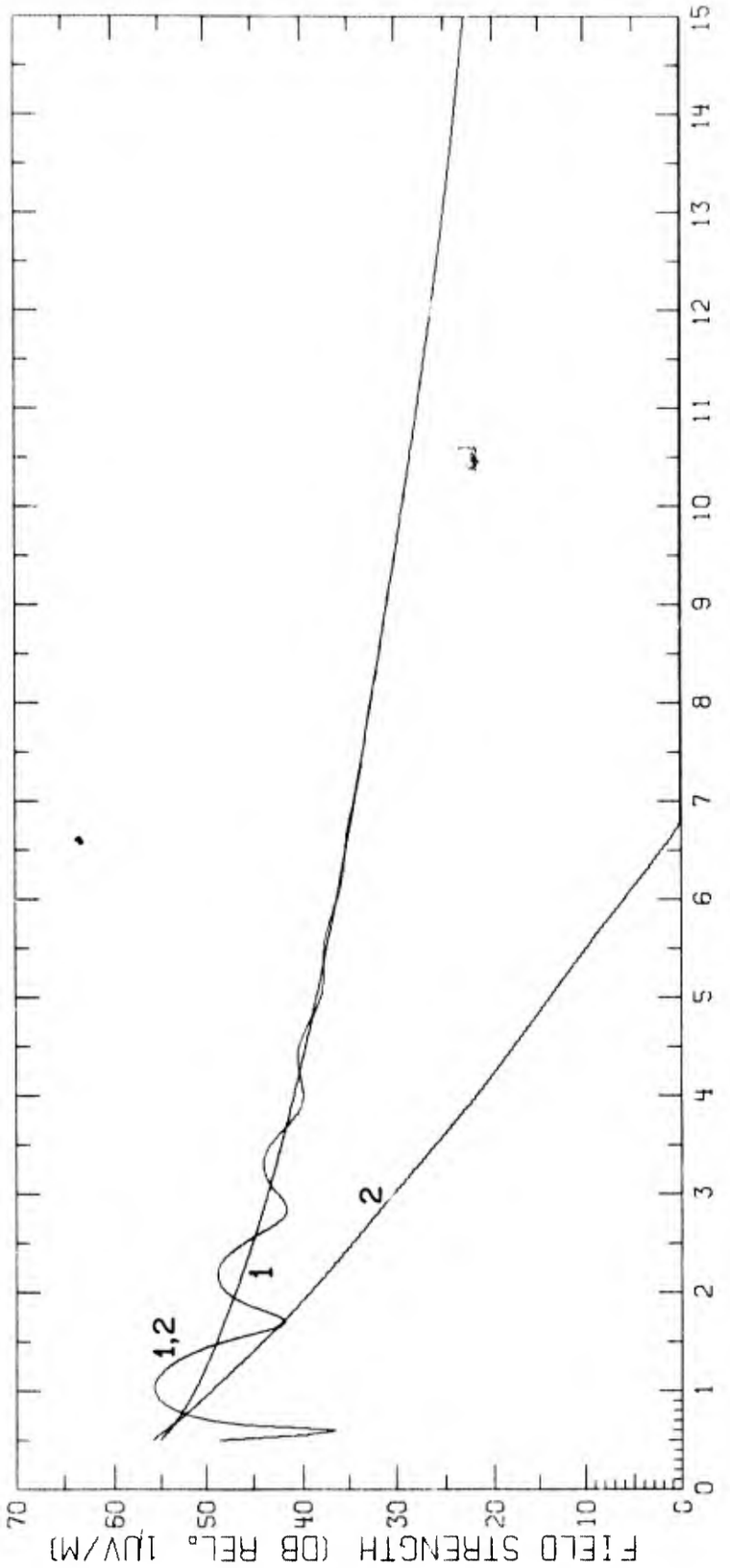

Fig. 33 - Predicted field strengths for f = 17.8 kc/s and h = 70 km

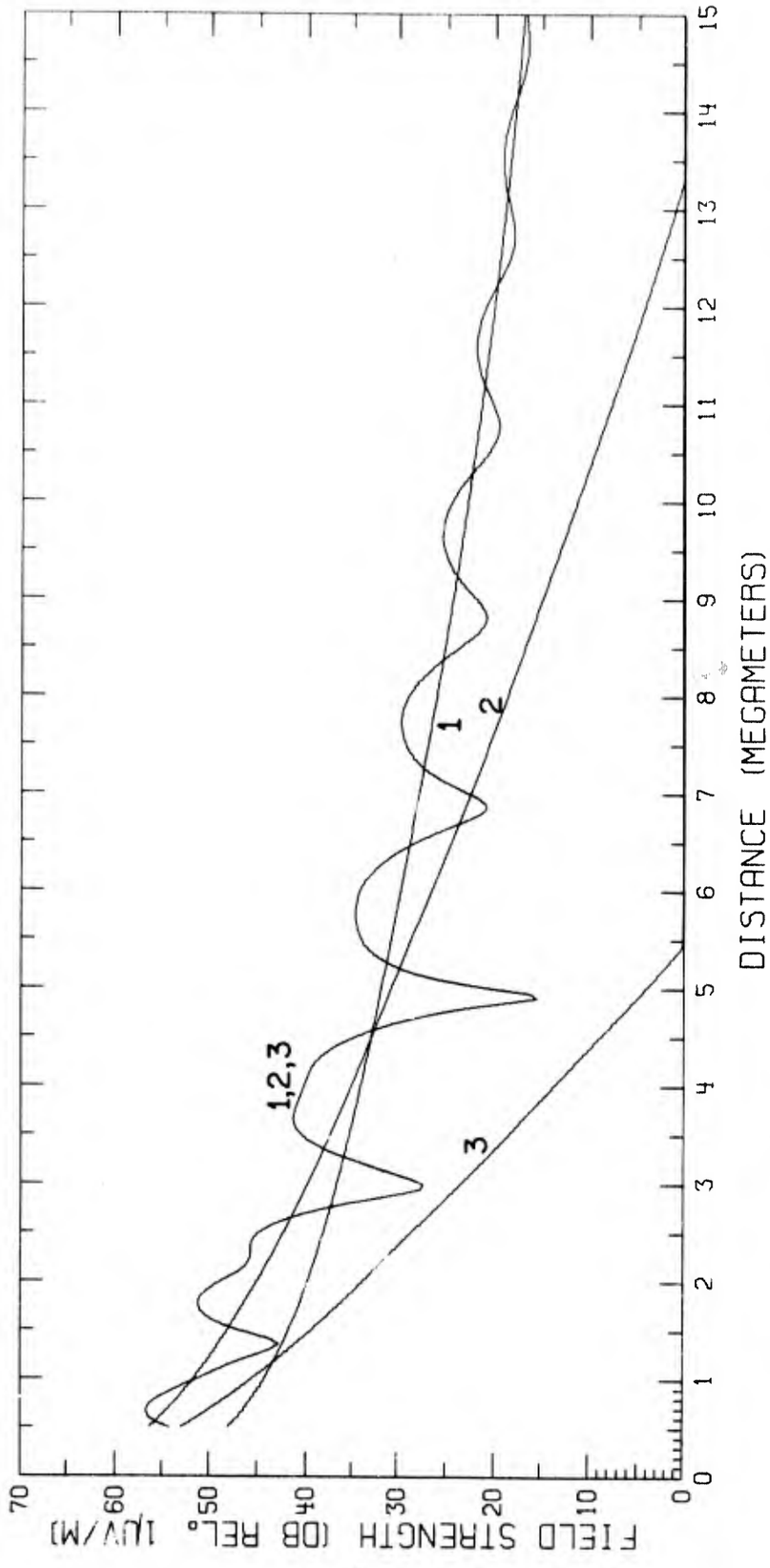

Fig. 34 - Predicted field strengths for f = 17.8 kc/s and h = 90 km

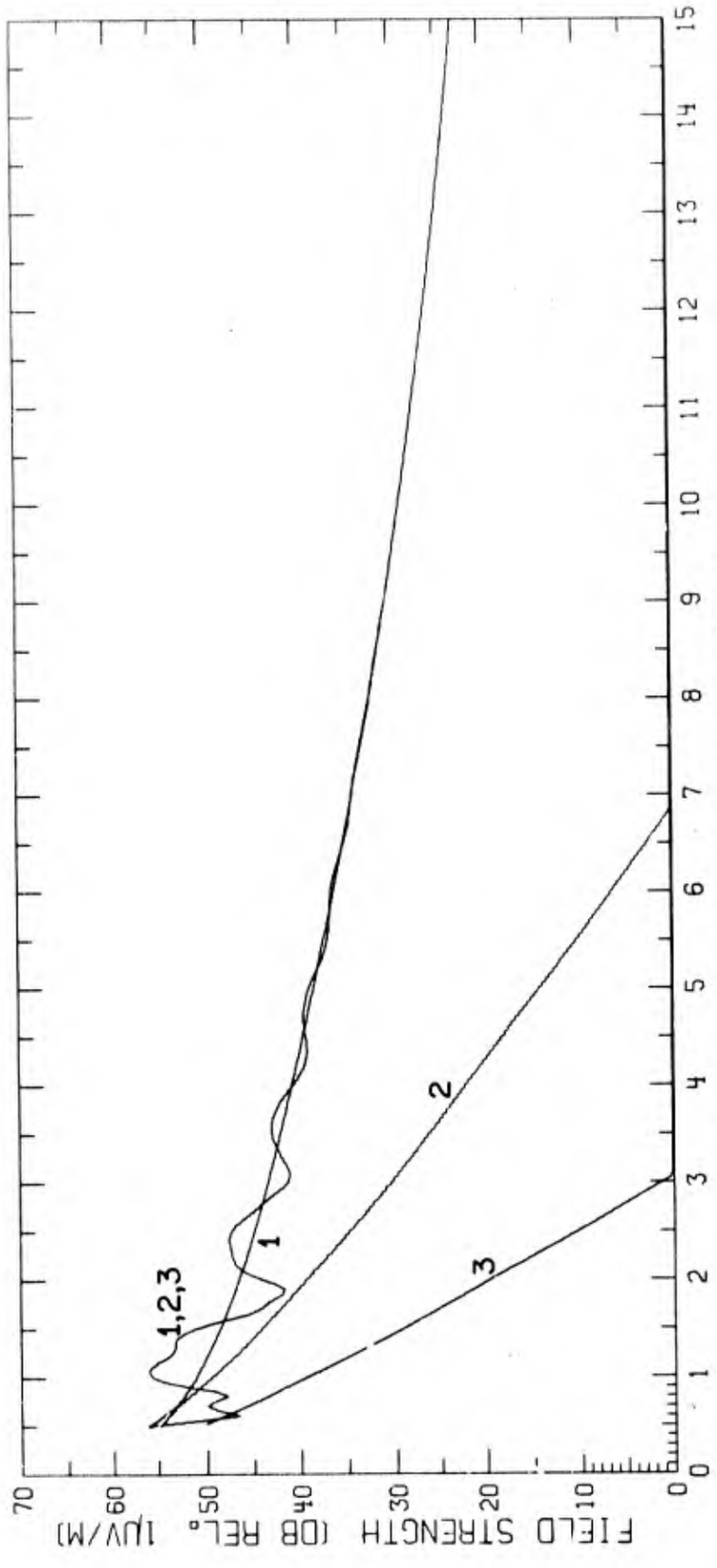

Fig. 35 - Predicted field strengths for f = 18.0 kc/s and h = 70 km

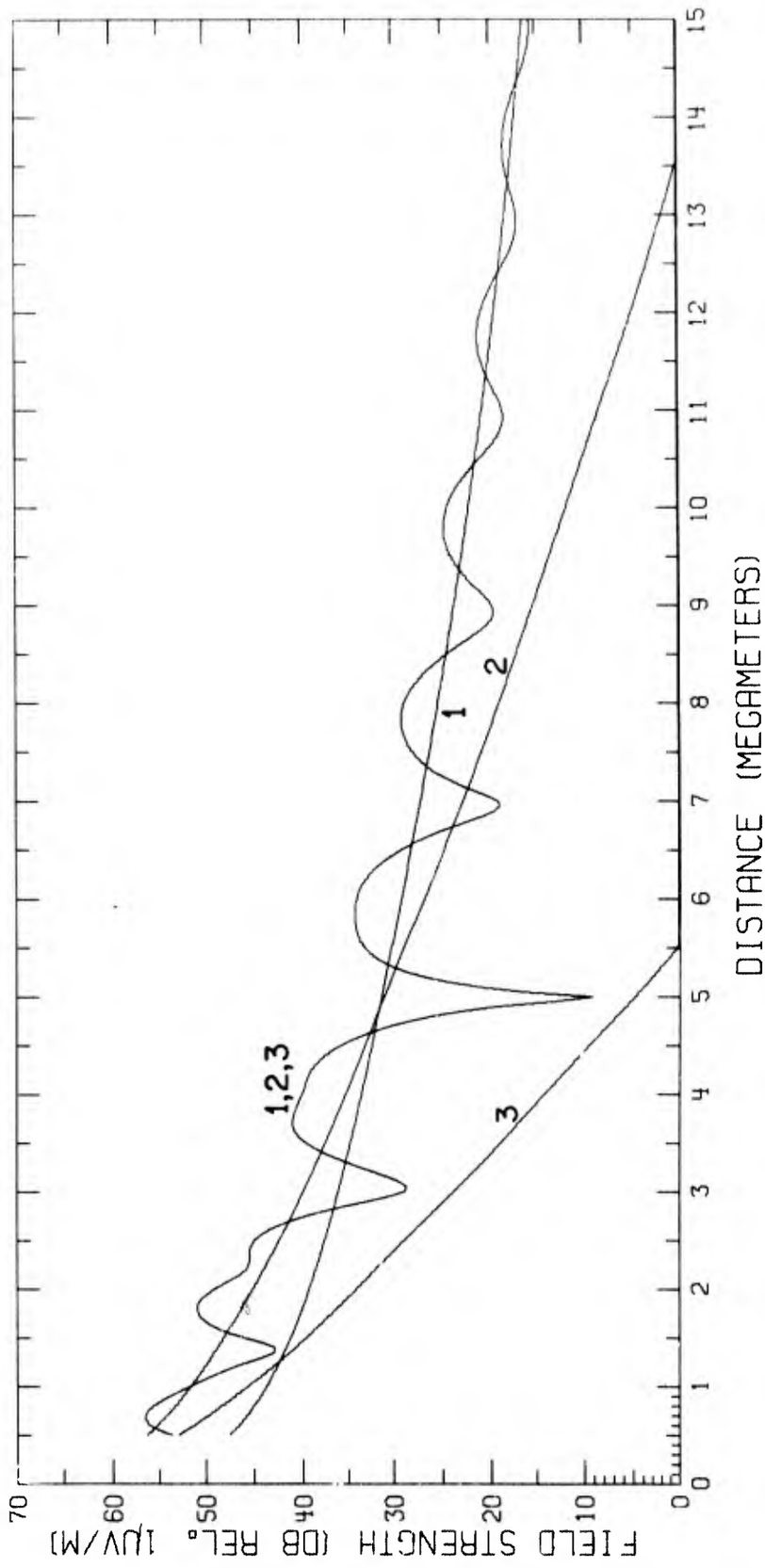

Fig. 36 - Predicted field strengths for f = 18.0 kc/s and h = 90 km

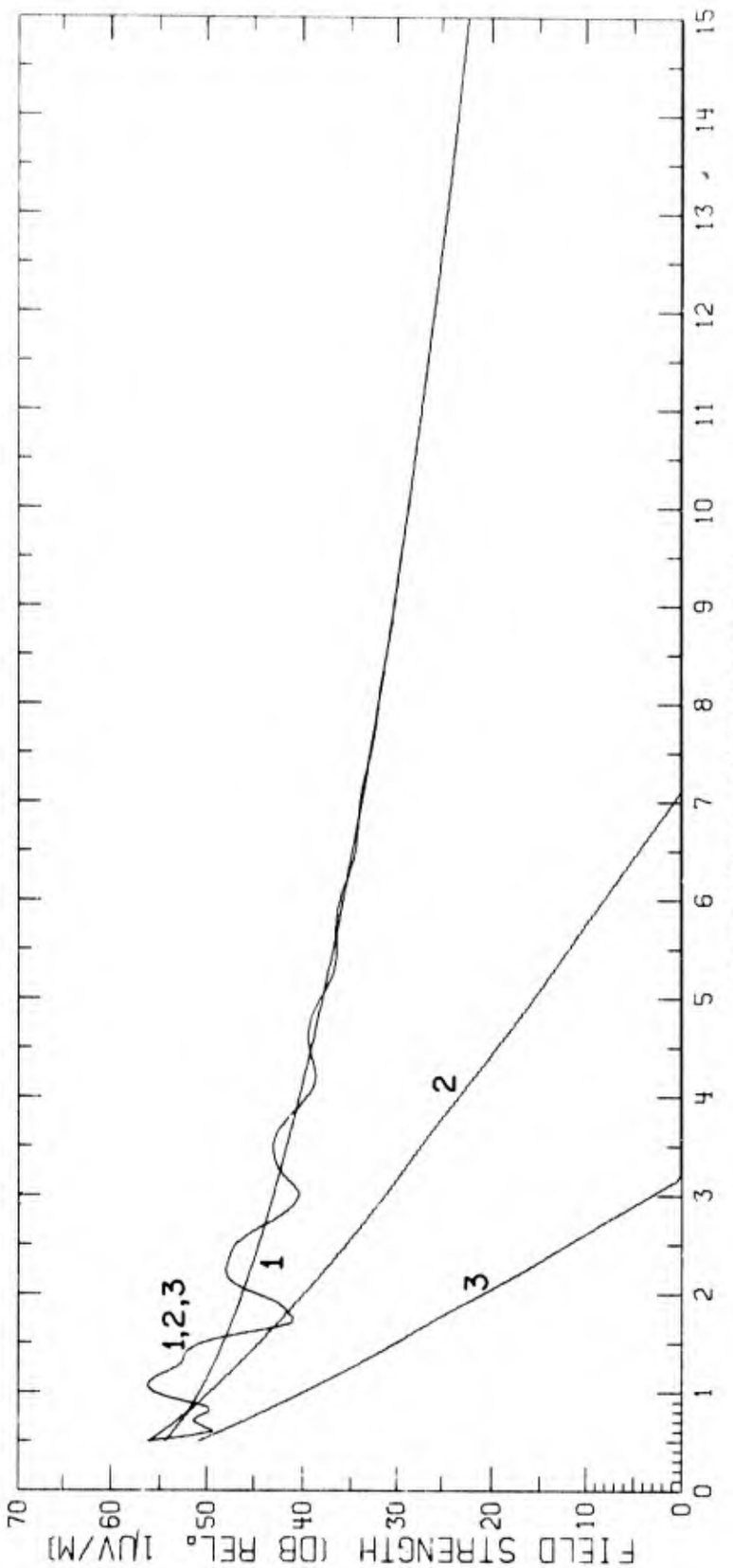

Fig. 37 - Predicted field strengths for f = 18.6 kc/s and h = 70 km

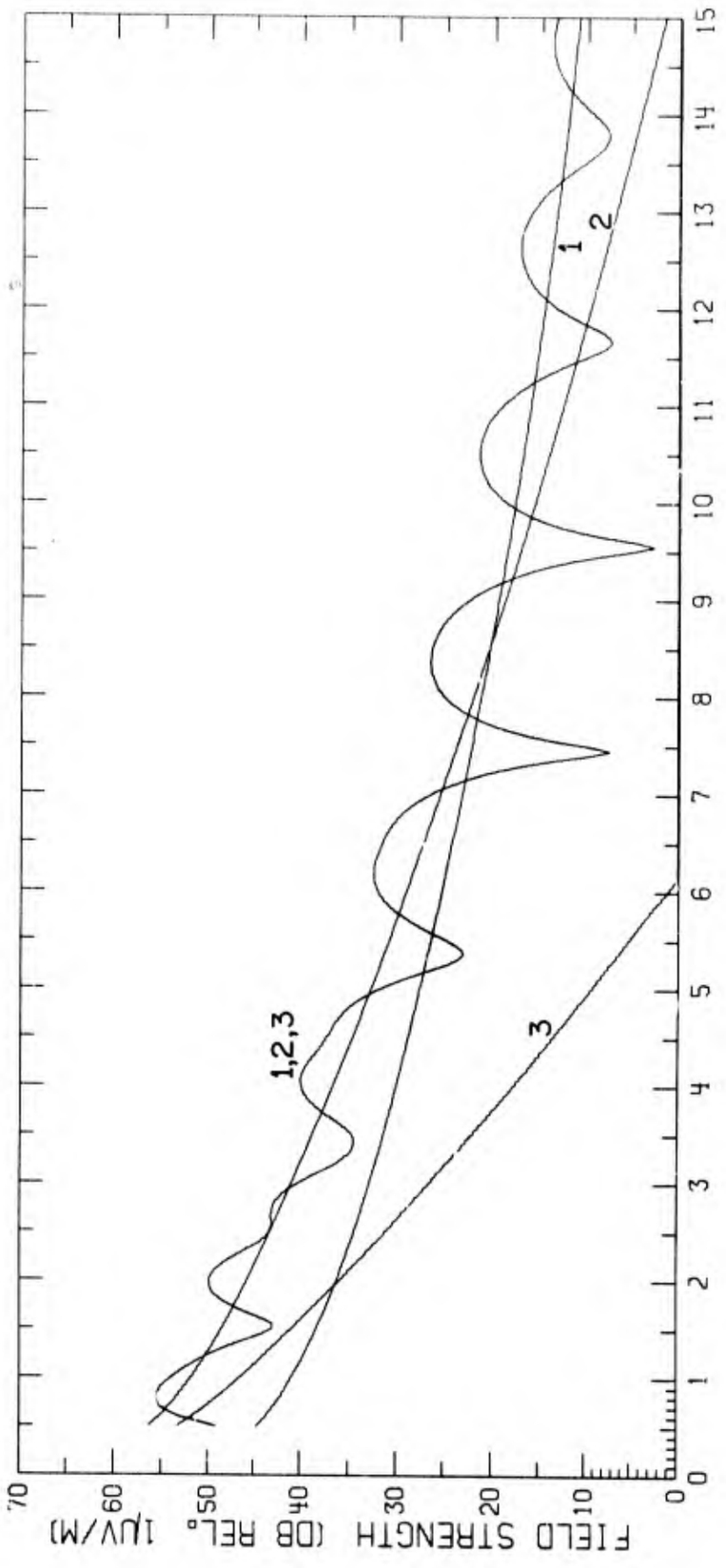

Fig. 38 - Predicted field strengths for f = 18.6 kc/s and h = 90 km

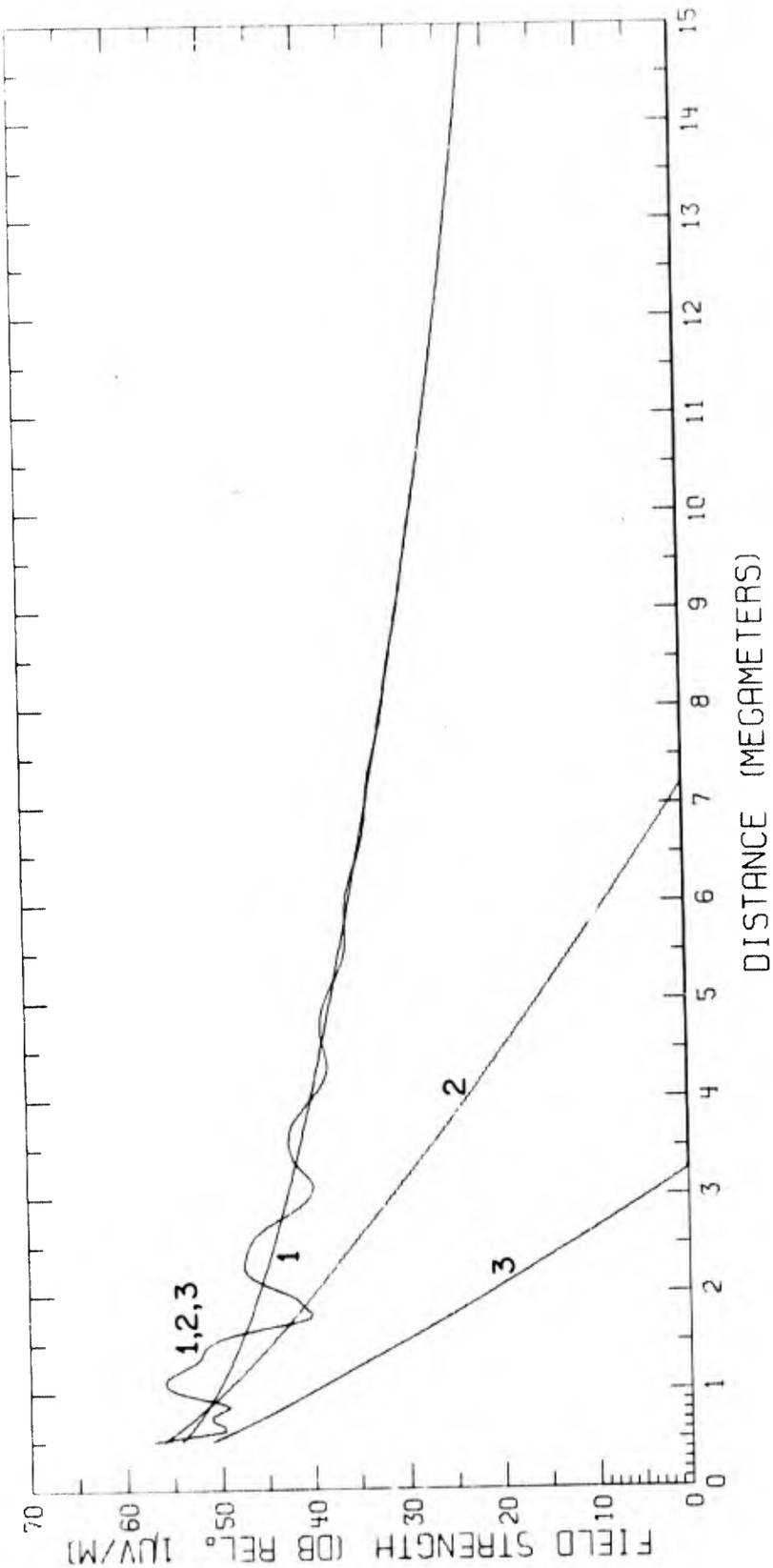

Fig. 39 - Predicted field strengths for f = 19.0 kc/s and h = 70 km

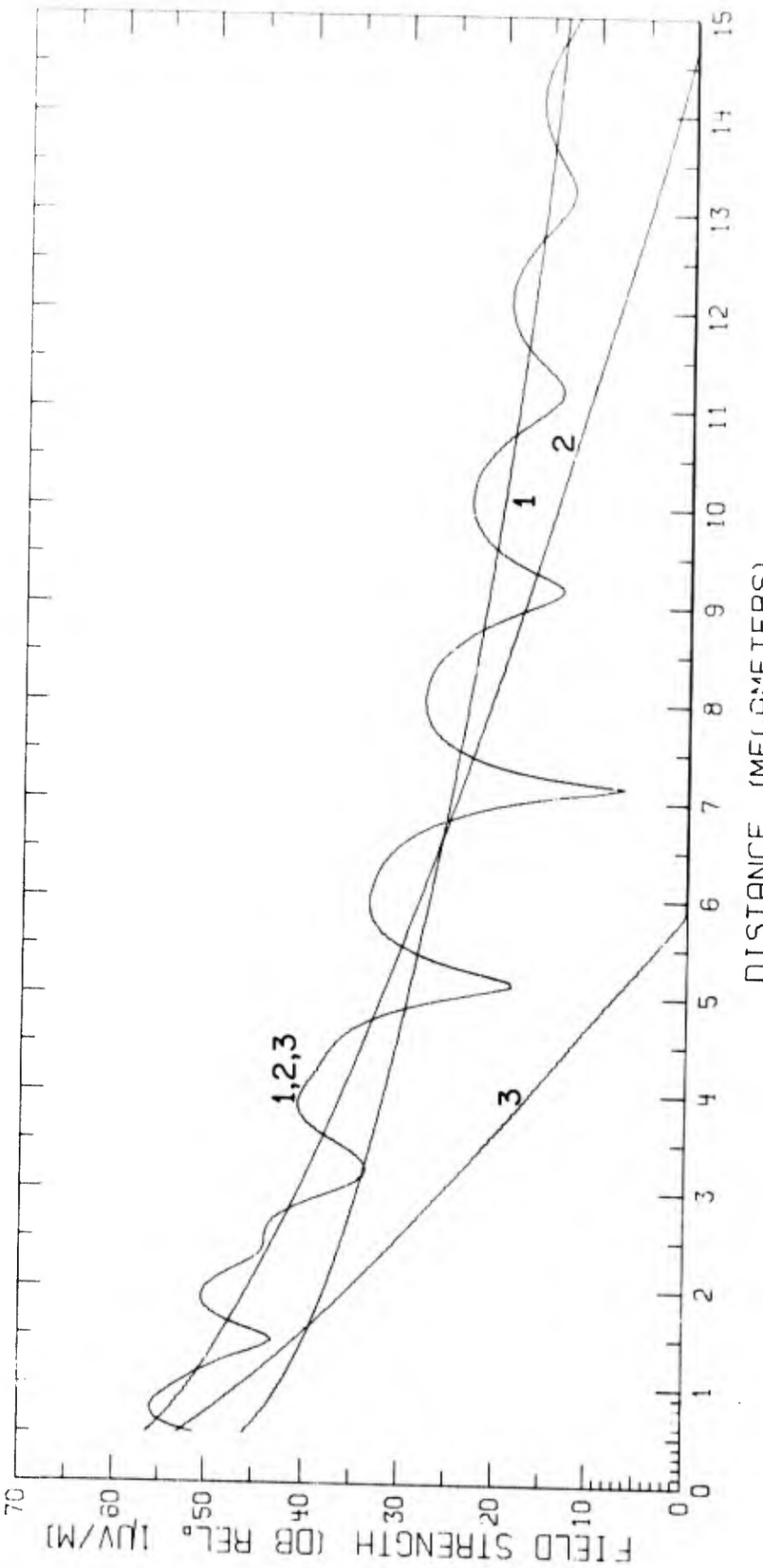

Fig. 40 - Predicted field strengths for f = 19.0 kc/s and h = 90 km

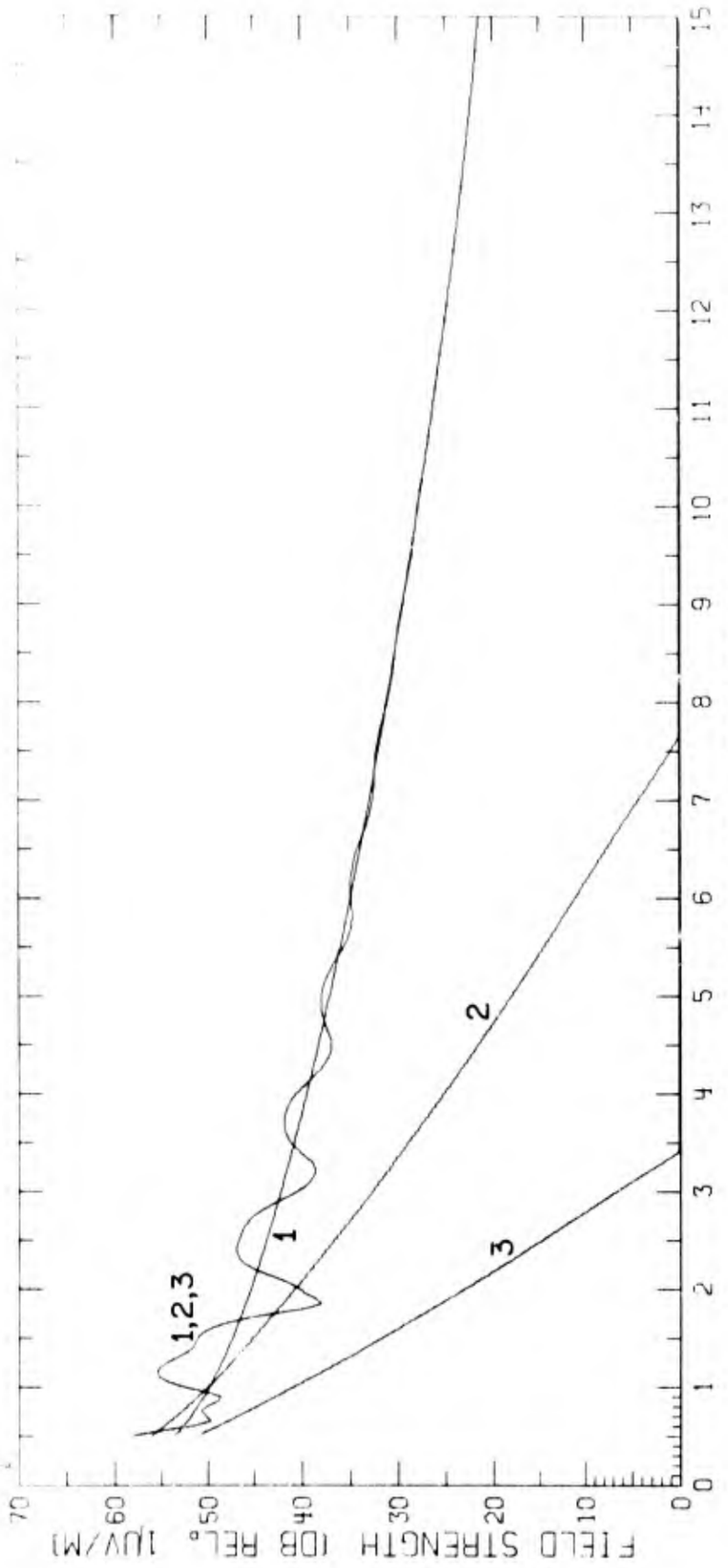

Fig. 41 - Predicted field strengths for f = 19.8 kc/s and h = 70 km

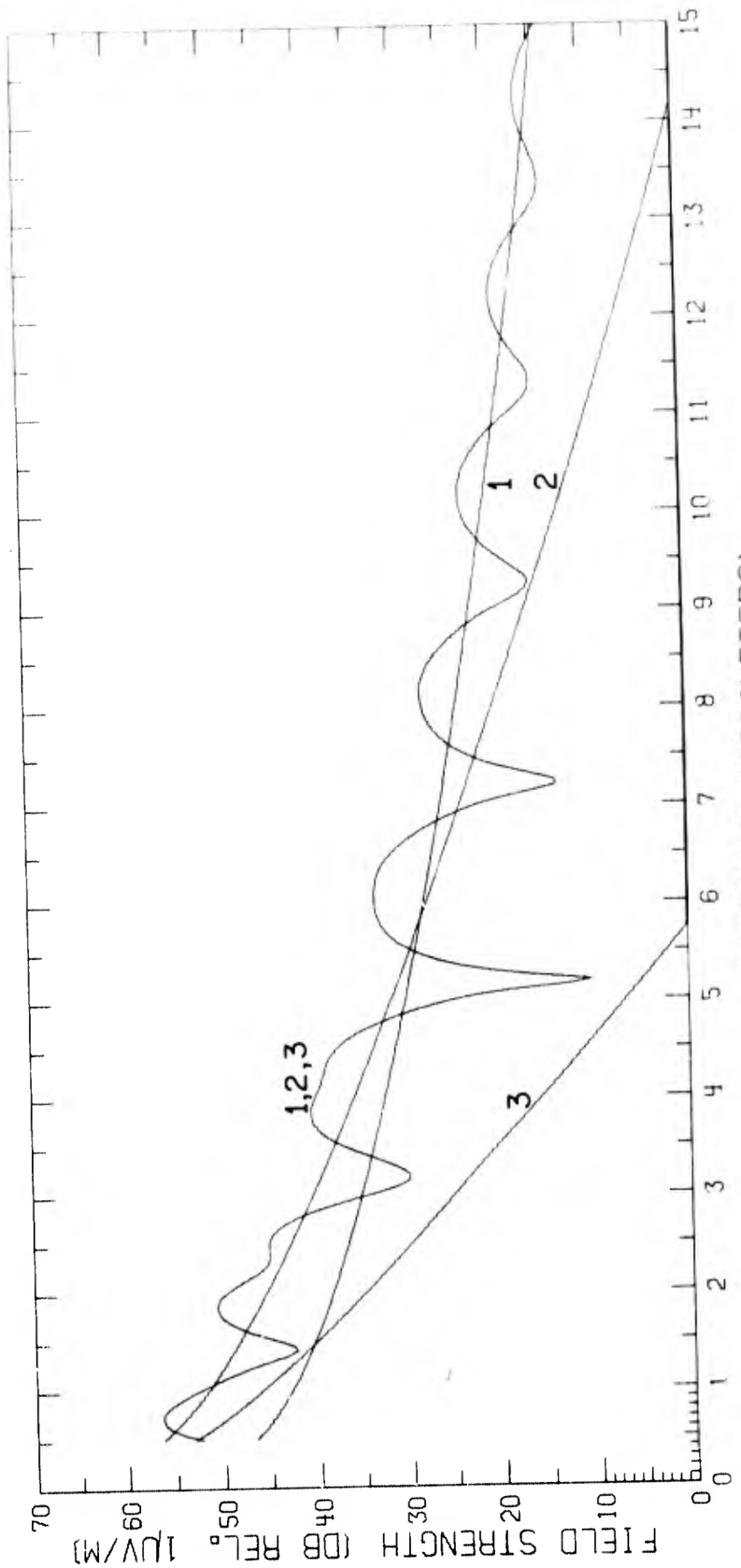

Fig. 42 - Predicted field strengths for / = 19.8 kc/s and ' = 90 km

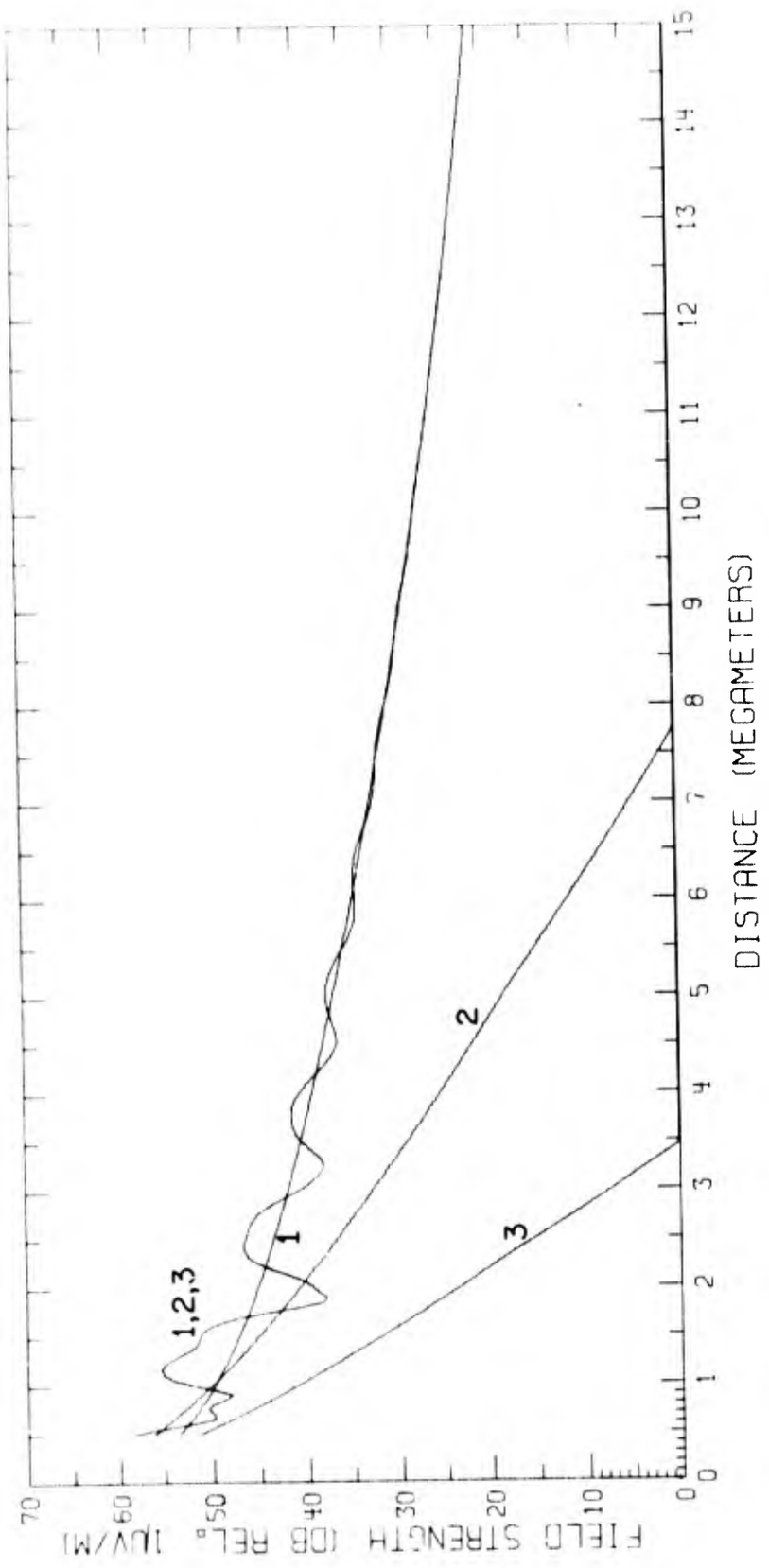

Fig. 43 - Predicted field strengths for f = 20.0 kc/s and h = 70 km

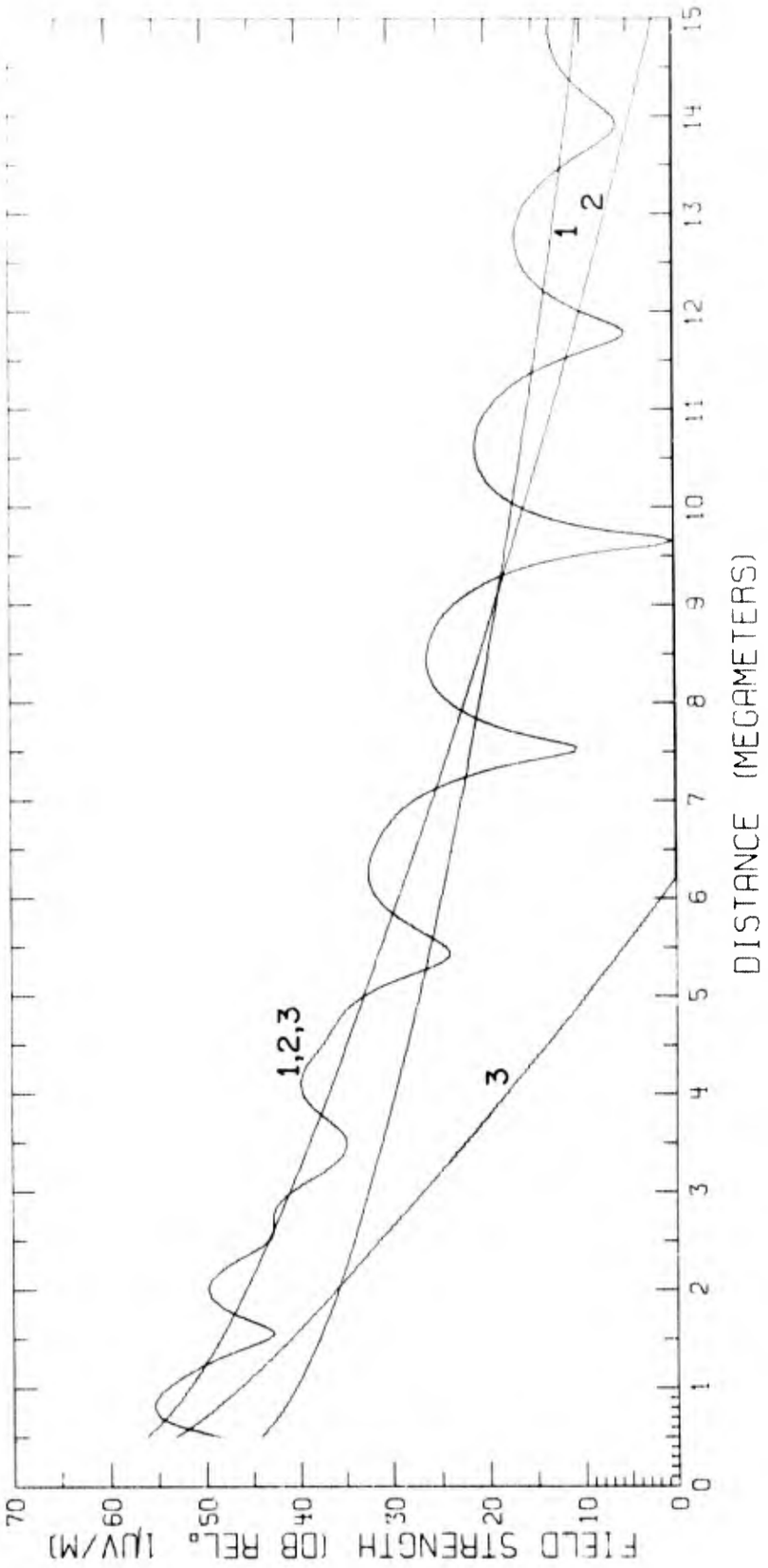

Fig. 44 - Predicted field strengths for f = 20.0 kc/s and h = 90 km

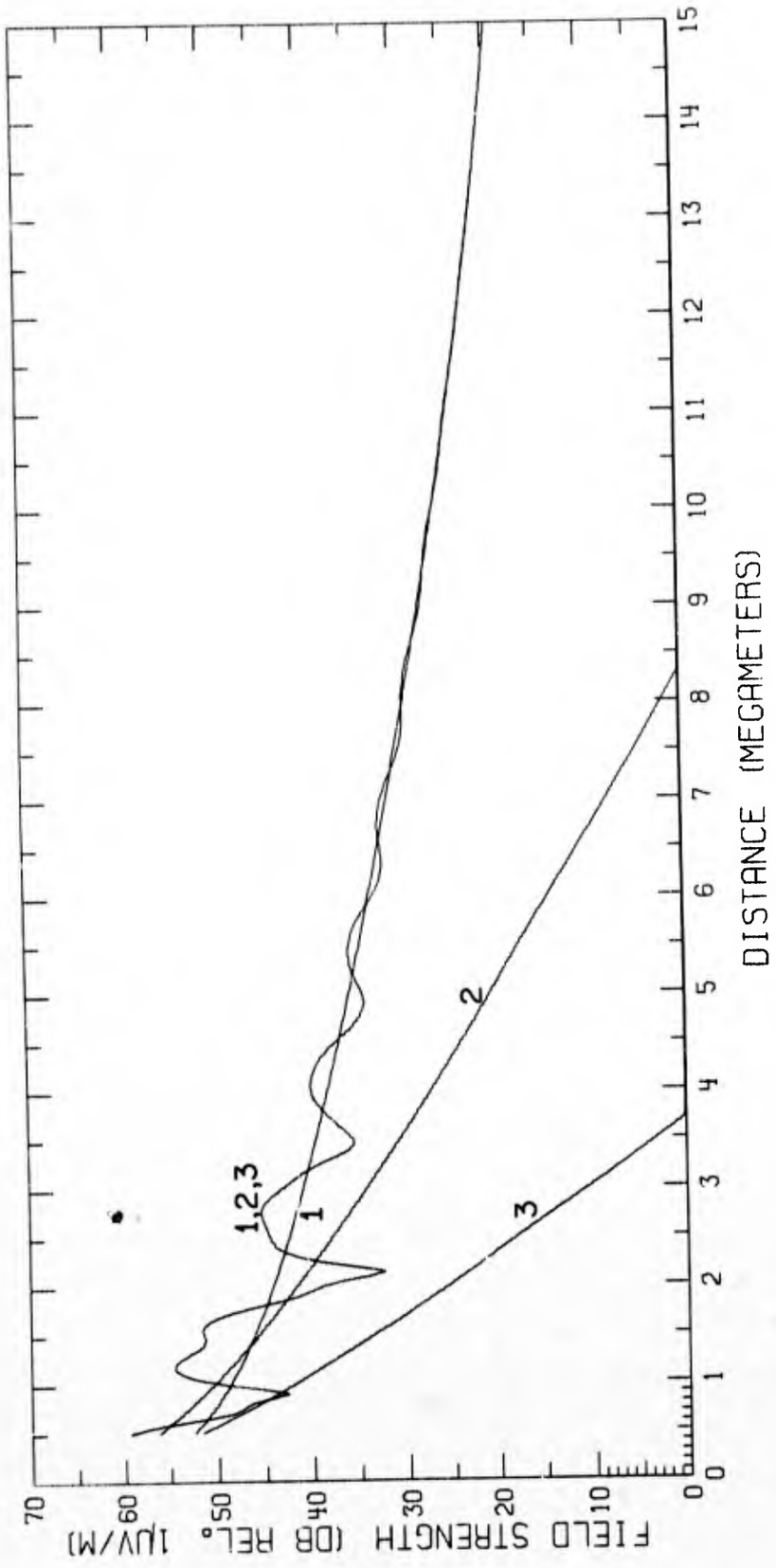

Fig. 45 - Predicted field strengths for f = 21.4 kc/s and $'$ = 70 km

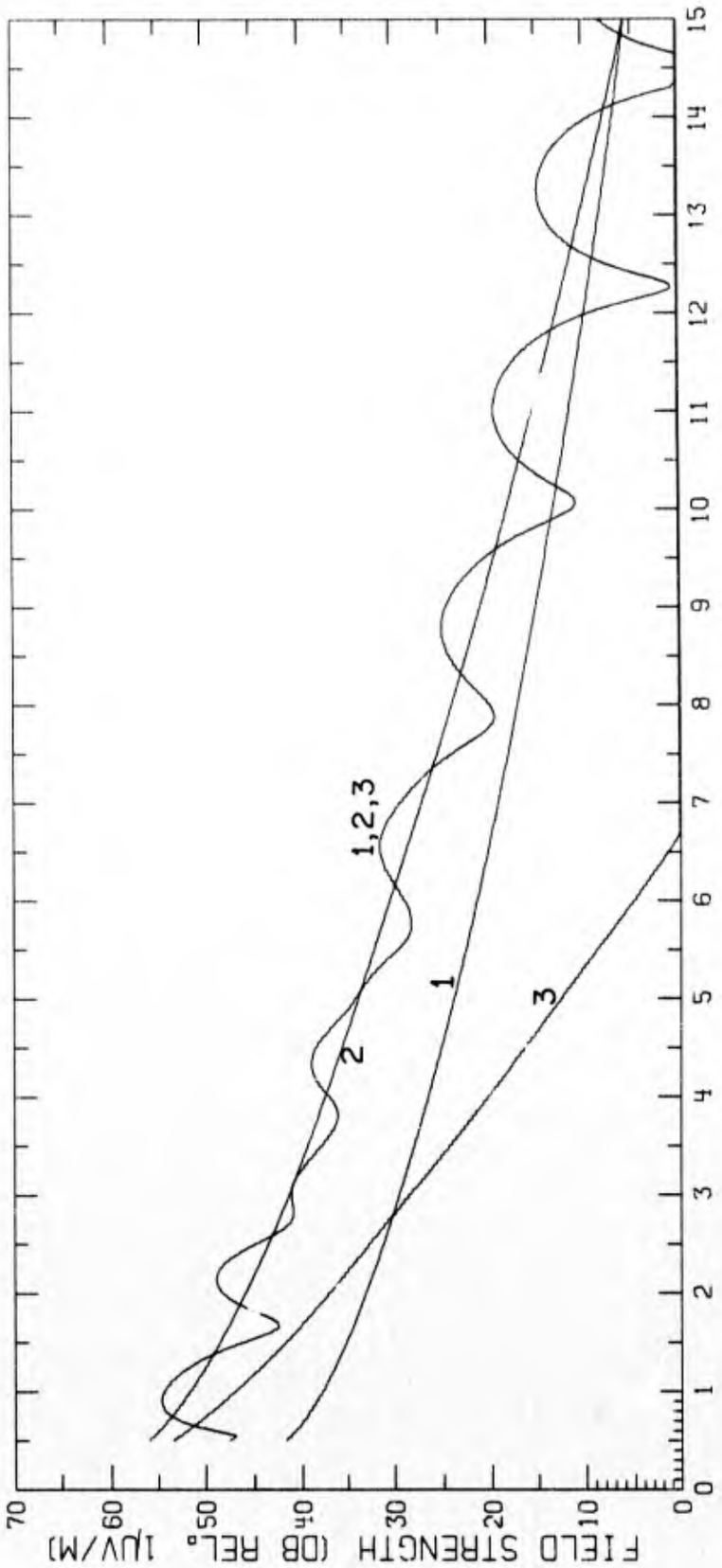

Fig. 46 - Predicted field strengths for f = 21.4 kc/s and h = 90 km

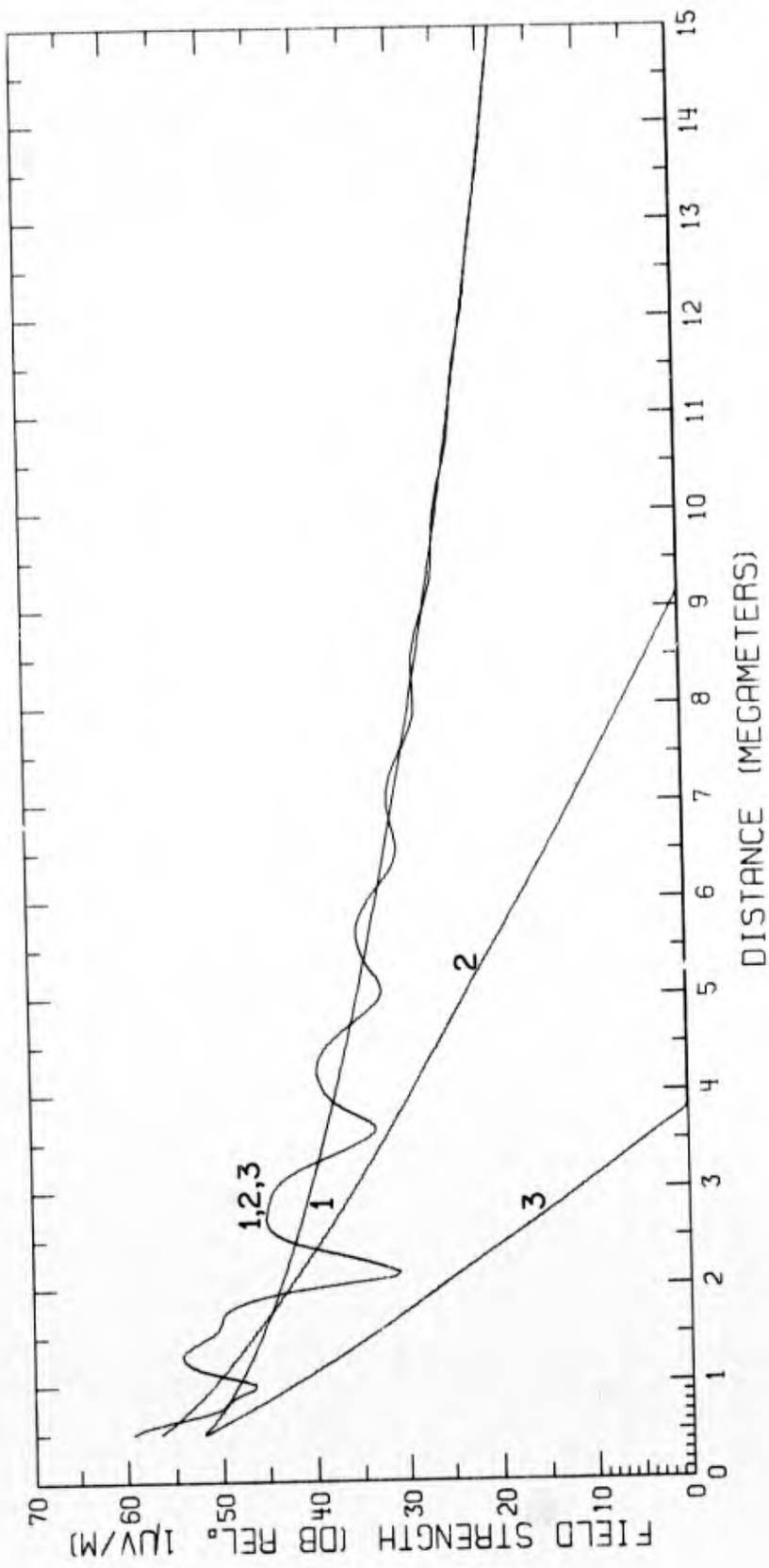

Fig. 47 - Predicted field strengths for f = 22.0 kc/s and h = 70 km

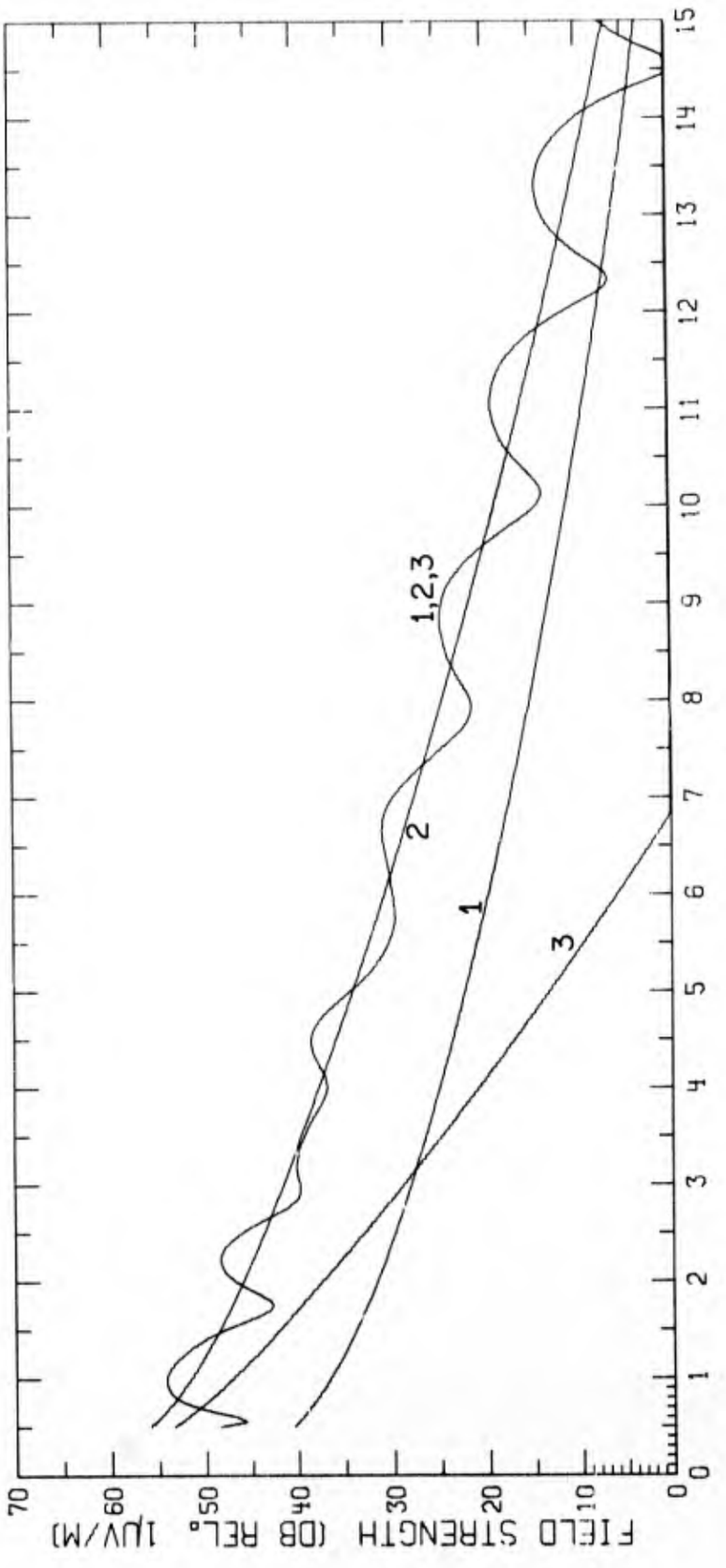

Fig. 48 - Predicted field strengths for f = 22.0 kc/s and h = 90 km

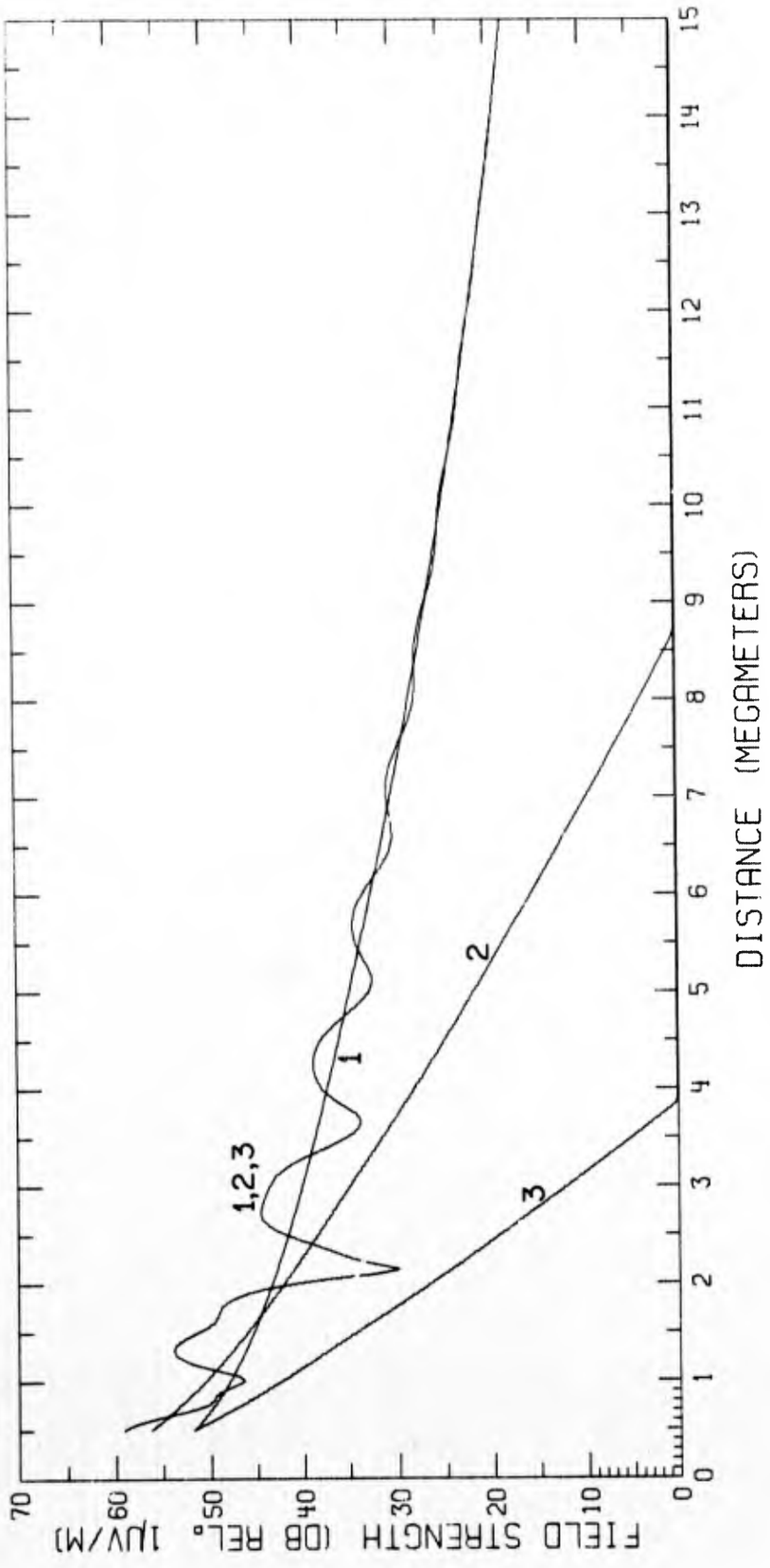

Fig. 49 - Predicted field strengths for f = 22.3 kc/s and h = 70 km

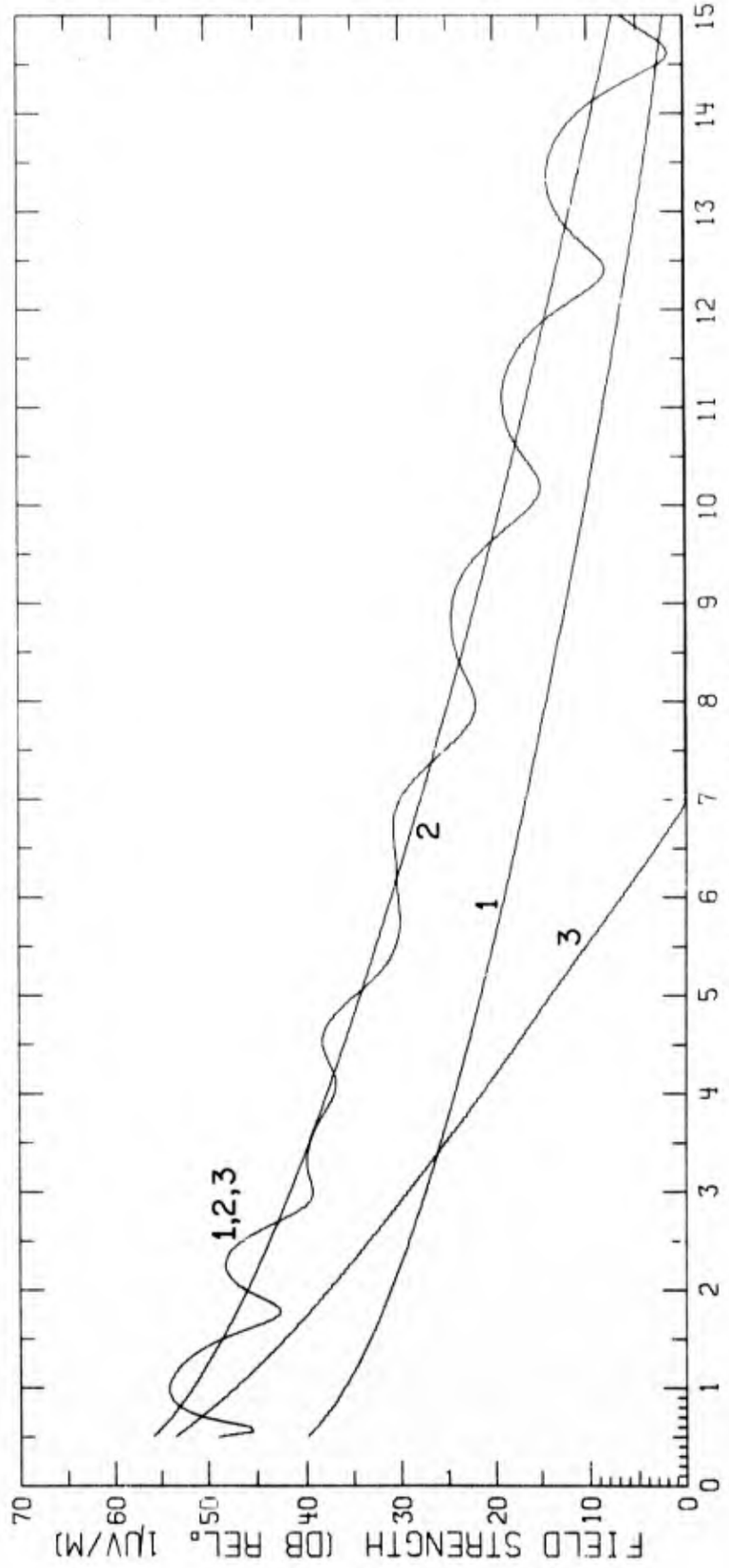

Fig. 50 - Predicted field strengths for f = 22.3 kc/s and h = 90 km

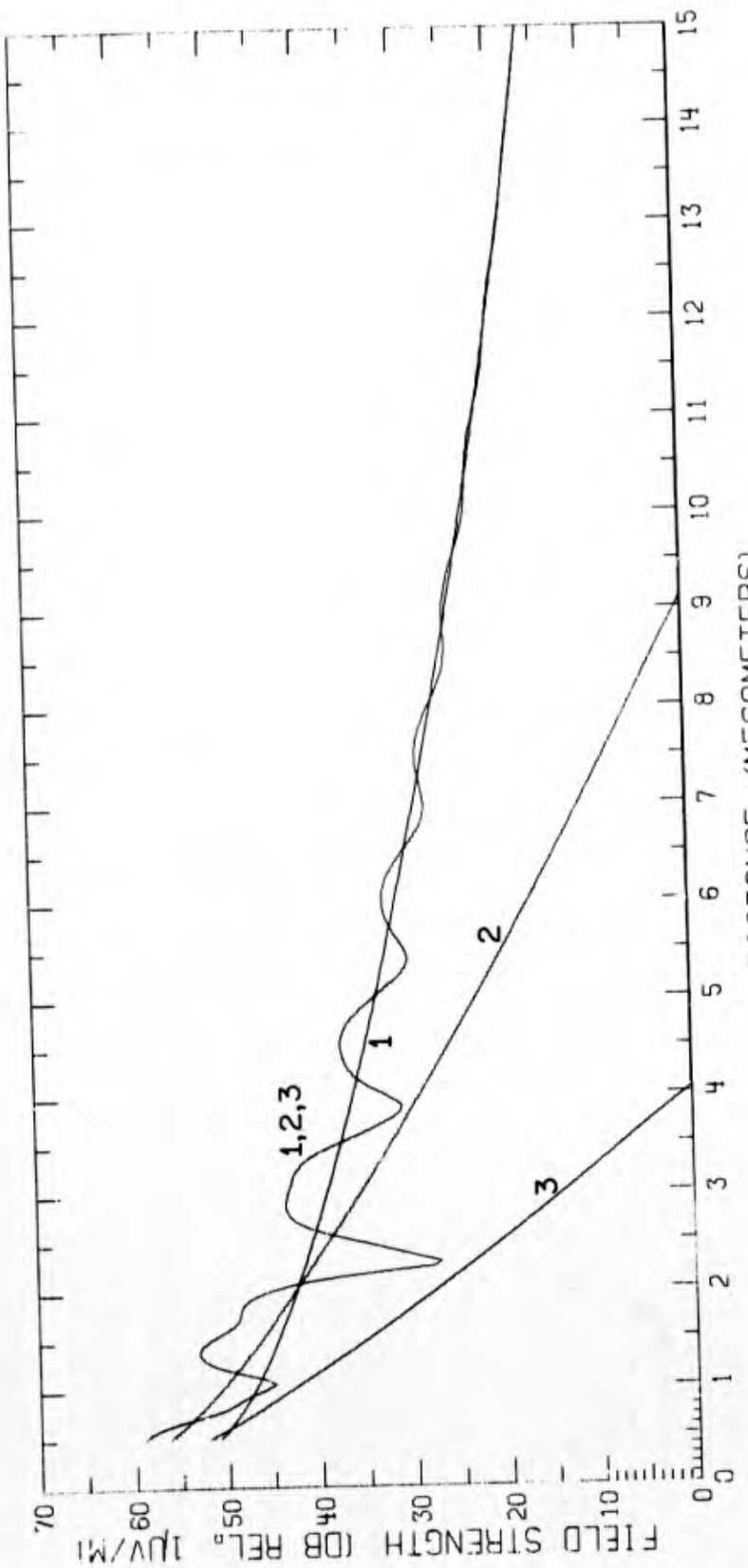

Fig. 51 - Predicted field strengths for f = 23.4 kc/s and h = 70 km

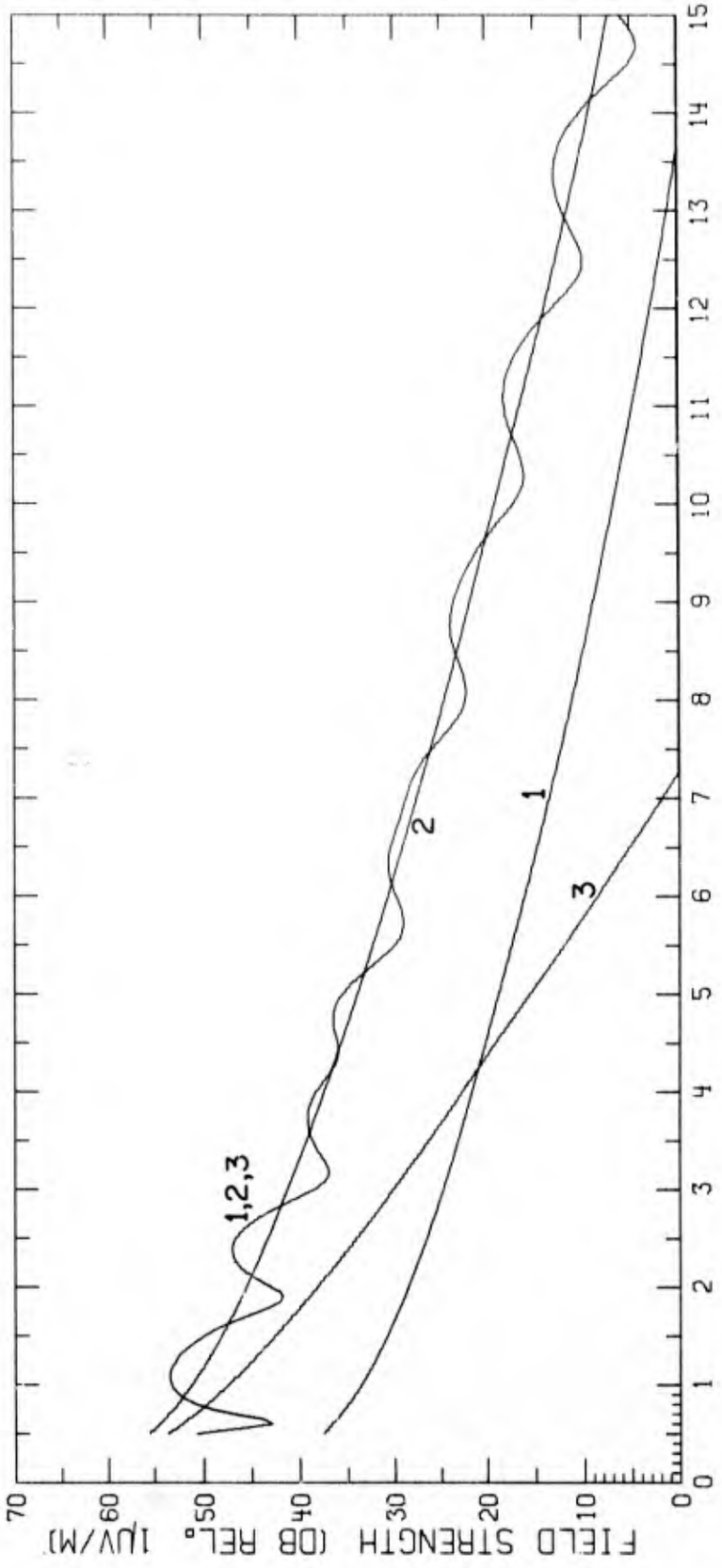

Fig. 52 - Predicted field strengths for f = 23.4 kc/s and h = 90 km

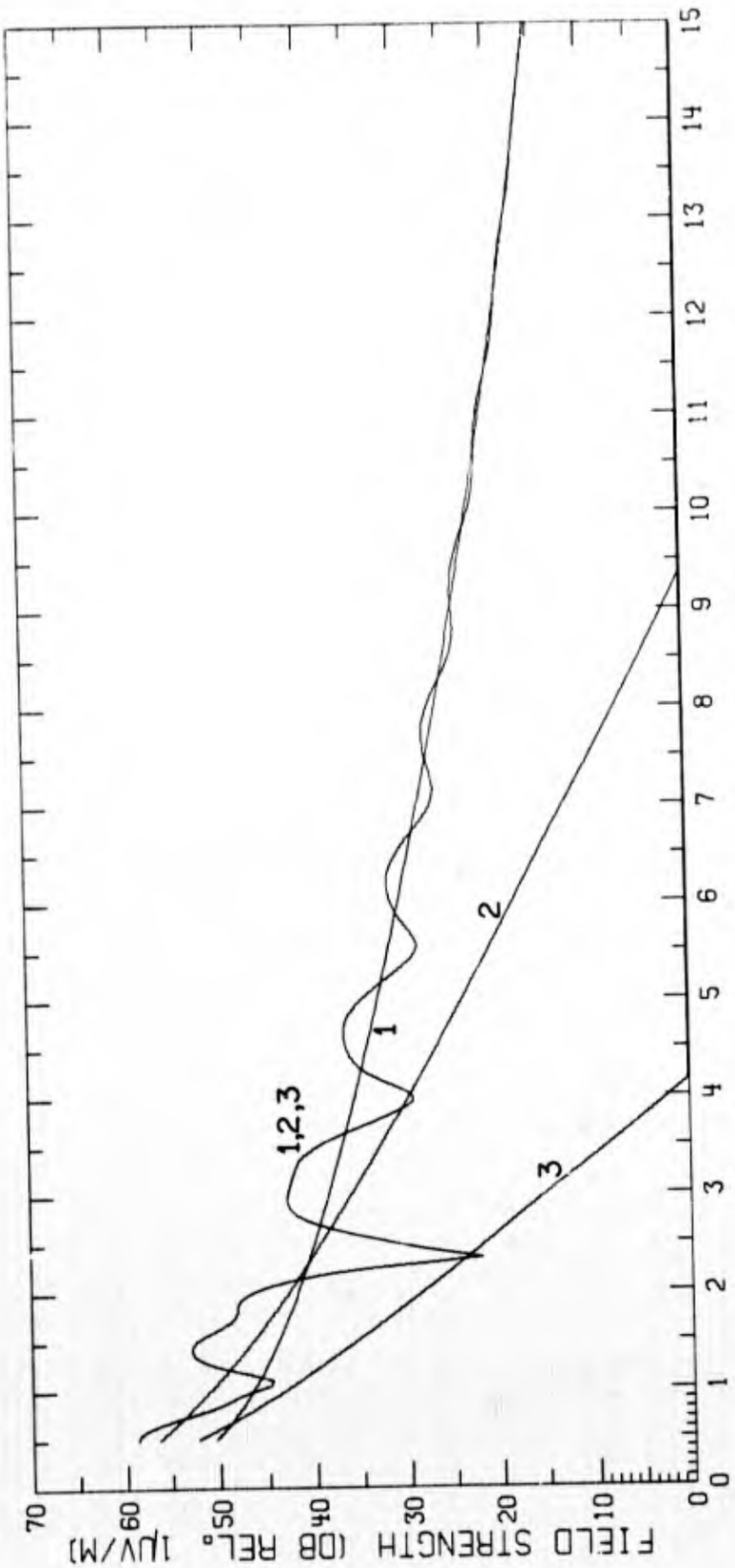

Fig. 53 - Predicted field strengths for f = 24.0 kc/s and h = 70 km

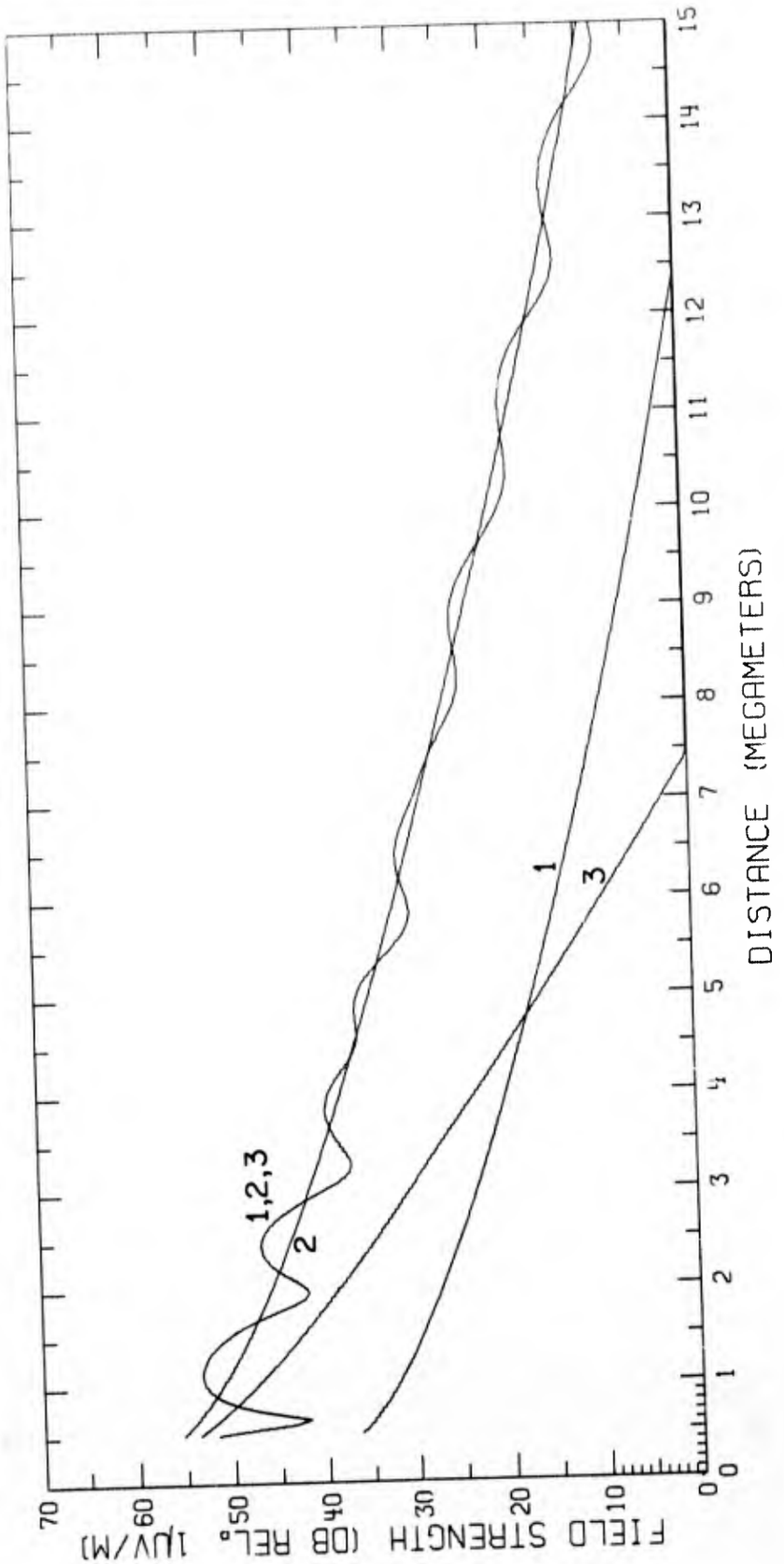

Fig. 5 - Predicted field strengths for f = 24.0 kc/s and h = 90 km

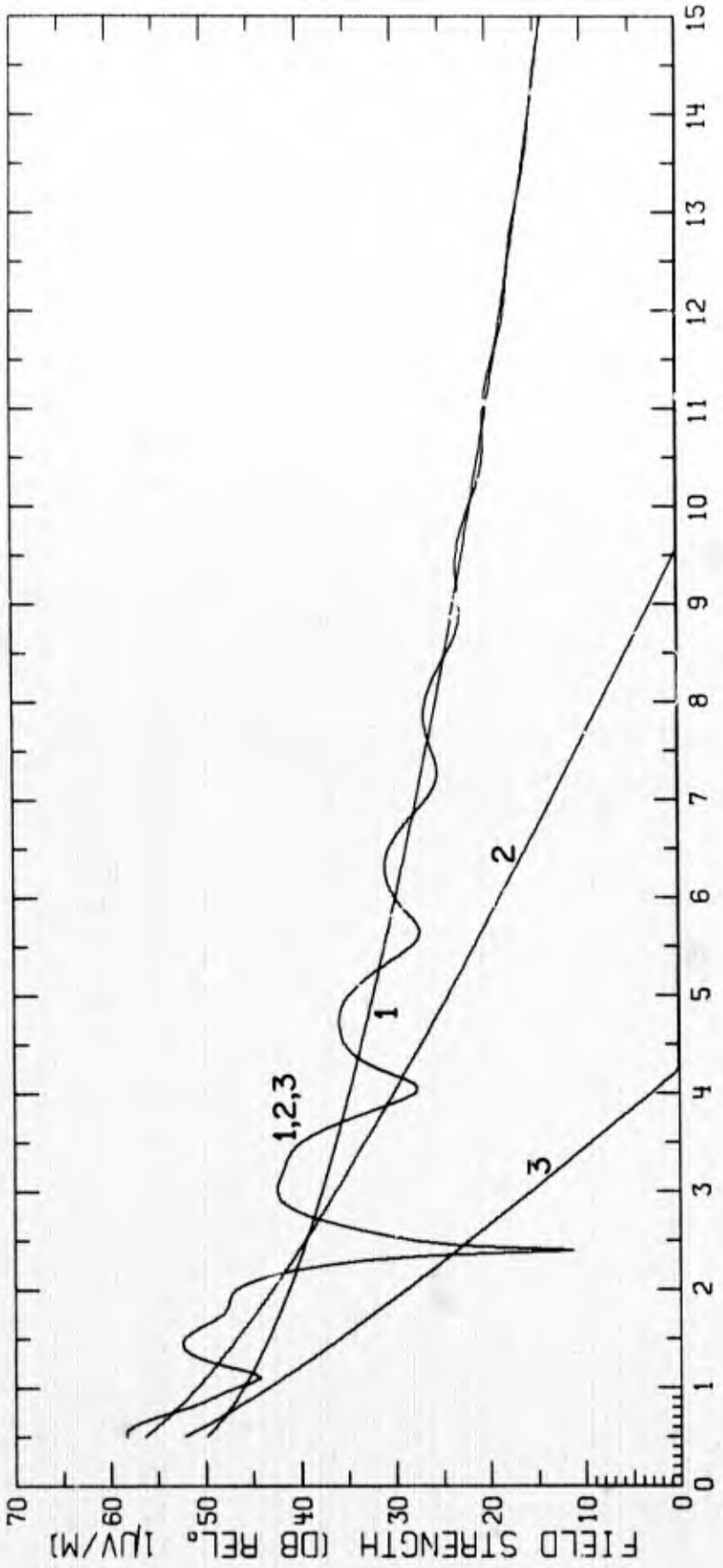

Fig. 55 - Predicted field strengths for f = 24.5 kc/s and h = 70 km

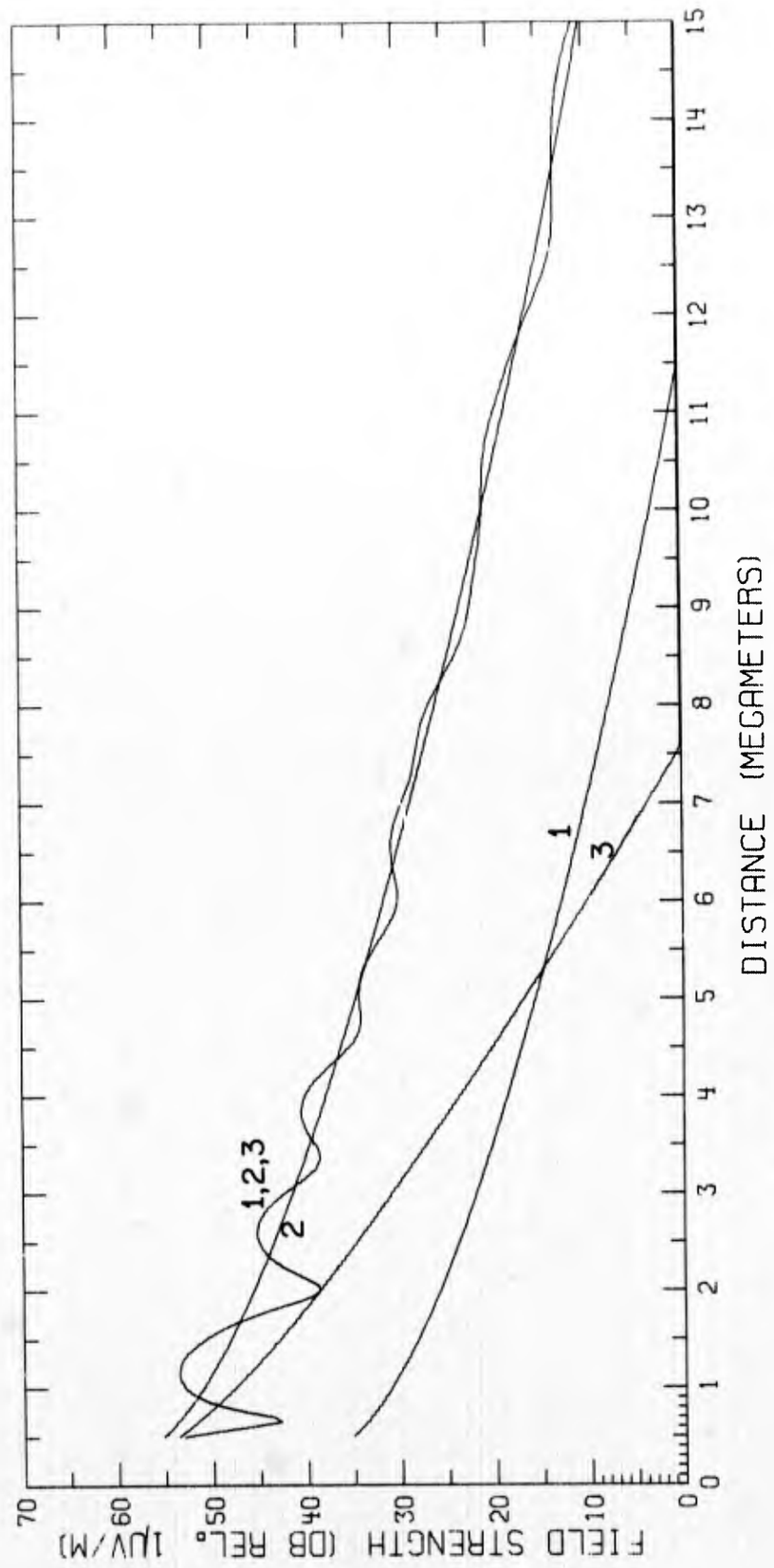

Fig. 56 - Predicted field strengths for f = 24.5 kc/s and h = 90 km

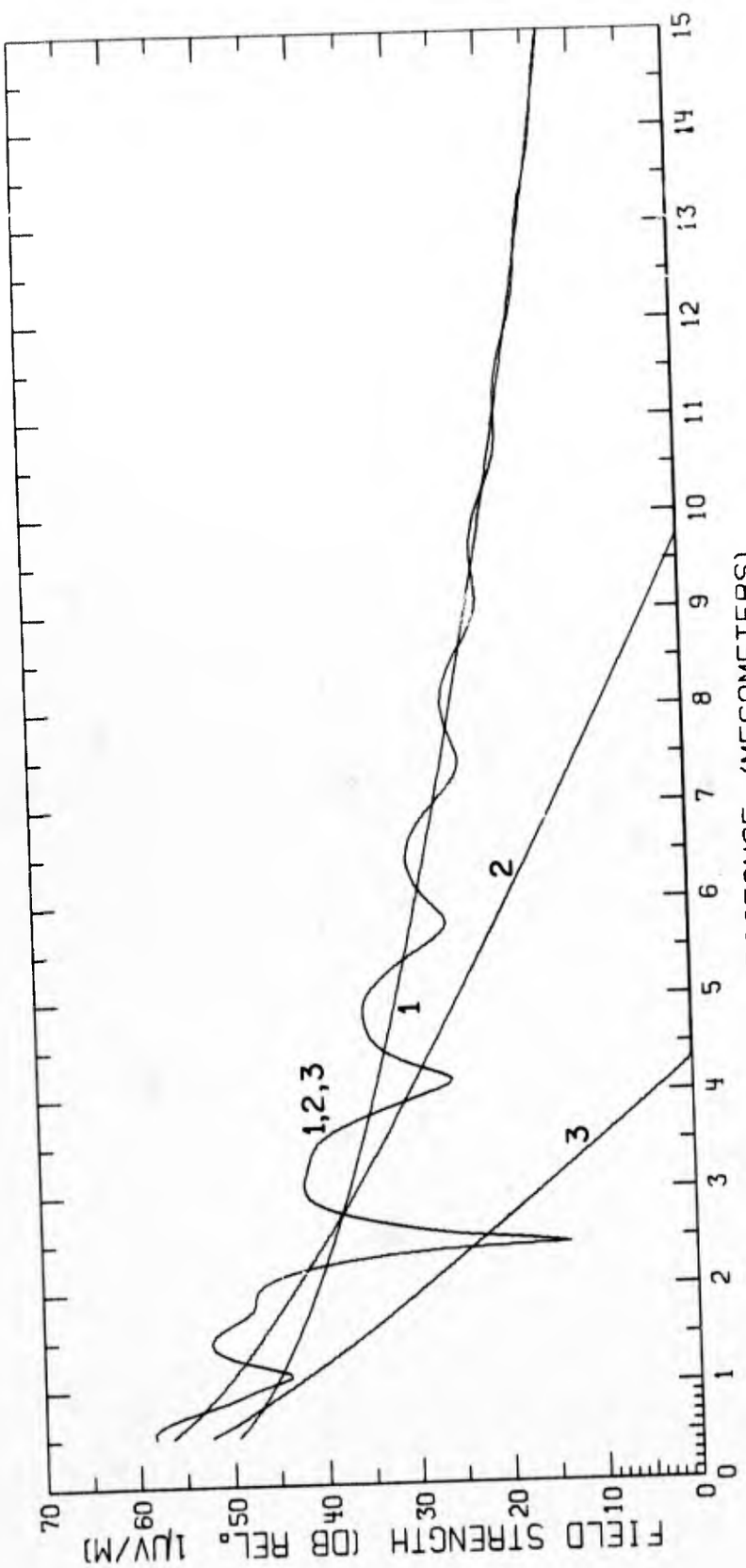

Fig. 57 - Predicted field strengths for f = 24.9 kc/s and h = 70 km

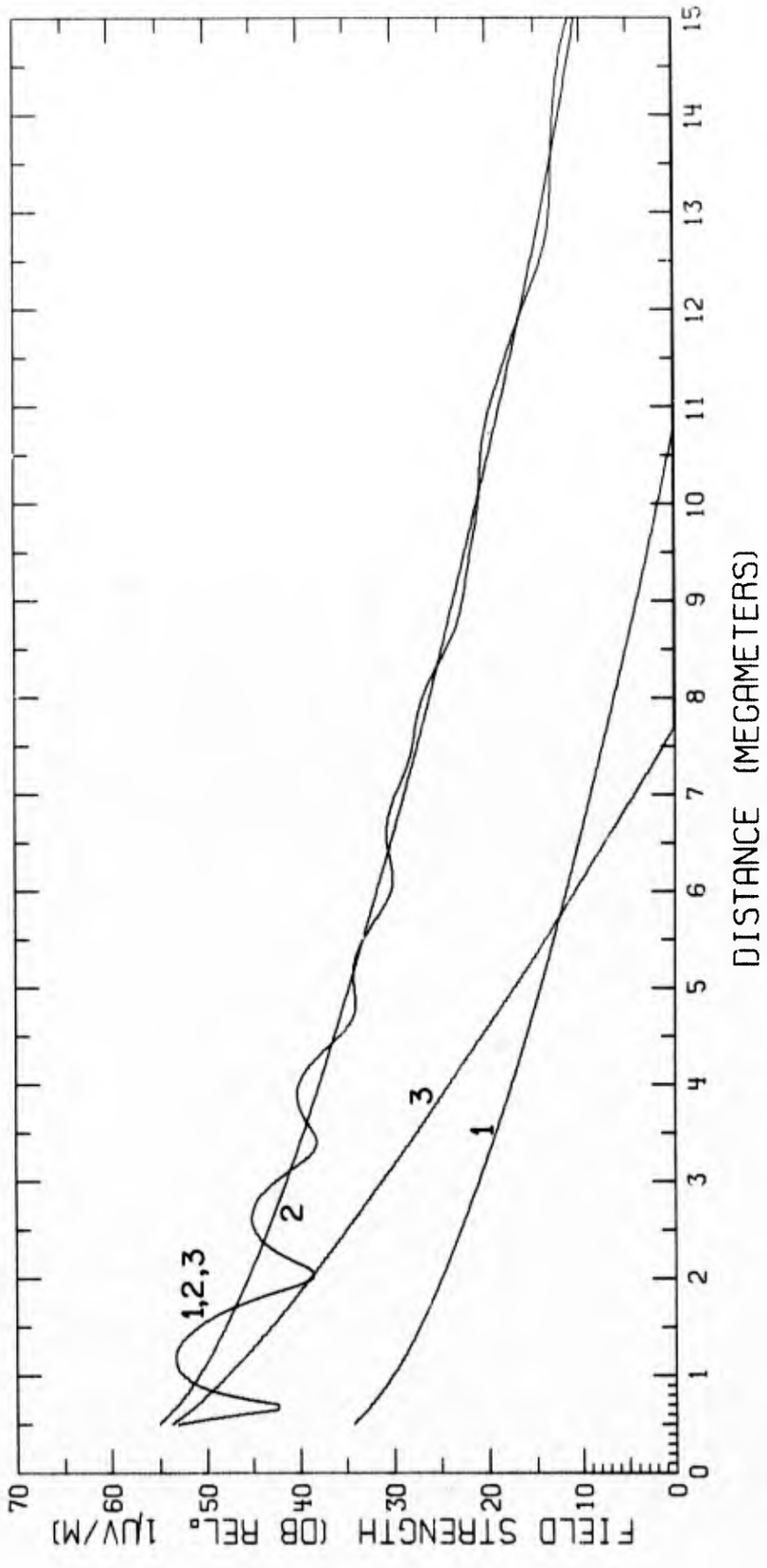

Fig. 58 - Predicted field strengths for f = 24.9 kc/s and h = 90 km

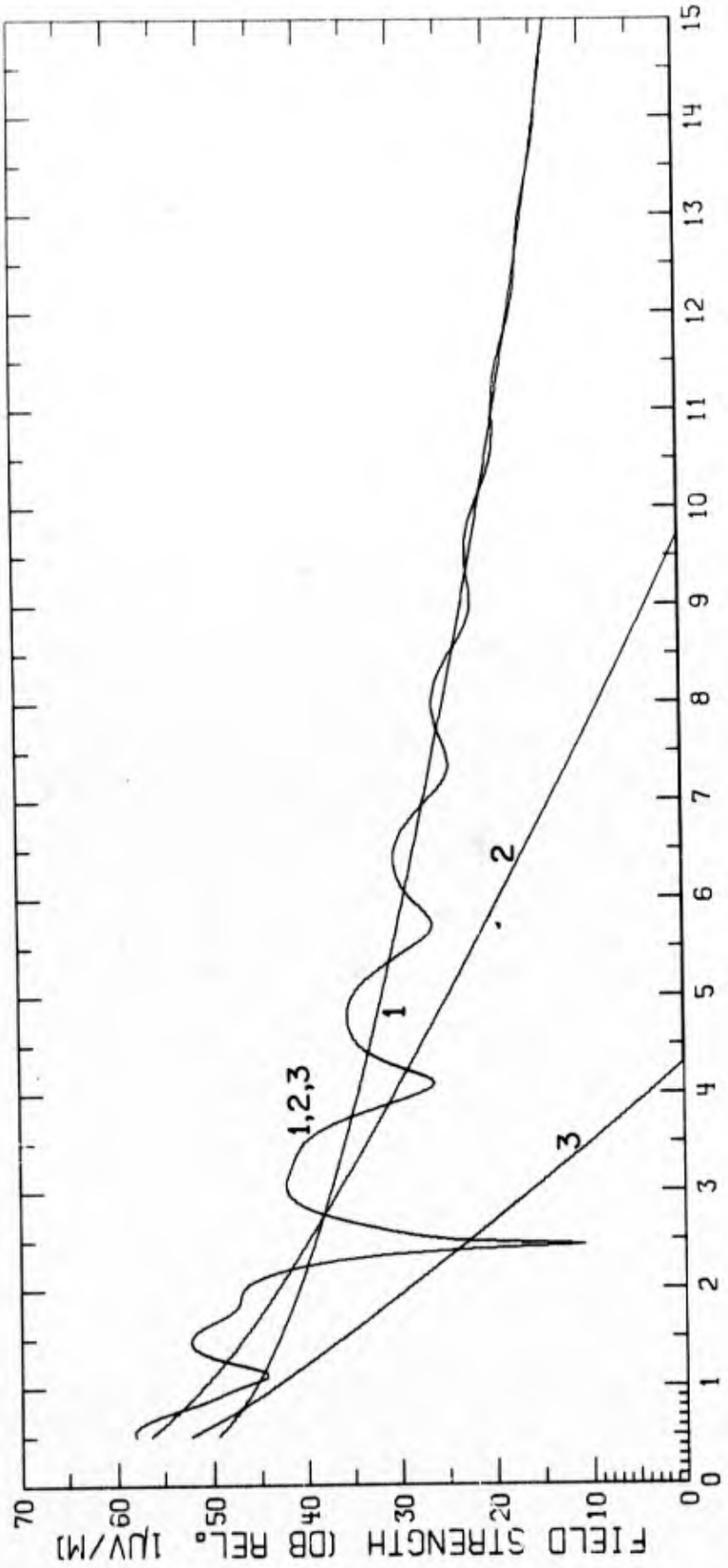

Fig. 59 - Predicted field strengths for f = 25.0 kc/s and h = 70 km

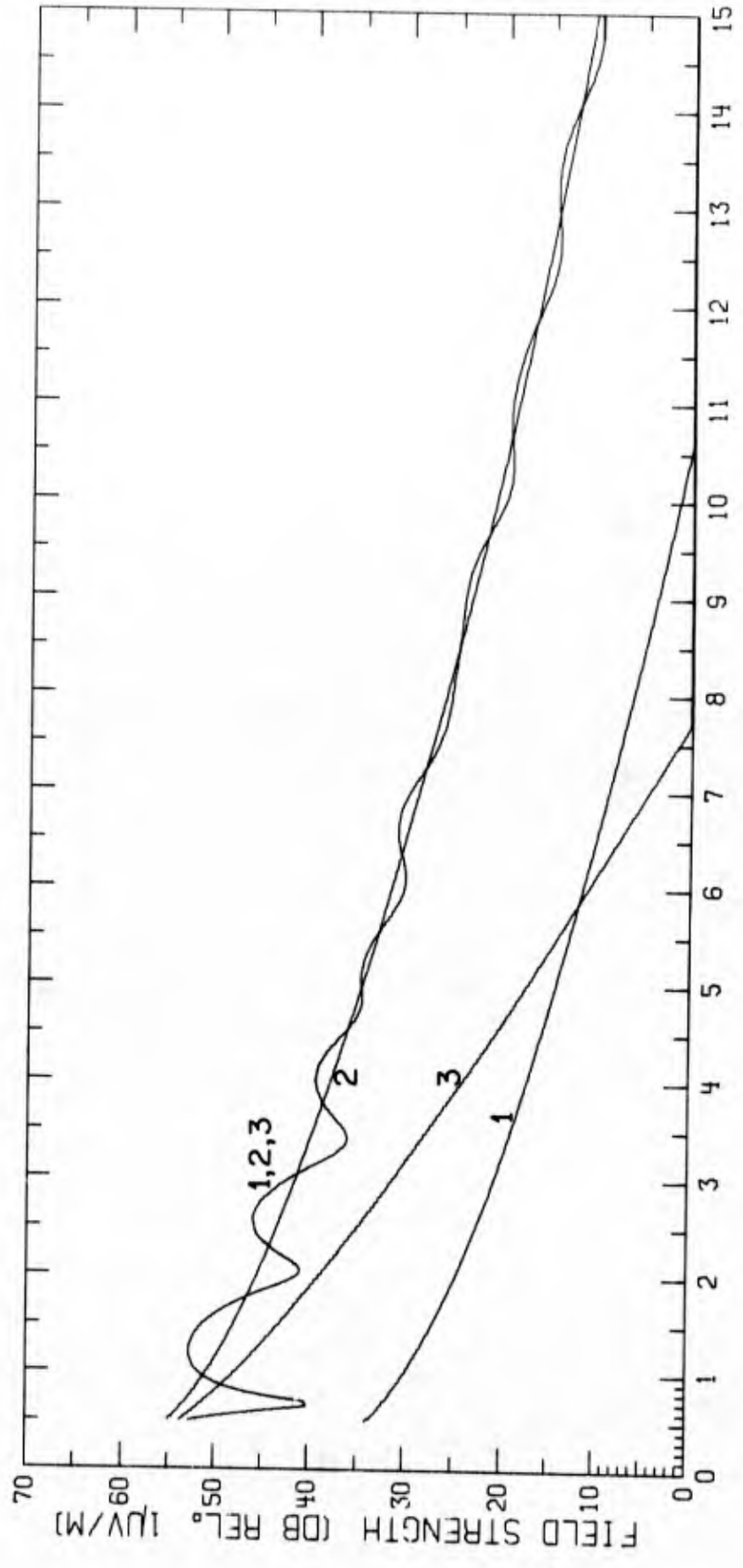

Fig. 60 - Predicted field strengths for f = 25.0 kc/s and h = 90 km

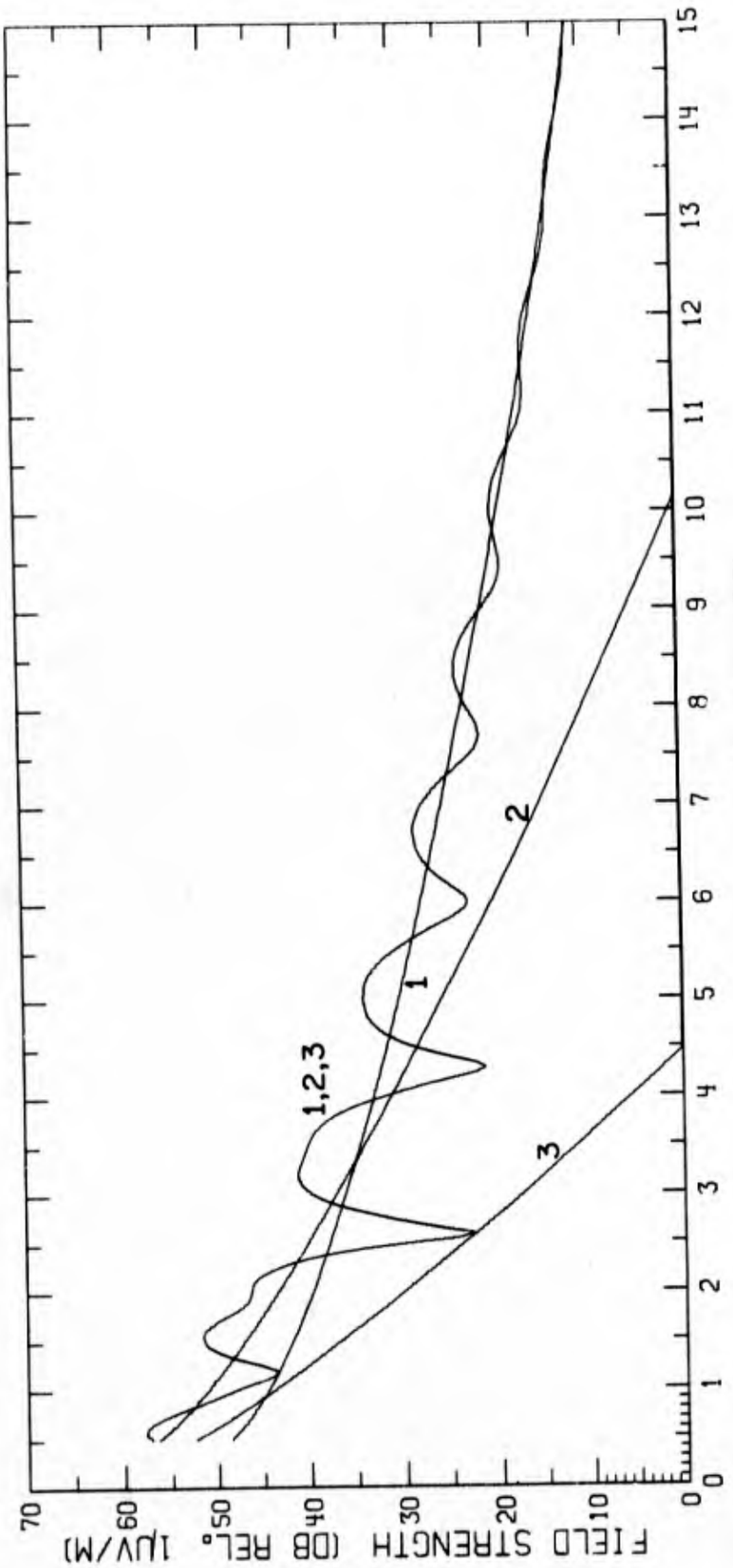

Fig. 61 - Predicted field strengths for f = 26.0 kc/s and h = 70 km

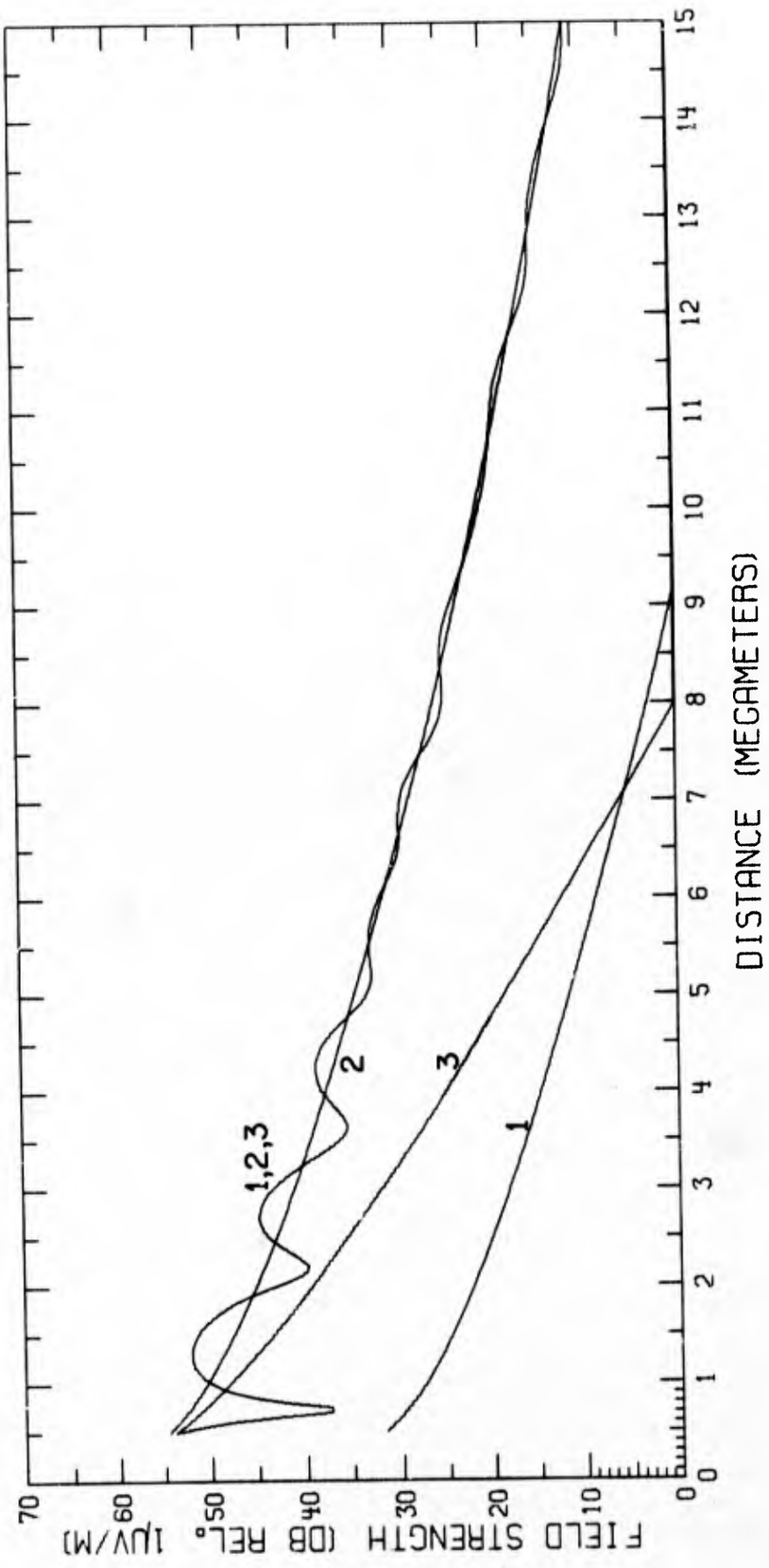

Fig. 62 - Predicted field strengths for f = 26.0 kc/s and h = 90 km

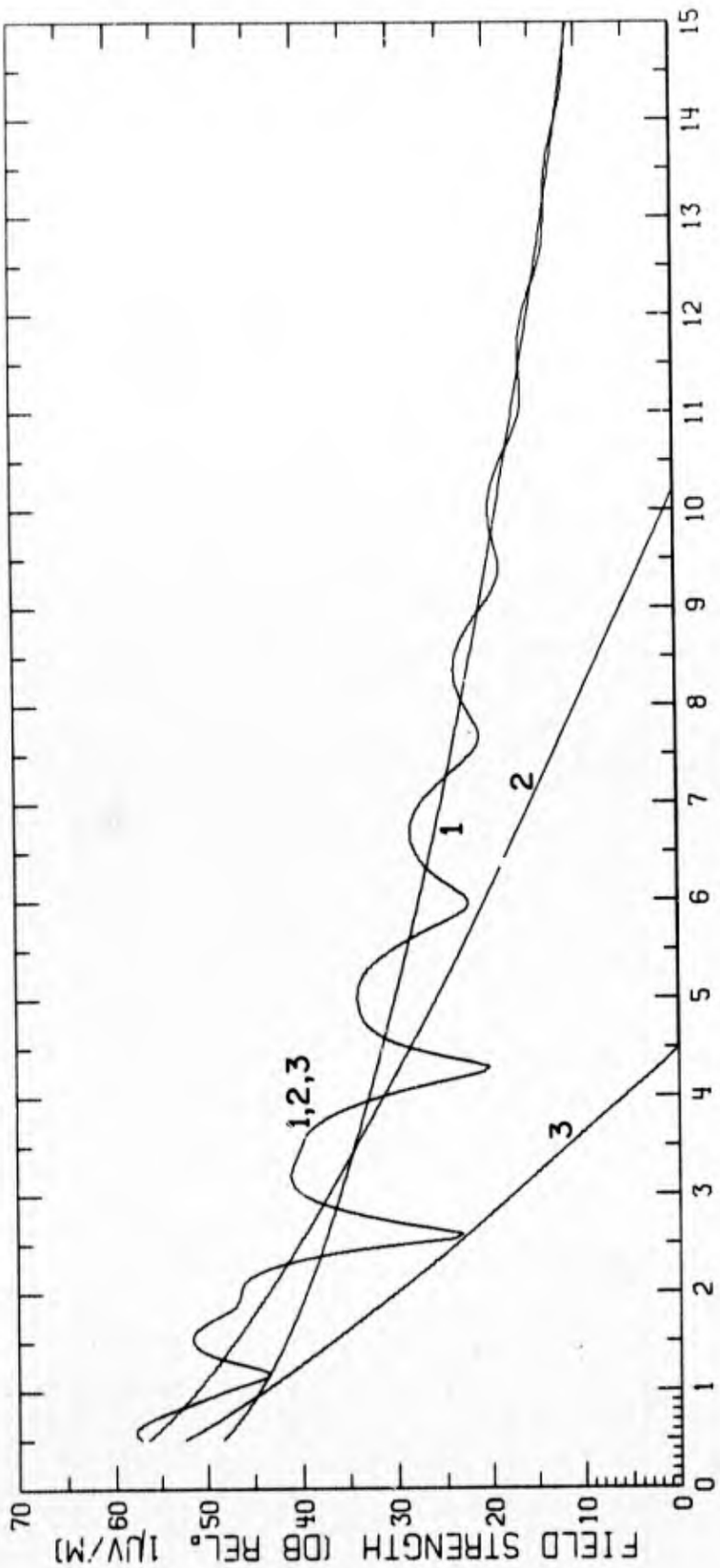

Fig. 63 - Predicted field strengths for f = 26.1 kc/s and h = 70 km

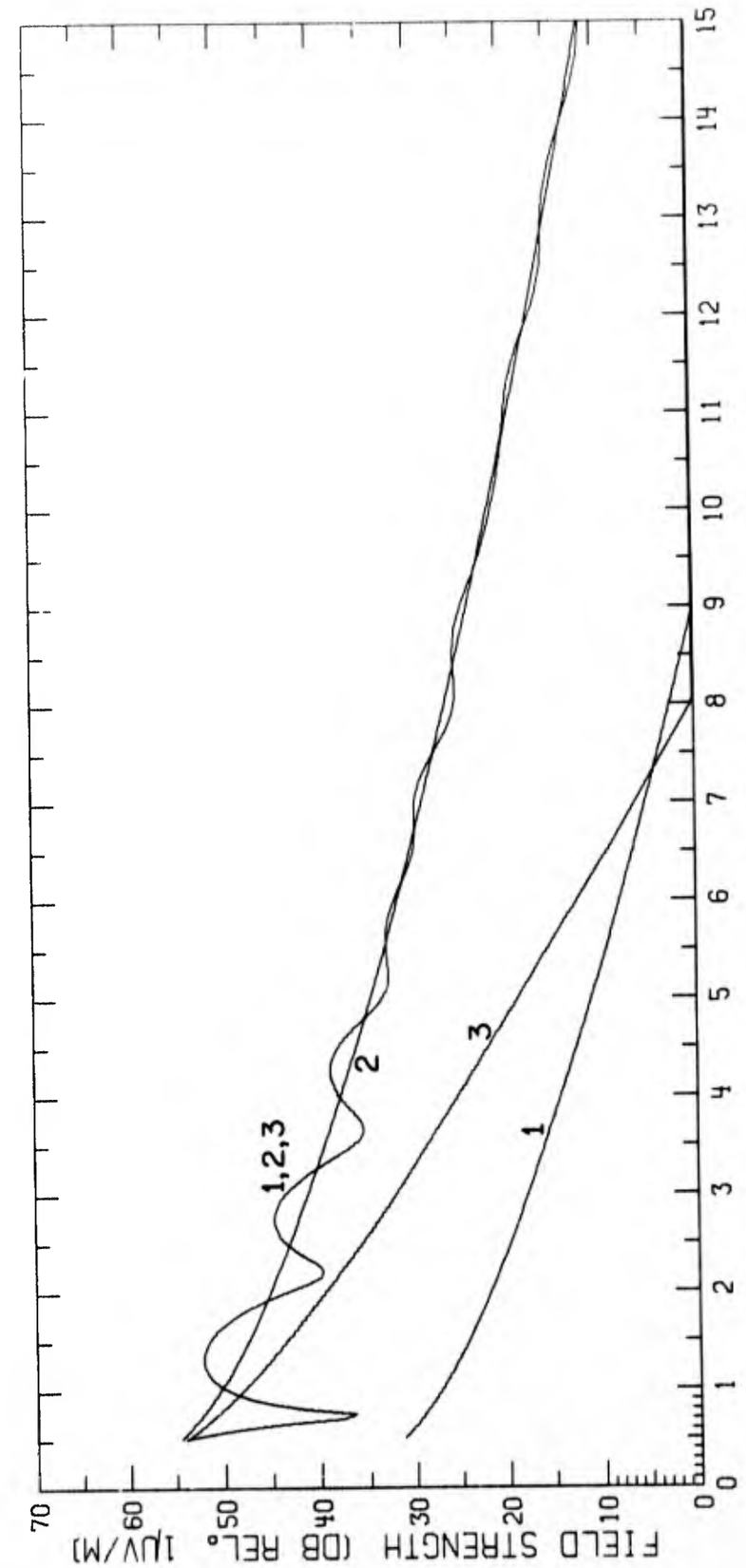

Fig. 64 - Predicted field strengths for f = 26.1 kc/s and h = 90 km

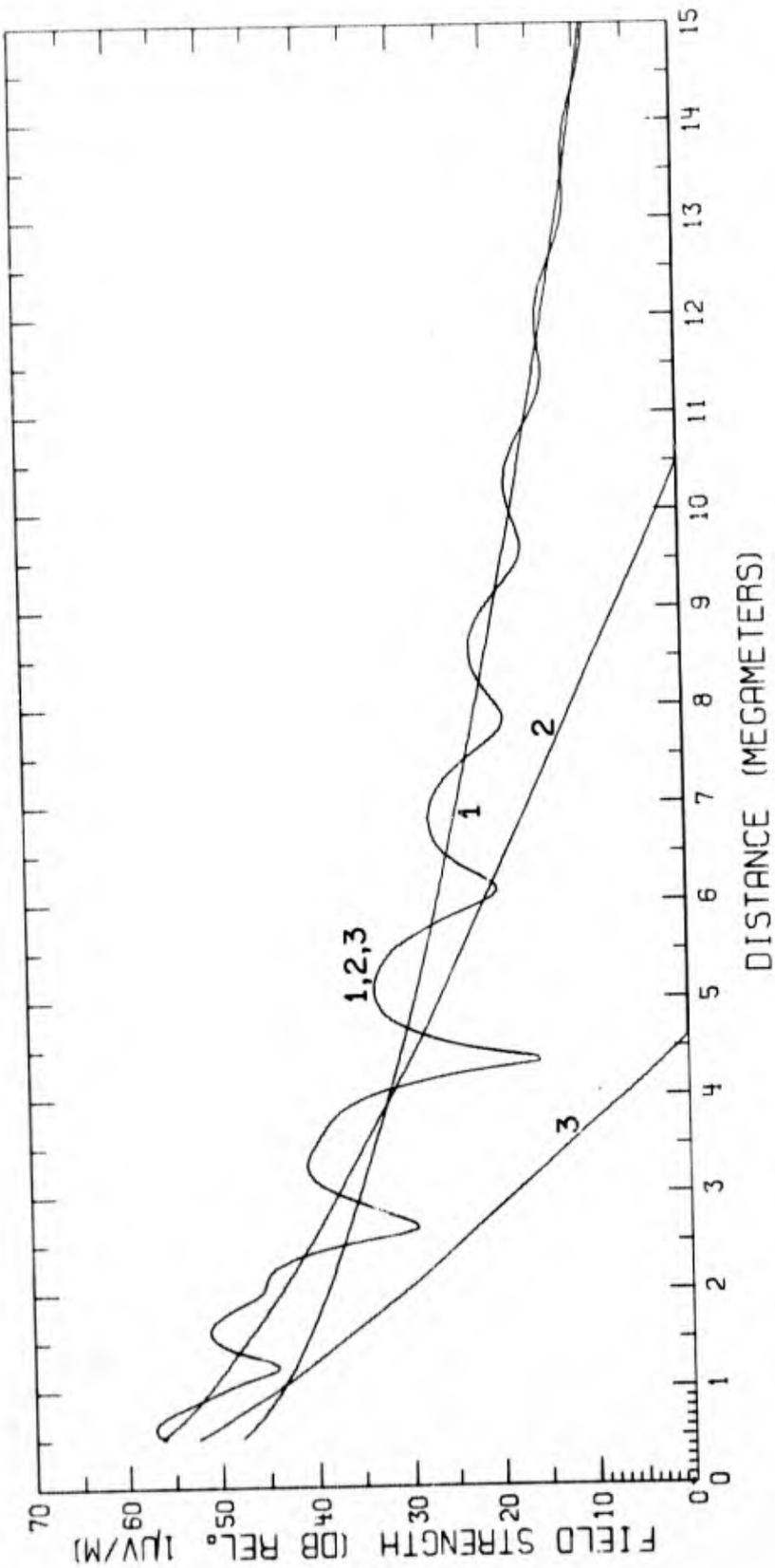

Fig. 65 - Predicted field strengths for f = 26.8 kc/s and h = 70 km

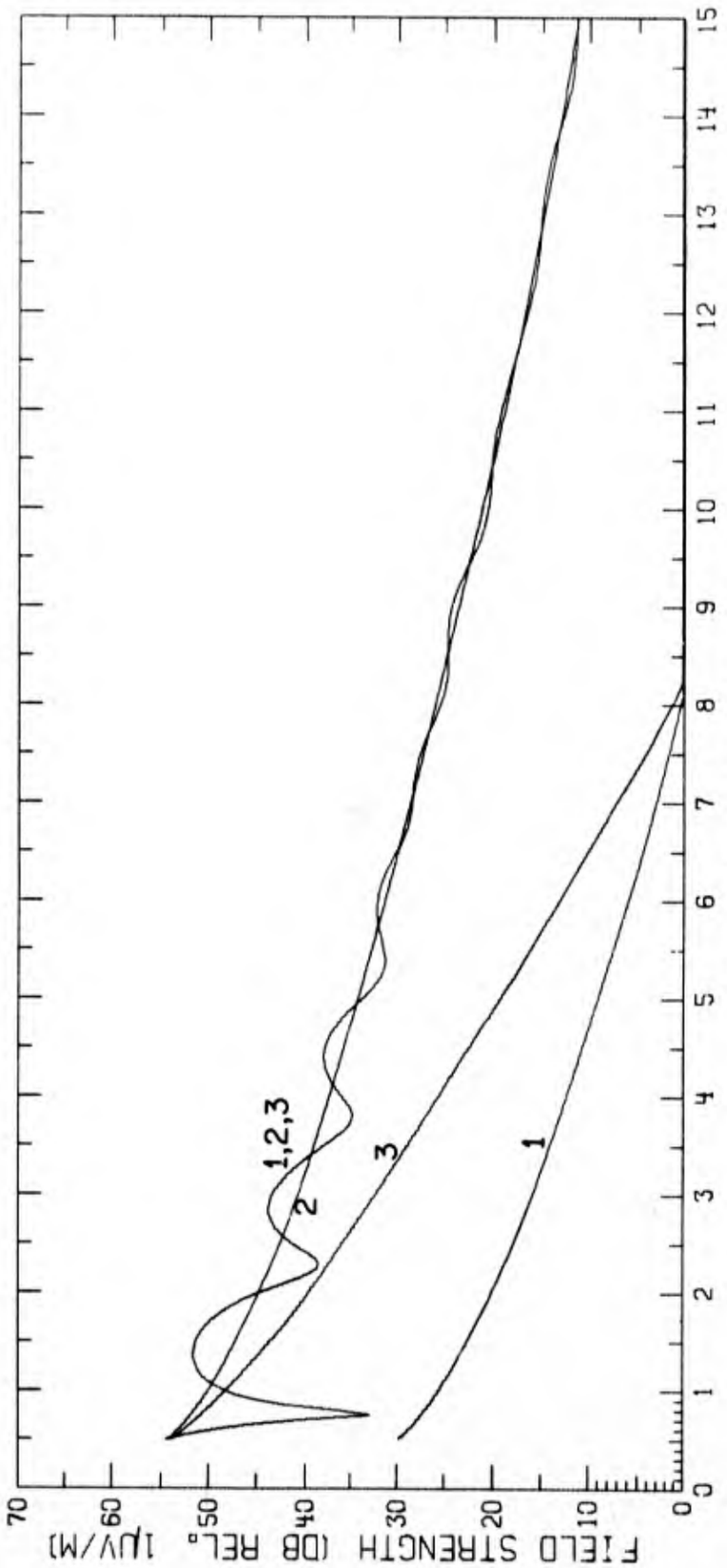

Fig. 66 - Predicted field strengths for f = 26.8 kc/s and h = 90 km

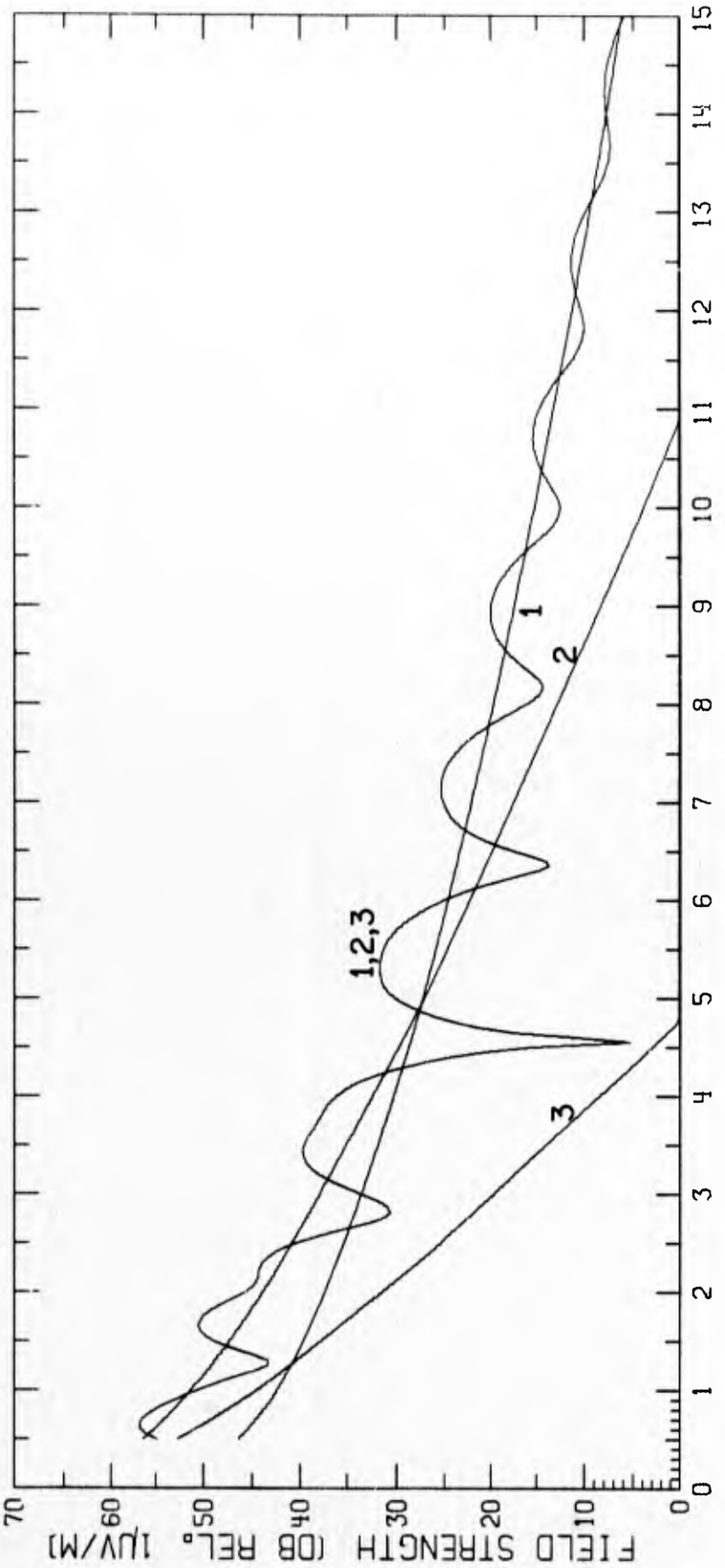

Fig. 67 - Predicted field strengths for f = 28.0 kc/s and h = 70 km

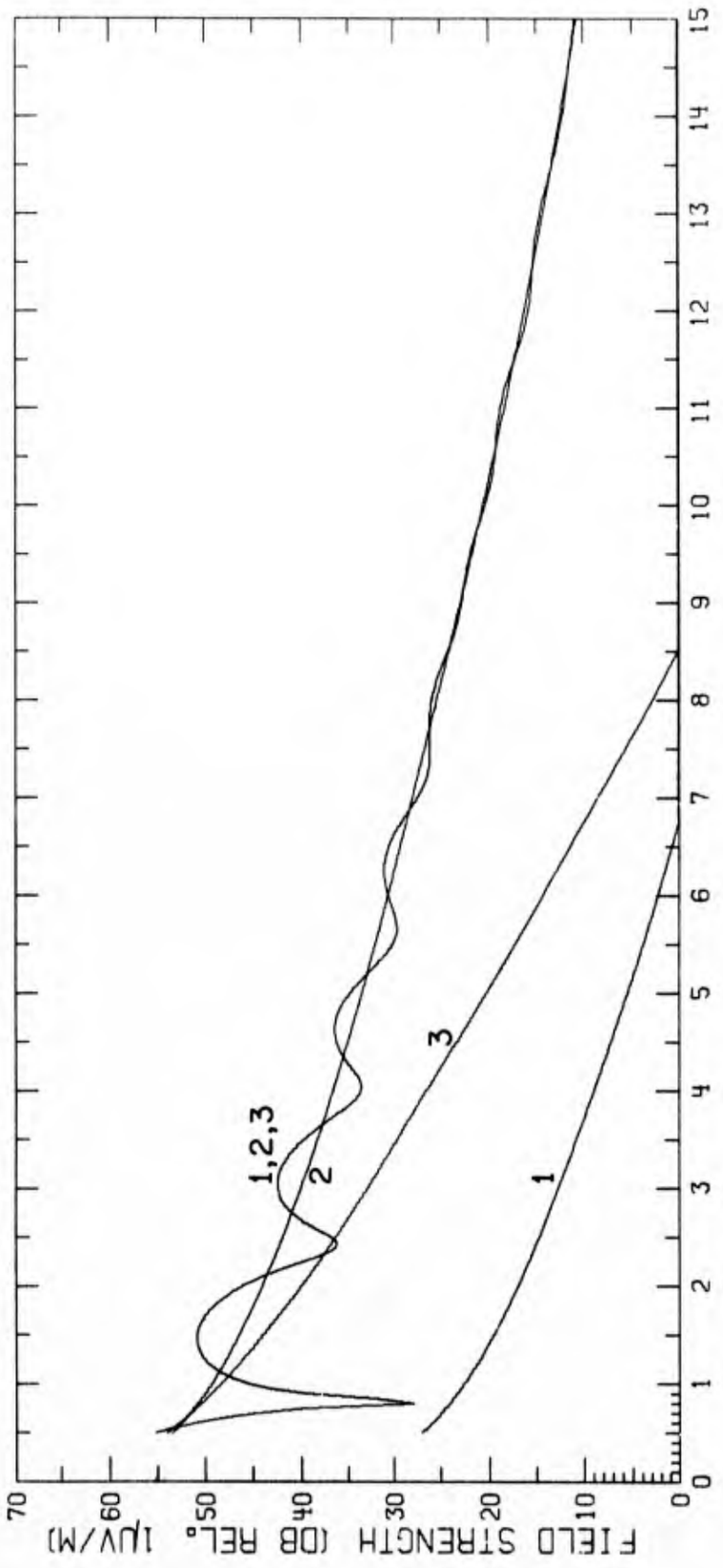

Fig. 68 - Predicted field strengths for f = 28.0 kc/s and h = 90 km

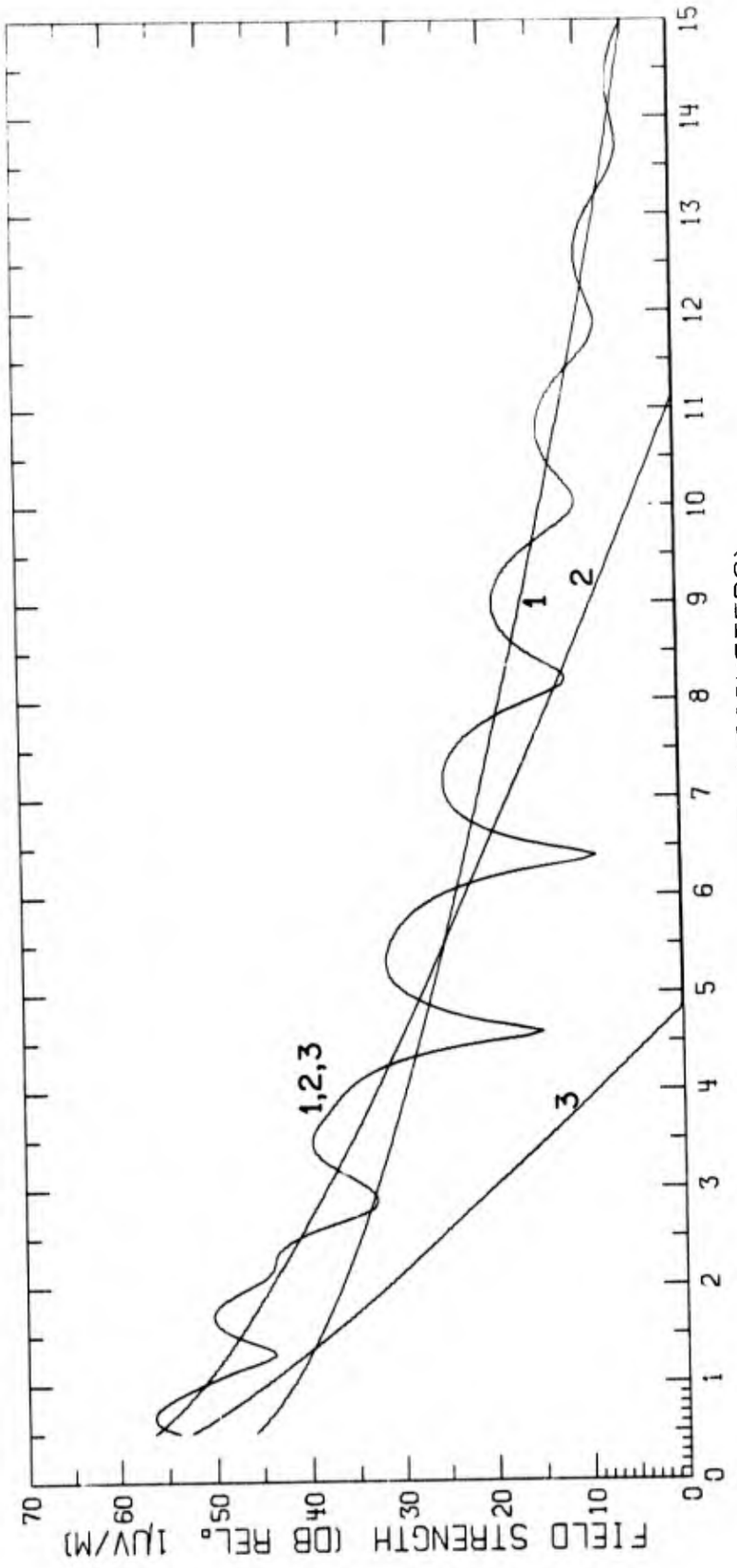

Fig. 69 - Predicted field strengths for f = 28.5 kc/s and h = 70 km

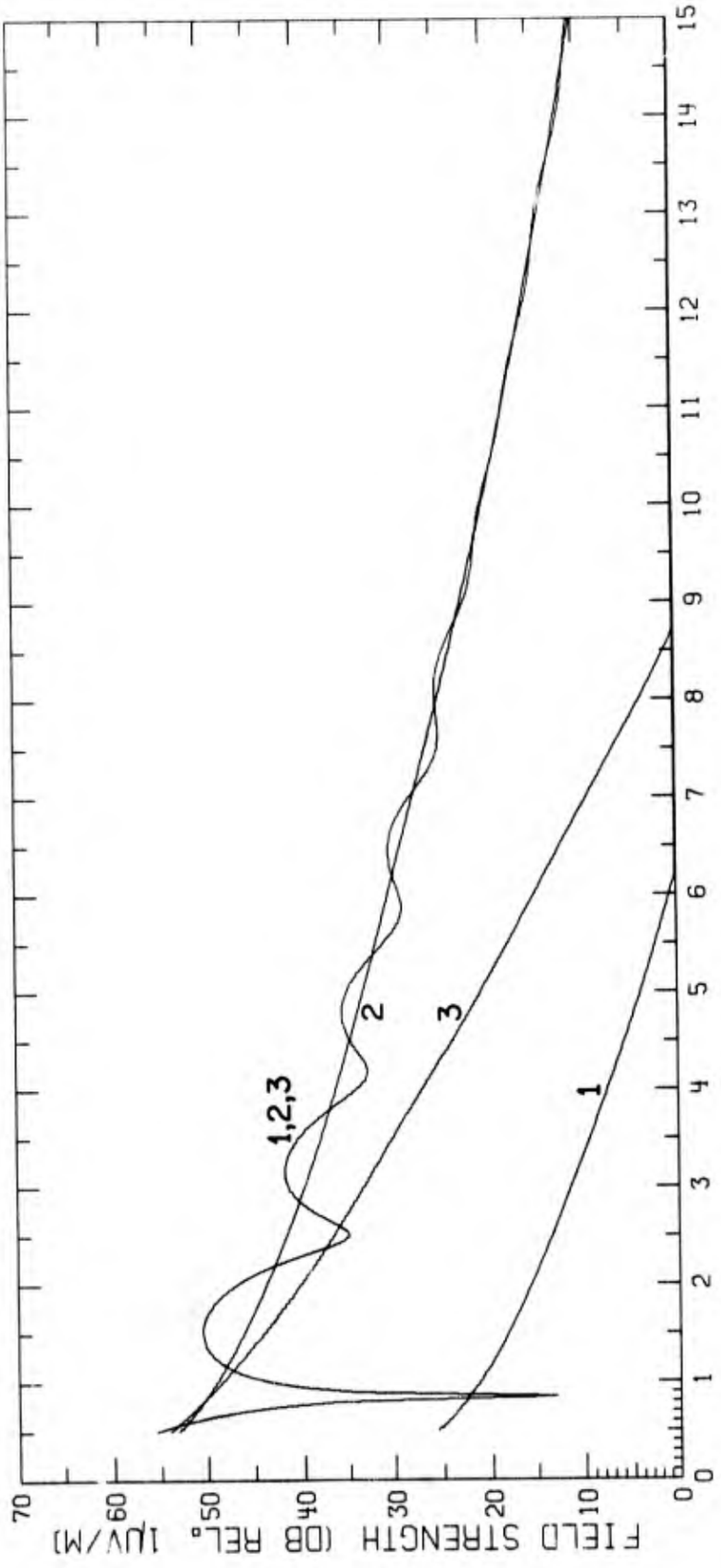

Fig. 70 - Predicted field strengths for f = 28.5 kc/s and h = 90 km

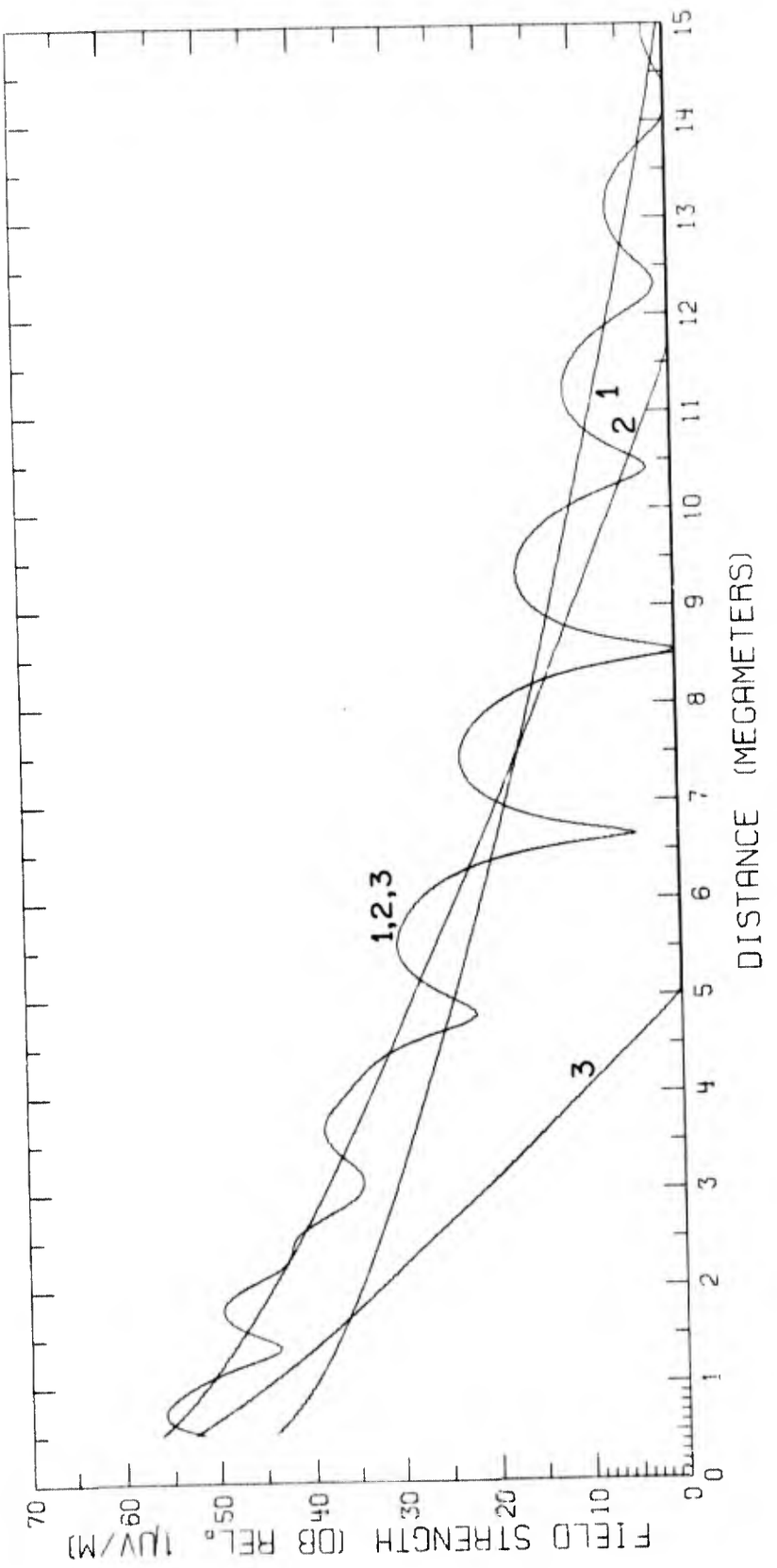

Fig. 71 - Predicted field strengths for f = 30.0 kc/s and h = 70 km

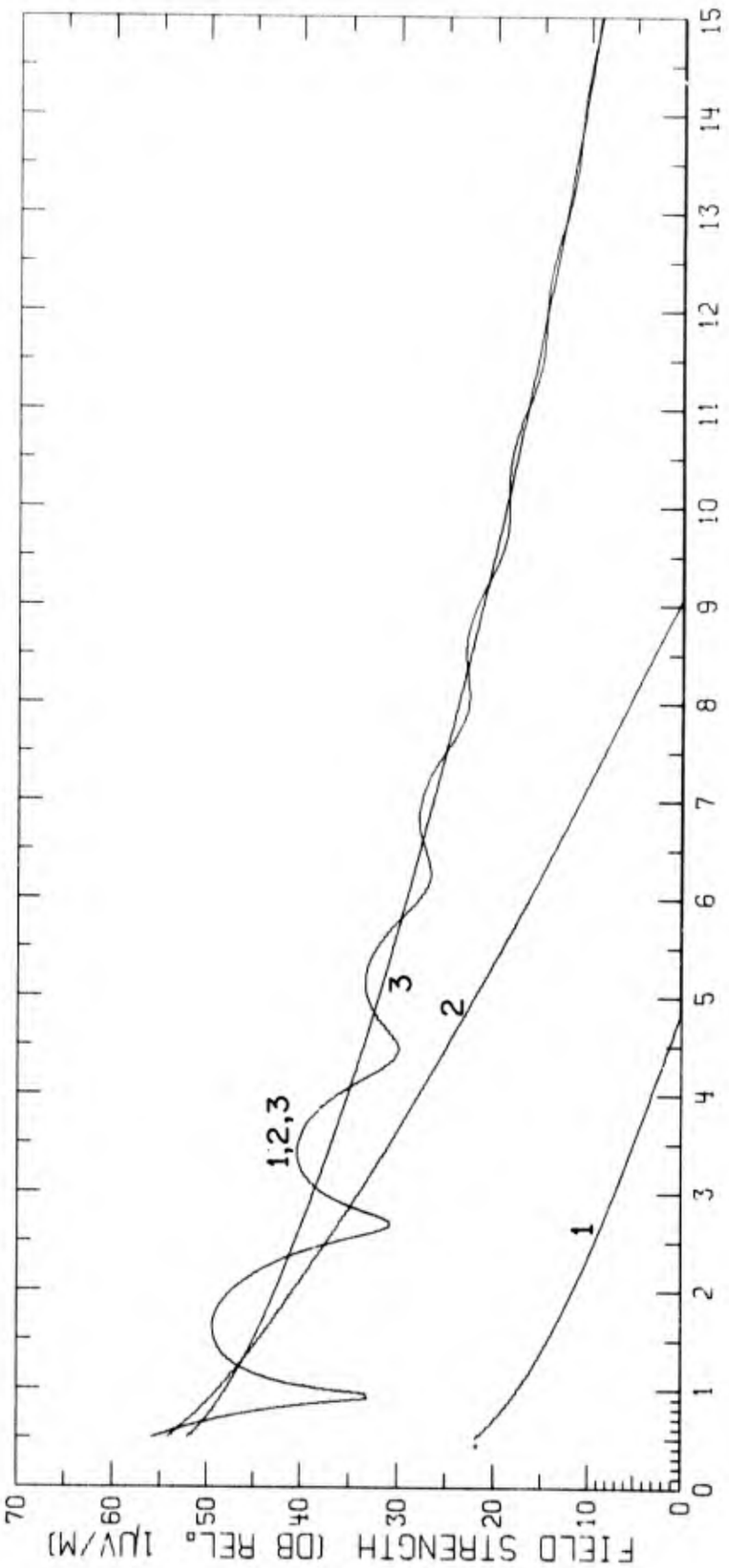

Fig. 72 - Predicted field strengths for f = 30.0 kc/s and h = 90 km

Security Classification

DOCUMENT CONTROL DATA - R & D

Security classification of title, body of abstract and indexing annotation must be entered when the overall report is classified)

1. ORIGINATING ACTIVITY (Corporate author)
Naval Research Laboratory
Washington, D.C. 20390

2a. REPORT SECURITY CLASSIFICATION
Unclassified

2b. GROUP

3. REPORT TITLE
THEORETICAL VLF MULTIMODE PROPAGATION PREDICTIONS

4. DESCRIPTIVE NOTES (*Type of report and inclusive dates*)
A final report on one phase of the problem; work on other phases continues.

5. AUTHOR(S) (*First name, middle initial, last name*)
C.B. Brookes, Jr., J.H. McCabe, and F.J. Rhoads

6. REPORT DATE	7a. TOTAL NO. OF PAGES	7b. NO. OF REFS
December 1, 1967	86	4

8a. CONTRACT OR GRANT NO	9a. ORIGINATOR'S REPORT NUMBER(S)
NRL Problem R01-39	NRL Report 6663
b. PROJECT NO X-1508, Task 82205	
c.	9b. OTHER REPORT NO(S) (*Any other numbers that may be assigned this report*)
d.	

10. DISTRIBUTION STATEMENT
This document has been approved for public release and sale; its distribution is unlimited.

11. SUPPLEMENTARY NOTES	12. SPONSORING MILITARY ACTIVITY
	Department of the Navy (Naval Electronic Systems Command), Washington, D.C. 20360

13. ABSTRACT

A computer program in Fortran has been written for the Control Data Corporation (CDC) 3800 computer to predict the field strength of multimode very-low-frequency (vlf) propagation for distances from 0.5 megameters to 15 megameters.

Although the propagation parameters used in the computations appear in various forms elsewhere in the literature, the curves presented here can be directly compared with experimental data without further computations.

Curves based on the theoretical results for seawater paths are presented for frequencies between 8.0 kc/s and 30.0 kc/s for ionospheric heights of 70 km and 90 km.

DD FORM 1 NOV 65 1473 (PAGE 1)

S/N 0101-807-6801

Security Classification

14 KEY WORDS	LINK A		LINK B		LINK C	
	ROLE	WT	ROLE	WT	ROLE	WT
Vlf radio wave propagation Communications reliability Field strength Multimodes						